CELLULAR SIGNALLING PATHWAYS INVOLVED IN THERMOPROTECTION OF NEURAL CIRCUIT FUNCTION IN THE LOCUST.

by

Gary Alan Barclay Armstrong

A thesis submitted to the Department of Biology

In conformity with the requirements for

the degree of Doctor of Philosophy

Queen's University

Kingston, Ontario, Canada

(August, 2009)

Abstract

Environmental temperature is arguably one of the most important abiotic physical factors affecting insect behaviour. Temperature affects virtually all physiological processes including those that regulate nervous system function. It is therefore not surprising that animals have evolved adaptations that confer tolerance to heat stress and allow for continued behaviour as ambient temperature fluctuates. Most animals have central nervous system (CNS) responses to heat shock (HS) preconditioning which extend the thermal operating range of neural circuits during exposure to extreme heat. It is unclear how HS preconditioning confers CNS thermotolerance. I used the migratory locust (*Locusta migratoria*), an animal that inhabits environments that can have large fluctuations in ambient temperature daily, to examine how neuronal circuits cope with temperatures stress. Using the ventilatory central pattern generator (vCPG) as a model circuit I was able to address how the CNS switches on adaptations which provide protection against heat stress. vCPG thermotolerance was manifested as an increase in the thermal operating range and a decrease in the length of time required to recover vCPG activity when temperature stress was removed. I investigated the octopaminergic (OA/cAMP/PKA) and nitrergic (NO/cGMP/PKG) signalling pathways and tested their involvement in conferring thermotolerance to the vCPG during heat stress. I found that long applications of octopamine, or increased adenylate cyclase activity generated vCPG thermotolerance and was dependent upon transcription and translation. In addition I found that HS-treated locust had significantly reduced nitric oxide (NO) production during heat stress, and when I pharmacologically reduced PKG activity vCPG

thermotolerance was generated. However, unlike octopamine treatment thermotolerance could be observed within minutes following PKG inhibition. Thus I conclude that the octopaminergic and nitrergic pathways coordinate long- and short-term protective modulation of the locust CNS.

Co-Authorship

This thesis consists of 5 manuscripts on three of which I am first author and for the two others I am second author.

Chapter I (Introduction): Temperature regulation and heat tolerance in locusts.

Authors: Armstrong GAB and Robertson RM.

In preparation for a review article including the General Discussion

I researched the literature and wrote this paper. Robertson gave editorial input.

Chapter II: Octopamine Mediates Thermal Preconditioning of the Locust Ventilatory Central Pattern Generator via a cAMP/Protein Kinase A Signalling Pathway.

Authors: Armstrong GAB, Shoemaker, KL, Money TGA, and Robertson RM.

The Journal of Neuroscience (2006) 26: 12118-12126.

I was primarily responsible for design of all the experiments. I collected and analyzed all of the data except the HPLC results which were collected by Shoemaker, and intracellular datasets which were collected by Money. I wrote the manuscript, with editorial input from Shoemaker and Robertson.

<u>Chapter III:</u> Natural Variation in the Thermotolerance of Neural Function and Behavior Due to a cGMP-Dependent Protein Kinase.

Authors: Dawson-Scully K, Armstrong GAB, Kent C, Robertson RM, and Sokolowski MB.

PLoS ONE (2007) e773.

This project used two experimental animal models to highlight the probable ubiquity of PKG activity in regulating heat stress-tolerance across species. Data from both *Drosophila* and *Locusta* were used equally in this manuscript. I collected all the *Locusta* data. *Drosophila* datasets were obtained primarily by the work of Dawson-Scully in Sokolowski's lab with the help of Kent. I wrote methods, results and figure captions of this manuscript pertaining to the use of the locust with editorial input from Robertson. The majority of this manuscript was written by Dawson-Scully.

<u>Chapter IV:</u> Stress Preconditioning of Spreading Depression in the Locust CNS.

Authors: Rodgers CI, Armstrong GAB, Shoemaker KL, LaBrie JD, Moyes CD, Robertson RM.

PLoS ONE (2007) e1366.

This bulk of the data included within this project was collected by Rodgers. I collected the datasets for: ATP assays (with supervision and help from Moyes), experiments which used local injections of KCl to evoke SD, and the SD propagation datasets. Shoemaker helped to collect ATP data and LaBrie was an undergraduate who provided Fig. 2A and

associated results from his Honours thesis. I designed the N_2 chamber used for the hypoxia dataset. This manuscript was written by Rodgers with editorial help from Robertson.

<u>Chapter V:</u> Suppression of spreading depression-like events in locusts by inhibition of the NO/cGMP/PKG pathway.

Authors: Armstrong GAB, Rodgers CI, Money TGA, Robertson RM.

The Journal of Neuroscience (2009) 29:8225-8235.

I designed all the experiments, collected and analyzed the majority of data and wrote the manuscript with input and additional help from Robertson. Rodgers collected two datasets.

Acknowledgements

After nine long years in the Department of Biology, five of which spent as a graduate student, I find myself wanting to say so much to so many people but find it difficult to properly express myself. It has been a journey. I have experienced great joys in Kingston and met many wonderful people, many of whom have played instrumental roles in shaping my character. Foremost of these individuals is my supervisor and friend Mel. Mel you have made me a better person. Your generosity, kindness, and compassion have been a source of great strength for me during difficult times. You have cultivated a passion for science in me and for that I am sincerely grateful. To Nathan, Corinne, Kelly and Tomas you have been there for me through thick and thin. I thank you for everything you did to get me here. I cannot find the words to properly express my gratitude.

I would also like to thank Chris Moyes and Donald Maurice for serving as committee members and helping with various projects. I would also like to acknowledge David Andrew, Laurent Seroude, Yuxiang Wang, Ian Chin-Sang, Paul Young, Sharon Regan, William Bendena, Virginia Walker, the members of the Robertson lab, and my friends who aided me in my studies. I would also like to especially thank John Leperre; you have been a beacon of light this last year, thank you for patiently waiting for me to finish.

I dedicate this thesis to my family: Mum, Dad, Jackson, Molly and Maggie. Who would have thought that the little kid who could not read or write would be here now? I could not have done it without your love and never wavering support and encouragement, I thank you.

Table of Contents

List of Figures

List of Tables

List of Abbreviations

$[K^+]_o$	Extracellular potassium ion concentration
8-Br-cGMP	8-bromo-guanosine 3',5'-cyclic monophosphate
ACTD	Actinomycin D
ATP	Adenosine triphosphate
cAMP	Cyclic adenosine monophosphate
Can	Cantharidin
cGMP	Cyclic guanosine monophosphate
CHX	Cycloheximide
Con	Control group
CPG	Central pattern generator
CSD	Cortical spreading depression
DA	Dopamine
DAF-2 DA	Diaminofluorescein 2-diacetate
E_k	Potassium equilibrium potential
EP	Epinastine
FOR	Forskolin
For	*foraging gene*
HS	Heat shock
HSE	Heat shock element
HSF	Heat shock transcription factor
HSP	Heat shock protein
L-NAME	N_ω-Nitro-L-arginine methyl ester
MSG	Mesothoracic ganglion
MTG	Metathoracic ganglion
NaN_3	Sodium azide

NO	Nitric oxide
NOS	Nitric oxide synthase
OA	Octopamine
OUA	Ouabain
PKA	Protein kinase A
PKG	Protein kinase G
PP2A	Protein phosophatase 2A
Rp-cAMPs	Rp-adenosine 3',5'-cyclic monophosphorothioate triethylammonium salt
SD	Spreading depression
SNAP	S-Nitroso-N-acetyl-DL-penicillamine
SNOG	S-Nitrosoglutathione
Sp-cAMPs	Sp-adenosine 3',5'-cyclic monophosphorothioate triethylammonium salt
TA	Tyramine
TEA	Tetraethylammonium
TTX	Tetrodotoxin
V_m	Membrane potential

Chapter 1

General Introduction

Temperature regulation and heat tolerance in locusts.

Gary A.B. Armstrong* & R. Meldrum Robertson.

Department of Biology, Queen's University, Kingston, Ont., Canada K7L 3N6.

Email address: 9ga1@queensu.ca (Gary A.B. Armstrong).

* To whom correspondence should be sent: G.A.B. Armstrong, Department of Biology, Queen's University, Biosciences Complex, Kingston, Ontario, Canada K7L 3N6. Email (armstrog@biology.queensu.ca).

1.1 Introduction

A biological problem of fundamental importance concerns the physiological mechanisms which have evolved that permit insects to survive in inhospitable environments. Many insects can survive extremely hot environments and the Saharan silver ant (*Cataglyphis bombycina*) is an excellent example. Individuals of this species emerge in groups from underground burrows to forage at midday in scorching conditions where surface temperatures can be in excess of 60 ºC (Wehner et al. 1992). They leave their burrows when temperatures rise above 46 °C and in doing so reduce their chance of being preyed upon by opportunistic predators unable to forage during these extreme environmental conditions. Foraging bouts last for only short period of time, often less than a few minutes, and are punctuated by stops in thermal refuges to dissipate body heat. How animals maintain behaviours at such temperatures while others cannot is poorly understood. Fundamentally, all animals behaving near their particular thermal limit encounter challenges. Many of these organisms make convenient models to study stress tolerance, but only a few are suitable for examining how neuronal circuits handle temperature stress.

Temporal variation in environmental temperature occurs daily and profoundly affects an organism's ability to survive and reproduce. Variation over longer time scales, such as seasonal changes in temperature, have many ramifications for organisms, for example dictating food availability and consequently when to reproduce and migrate. In addition, temperature gradients across a species' range and within microclimates constitute a

spatial variable which organisms must cope with. Many of these heat gradients can be large and can occur over a small distance.

Thermal relationships between an individual and its environment are often complex. Air temperature is a poor proxy of thermal conditions in an environment. On a cool day, radiant energy from the sun can drive up an insect's body temperature many tens of degrees Celsius. Heat gained or lost due to substrate conduction and convection can heat or cool a locust rapidly. In some species of insects temperature disparity between the thorax and abdomen can be several degrees Celsius (Casey, 1981) affecting heat transfer within the organism. In the context of investigating nervous system tolerance to heat stress one must be aware that the temperature of the CNS may be different from air temperature, substrate temperature or even temperature at different locations in the organism.

I am interested in mechanisms of heat tolerance in the migratory locust (*Locusta migratoria*), a eurythermic animal inhabiting environments that can fluctuate daily by 45 °C (Uvarov, 1977). Mature individuals of this species have a range of "preferred" ambient temperature between 22 and 38 °C (Bodenheimer and Segal, 1929). Conveniently, much is known about the neuronal circuitry for flight and ventilation along with axonal and synaptic properties of particular neurons in this species (Burrows, 1996). Thus, the use of this organism allows the integration of cellular and subcellular neuronal adaptations with physiological and behavioural responses.

1.1.1 Behavioural thermoregulation in locusts

Insects rely upon behavioural mechanisms to regulate body temperature. Many of these behaviours are seemingly simple but can profoundly regulate body temperature. Postural adjustments can regulate body temperature. Moving from a semi-stilted posture (abdomen touching substrate) to a stilted posture (abdomen not touching substrate) dramatically reduces body temperature to 43 °C from the much hotter 56 °C temperature of the substrate (Waloff, 1963). More complex behavioural responses to heat sources can be directed (thermotaxis) or undirected (thermokinesis) (Uvarov, 1977). These responses to heat can be very rapid (Chapman, 1965; Altner et al. 1981; Robertson et al. 1996). Moving onto the shade-cast side of a leaf or branch has been well documented in insects and temperature gradients between shaded and non-shaded sides can be large.

A second kind of postural adjustment facilitates basking. This entails alignment changes to alter body axis orientation with incident light rays (men-akinetic behaviour). During windless conditions, basking can rapidly raise the thoracic body temperature many degrees Celsius in a matter of minutes. Results obtained from an intact, basking brown locust (*Locustana pardalina*) in its environment revealed a rise in body temperature from 21.2 °C to 37.7 °C in 5 minutes (Smit, 1960). Many species begin basking following sunrise. African desert locusts (*Schistocerca gregaria*) leave their roosts and begin basking behaviour 30 minutes after sunrise when body temperature is as low as 10 °C (Uvarov, 1977). When internal temperature reaches 39-40 °C *L. migratoria* faces the sun

paralleling its posture with sunlight (*Tel-akinesis*), and in doing so reduces total light exposed surface area by four-fifths (Volkonsky, 1939). Many species of insects, including *Locusta* and *Schistocerca*, rely upon basking behaviour to increase thoracic temperature and thus temperature of the wing musculature needed for flight (Uvarov, 1977). Both *S. gregaria* and *L. migratoria* are unable to achieve flight when body temperature is below 20 °C and strong sustained flight only occurs when body temperature is above 24 °C (Gunn *et al.*, 1948; Waloff and Rainey, 1951). However, locusts have been observed to fly in air temperature as low as 11 °C but basking behaviour was required first before commencing flight (Gunn *et al*, 1948).

In a locust's environment rapid rises in temperature are rare, but can occur. Inferred from above, basking brown locusts have heating rates of 3.3 °C/min. Pre-flight warm up in *Manduca sexta* raises the thoracic temperature at a minimum rate of 4.5 °C/min (Heinrich and Bartholomew, 1971). In flying locusts, metabolic heat production and radiant energy raise the thoracic temperature of the locust 13-14 °C above air temperature in the first few minutes of flight (Uvarov, 1977). Along with rapid rises in temperature from conduction and convection, heating rates of locusts behaving in their environment can be fast. An important question that arises is how does the nervous system cope with rapid rises in temperature?

1.2 CNS dysfunction due to heat stress

I examined how heat stress affects the neural circuit controlling ventilation in the locust. Ventilatory motor patterns are coordinated by a robust central pattern generator (vCPG) situated in the metathoracic ganglion (MTG) (Burrows, 1996). This motor pattern is responsible for delivering and removing oxygen and carbon dioxide via the tracheal system in the locust (Albrecht, 1953). In intact behaving locusts the frequency of the rhythm is variable, ranging from 0.08 - 4 Hz (Burrows, 1996). However, this rhythm can become less regular during quiescence, termed discontinuous ventilation, and is characterized by periods of no ventilation lasting for several minutes (for review see Lighton, 1994). In semi-intact locusts the ventilatory rhythm is around 1 Hz at 20 °C (Newman et al. 2003) and fictive motor patterns are slower in isolated nerve cord preparations (removed from the animal with no afferent feedback), less than 0.5 Hz at 18-19 °C (Bustami and Hustert, 2000). Faster and more regular ventilatory rhythms occur during increased activity (e.g. flight), octopamine neuromodulation, and heat stress (Ramirez and Pearson, 1989b; Sombati and Hoyle, 1984; Armstrong and Robertson, 2006). At higher temperatures faster ventilatory rates increase heat loss via tracheal evaporation and keep body temperature much below air temperature (Prange, 1990).

Semi-intact preparations superfused with saline at room temperature (~20 °C) ventilate at a frequency around 1 Hz (Newman et al. 2003). As temperature of the saline is raised the frequency of the motor pattern increases. At 40 °C the frequency is around 3 Hz. If temperature increases, irregularities in vCPG activity occur and eventually motor pattern

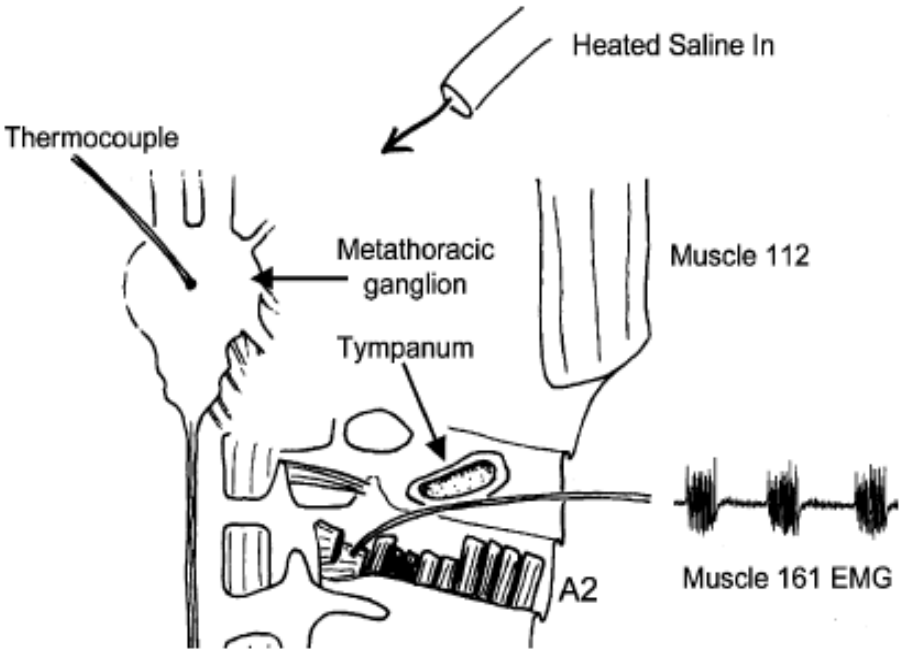

Figure 1.1

Schematic representation of the semi-intact locust preparation displaying the location of the electromyographic (EMG) recording electrode on muscle 161 in the second abdominal segment (A2) (Taken from Newman et al. 2003).

activity stops (Armstrong and Robertson, 2006). However if saline temperature is allowed to return to room level, motor pattern activity recovers. (Newman et al. 2003; Armstrong and Robertson, 2006). Measurements of extracellular potassium ion concentrations ($[K^+]_o$) made in the MTG during hyperthermic failure of the vCPG revealed a rapid rise and plateau from a 10 mM baseline levels of $[K^+]_o$ to around 42 mM (Robertson, 2004). When the heater was switched off and saline temperature returned to room levels, $[K^+]_o$ return to baseline levels and vCPG activity resumed. This is very similar to $[K^+]_o$ changes in the rat hippocampus during hyperthermia-induced spreading depression (SD) (Wu and Fisher, 2000).

1.3 Characteristics of spreading depression

SD is characterized by a propagating wave of cellular depolarizations and redistribution of ionic concentrations across the membrane of neurons lasting for several minutes. A notable feature of SD is a rapid rise in $[K^+]_o$ which may account for the neuronal depolarization. Inhibition of neuronal activity due to high $[K^+]_o$ in insects has previously been described (Hoyle, 1952), and SD was first proposed to occur in insects over 40 years ago (Rounds, 1966). In mammals, SD has been well documented and studied in the CNS including those of the mouse, rat, rabbit, cat, monkey and human (Leão, 1944; Van Harreveld and Khattab, 1967; Van Harreveld et al. 1956; Aitken et al. 1991; Gorji et al. 2001). The occurrence of SD is not limited to mammals having been observed in the CNS of a frog (*Rana*) and turtle (*Pseudemys*), and in the retinas of the chicken (*Gallus*), toad (*Bufo*), and lizard (*Tupinambis*) (Guedes et al. 2005; Lauritzen et al. 1988; Martins-

Ferreira and Castro, 1965: Streit et al 1995; Hanke and Fernandes De Lima, 2008; for reviews see Somjen 2001; Smith et al. 2006). SD arises in regions of the CNS that contain grey matter; in particular the hippocampus and neocortex are susceptible to it, whereas the spinal cord is more resistant to it (Czéh and Somjen, 1990). When SD occurs in the cortex it is referred to as cortical spreading depression (CSD). SD is initiated following mechanical (contusions), electrical (high frequency stimulation), and chemical (ouabain, KCl, metabolic blockers etc.) and thermal insults to the CNS (Leão, 1944; Leão and Morrison, 1945; Balestrino, 1999; Müller and Ballanyi, 2003; Wu and Fisher, 2000). SD is believed to be the manifestation of the aura that sometimes accompanies migraine (Hadjikhani et al. 2001). Additionally, anoxic depolarization (AD, sometimes called terminal depolarization), which occurs following ischemia and simulated stroke (oxygen/glucose deprivation) is considered to be a related phenomenon that differs in the severity of tissue damage (Somjen, 2001; Joshi and Andrew, 2001; Obeidat and Andrew, 1998). A milder version of AD occurs when brain tissue is briefly exposed to hypoxia (hypoxic SD), and unlike AD, neuronal recovery from hypoxic SD occurs (Müller and Somjen, 2000). SD is thought to be benign when compared to AD which is damaging, largely due to compromised energy production thereby leading to cell swelling and dendritic beading (Obeidat et al. 2000). Recently, SD has been shown to produce local regions of hypoxia as transient increases in the tissue's demand for oxygen outstrip vascular oxygen supply (Takano et al. 2007).

SD was first observed as a propagating wave of depressed neuronal activity over rabbit cortex (Leão, 1944). The commonly reported propagation speeds are around 3 mm/min but some studies report speeds as low as 2 mm/min and others as high as 9 mm/min, with propagation stopping at lesions or white matter (Van Harreveld, 1956; Grafstein, 1956; Hull and Van Harreveld, 1964; Nicholoson et al. 1978). The propagation of AD is infrequently observed as tissue is globally exposed to reduced energy levels. However, during hypoxic SD specific foci of SD initiation have been observed (Aitken et al. 1998). The use of electrophysiological measures to characterize SD, hypoxic SD, and AD has yielded considerable information about the physiological basis of this phenomenon. Membrane potential, measured from pyramidal neurons in the CA1 sector of the hippocampus, depolarized from baseline membrane potential to zero or close to zero before repolarizing and resuming activity (Snow et al. 1983; Czéh et al. 1993). Occasionally, a brief bust of prodromal spikes preceded the SD wave front (Müller and Somjen, 2000). Measurements of membrane potential from interneurons and glia also show a substantial depolarization during SD (Müller and Somjen, 2000). Depolarization of a sizable portion of neurons in the CNS accounts for the strong DC field potential shift used by many researchers to identify SD events.

The inability to produce spikes during SD reflects the large redistribution of ionic concentrations inside and outside cells that accompanies these events. Tightly controlled baseline levels of 3.0 - 3.5 mM extracellular potassium concentration ($[K^+]_o$) rapidly rises to 50.0 - 60.0 mM $[K^+]_o$ during SD in the rat hippocampus (Vyskočil et al. 1972; Müller

and Somjen, 2000). The rise in $[K^+]_o$ is concomitantly associated with a drop of extracellular ion concentrations of sodium (155 mM to around 64 mM), chloride (128 mM to 89 mM) and calcium (1.15 mM to 0.10 mM) (Müller and Somjen, 2000; Jiang et al. 1992; Basarasky et al. 1998). Measurements of input resistance during SD show a substantial collapse in the ability of neurons to regulate ion conductances. Hippocampal pyramidal cells during hypoxic SD have a peak decrease in input resistance between 56.4 and 88.5 % from initial levels (see Czéh, 1993; Muller and Somjen, 2000). However, decreases in input resistance can be variable, ranging from as little as 11% (Czéh, 1993) to as high as 97 % (Snow et al. 1983). Glia have a more moderate reduction in input resistance as well (Müller and Somjen, 2000).

Using K^+-sensitive electrodes we have observed a rapid rise in $[K^+]_o$ at the moment of heat-induced CNS failure that is reminiscent of SD (Robertson, 2004). However, it is unclear how similar these events are to SD. One aim of this thesis was to further describe the occurrence of these events in the locust.

1.4 Responses to heat shock in the locust CNS

The vCPG is a reliable proxy of CNS function during exposure to noxious stimuli. It is likely that protective adaptations are robustly expressed within the CNS. As previously suggested, before cells and tissues die, any dysfunction in CNS activity that coordinates crucial behaviours such as escape or ventilation could decrease the ability to avoid predation (Armstrong and Robertson, 2006). Nervous tissue in the locust and other

animals has repeatedly been observed to produce a strong response to preconditioning treatments e.g. heat shock (HS). Preconditioning is defined as a sublethal stress that confers subsequent protection for stress.

Across disparate phyla organisms display a universal response to elevated temperature by inducing a heat shock response (HSR), which can be characterized by the expression of a suite of heat shock proteins (HSPs) (Kiang and Tsokos, 1998; Sharp et al. 1999. The increased presence of HSPs allows cells, tissues, and whole organisms to withstand higher temperatures. It is believed that important changes like the up-regulation of HSPs occurs in the CNS forming a mechanistic cornerstone for continued CNS function during heat and other stresses (Parsell and Lindquist, 1993; Feder and Hofmann, 1999). In the laboratory the HSR can be induced by briefly exposing animals to heat. Depending upon the species this can usually be observed in as short as 20 minutes and as long as 3 hours. Heat shock (HS) protocols for *Drosophila melanogaster* larvae usually consist of 1 hr exposure to 36 °C followed by a 1 hr recovery at room temperature (25 °C) (Xiao et al. 2007); for *L. migratoria*, 3 hrs at 45 °C followed by 1 hr recovery at room temperature (Whyard et al. 1986); for mouse brainstem slices 20 minutes at 40 °C followed by a 2 hr recovery at 30 °C (Kelty et al. 2002). Following HS treatment one can observe a substantial increase in the upper thermal operating range of the nervous system. For example, following HS treatment the vCPG operating range is extended by 5-6 °C and the flight CPG by 6-7 °C (Armstrong and Robertson, 2006; Robertson et al. 1996). Excitatory junction potentials at the hindleg are maintained at temperatures 6.3-8.4 °C

higher than in control preparations, (Barclay and Robertson, 2000; Klose et al. 2004). Experiments using the descending contralateral movement detector (DCMD) neuron as a model for investigating changes in neuronal properties of the locust following HS, have concluded that firing frequency, half-width duration, amplitude and membrane potential are maintained at higher temperatures (Money et al. 2005; Money et al. 2006).

It remains unclear how neuronal circuits are able to remain operational at higher temperatures following HS treatment. One possibility is that neuromodulators might play a role in generating thermotolerance. My Ph.D. work investigated the role of octopaminergic and nitrergic neuromodulation in conferring thermotolerance.

1.5 Does octopamine neuromodulation play a role in vCPG thermotolerance?

Although most of our preconditioning treatments use heat stress to generate thermotolerance, similar protective responses can be generated in the locust following exposure to cold and anoxia (Newman et al. 2003). One possible mechanism that aids in this coordinated universal stress response is via the release of an endogenous compound. In insects, candidate compounds that can account for the diverse coordinated change in physiology are amines, such as octopamine (OA). OA can act as a neurotransmitter (Nathanson, 1979), a neuromodulator (Leitch et al. 2003) and a neurohormone (Orchard et al. 1982). Its multifaceted functions are widely accepted to activate a flight-or-fight

response in invertebrates that is analogous to the effect of norepinephrine in vertebrates (Hoyle, 1975; Evans, 1985; Roeder, 1999, 2005).

Many of the initial studies investigating the role of OA used locusts (*L. migratoria* and *S. gregaria*). From these studies the diverse physiological processes regulated by OA were first described. For example, during flight, OA coordinates a change from carbohydrate catabolism to lipid oxidation needed for long distance flight (Mentel et al. 2003). OA concentration in the haemolymph increases by 5 times during the first 10 minutes of flight (Goosey and Candy, 1980) and a similar increase in circulating haemolymph concentrations occurs after heat stress (Davenport and Evans, 1984). Peripherally, OA increases the performance of wing musculature during flight (Malamud et al. 1988), and increases hind leg muscle contraction force (Evans, and Myers, 1986; O'Shea and Evans, 1997), both essential for effective escape behaviours. Centrally released OA dishabituates the visual descending contralateral movement detector (DCMD) interneuron from repeated stimuli, keeping the animal more responsive to repetitive looming threats (Bacon et al. 1995). OA also excites CPGs for foregut activity, locomotion, flight and ventilation (Zilberstein *et* al., 2004; Sombati and Hoyle, 1984; Stevenson and Kutsch, 1986; Bellah et al. 1984; Ramirez and Pearson, 1989b, 1991).

The main source of OA in the locust CNS is from dorsal and ventral unpaired median neurons, situated in the ganglia of the ventral nerve cord (Bräunig and Burrows, 2004; Duch et al. 1999; Stevenson and Spörhase-Eichmann, 1995). These neurons can be

identified electrophysiologically, possessing a broad action potential, an excitable soma, and a prominent after-hyperpolarization (Hoyle and Dagan, 1978; Baudoux and Burrows, 1998). OA receptors were initially classified into 3 groups, based on agonist and antagonist binding efficacies and coupling to specific second messenger pathways (Evans, 1981; 1984a, b; Roeder, 1992). Recently a new classification scheme has been made based on the similarities of cloned *Drosophila* OA receptors and their signalling pathways to vertebrate adrenergic receptors and their signalling pathways (Evans and Maqueira, 2005). This scheme places OA receptors into two groups: α-adrenergic-like OA receptors, which raise intracellular calcium levels following receptor activation, and β-adrenergic-like OA receptors that are coupled to adenylate cyclase and increase cAMP concentrations (Bischof and Enan, 2004; Balfanz et al. 2005; Roeder and Gewecke, 1990; Roeder, 1992; 1995). β-adrenergic-like OA receptors are abundant in the locust CNS (Roeder, 1992) and are probably responsible for modulating the ventilatory rhythm (Armstrong and Robertson, 2006).

There are several possible roles for OA protecting the CNS from heat stress. First, OA excitation of the ventilatory motor pattern may promote evaporative cooling. Second, OA may augment synaptic potentials, thereby accommodating loss of synaptic strength as temperature is increased. Third, OA may initiate transcription and translation of genes and proteins which provide protection of neuronal function during stress.

1.6 Does nitrergic neuromodulation play a role in vCPG thermotolerance?

Nitric oxide (NO) is a highly diffusible diatomic molecule that acts as a transmitter and modulator of neuronal activity in vertebrates and invertebrates. Much is known about the NO pathway in animals (for vertebrate reviews see: Moncada et al. 1991; Hofmann et al. 2006; Calabrese et al. 2007; for invertebrate reviews see: Müller, 1997; Bicker, 1998; 2001; 2005; 2007; Davies, 2000). In the locust nervous system pharmacological manipulation of NO production has been implicated in modulating CPGs. These include the mandibular, heart, and egg-laying motor patterns (Rast, 2001; Bullerjahn et al. 2006; Newland and Yates, 2007). Nitrergic neuronal modulation of the vCPG has not been reported, although neurons expressing nitric oxide synthase (NOS), the enzyme responsible for producing NO are present in the MTG near the ventilatory neuropil (Ott and Burrows, 1998; Bullerjahn and Pflüger, 2003).

The presence of NO in the locust CNS was first reported by Elphick and colleagues (1993). Using NADPH diaphorase histochemistry, a marker for NOS activity, Ott and Burrows (1998, 1999) showed an extensive network of NOS-containing neurons throughout the entire thoracic nerve cord, including the MTG. These neurons can also be labeled using a universal NOS antibody, which has also revealed NOS-containing neurons (Bullerjahn and Pflüger, 2003). Interestingly, some reports have suggested that DUM neurons may also express this enzyme (Bullerjahn and Pflüger, 2003; Bullerjahn et al. 2006), however arguments against DUM neurons having NOS have been made (Ott and Burrows, 1999).

NO stimulates the production of cGMP via activating soluble guanylyl cyclase (sGC) (Elphick et al. 1993). In the locust brain, baseline levels of cGMP are around 200 fM which increase to 800 - 1600 fM following application of various NO donors to the saline (Elphick et al. 1993). Rises in cGMP concentrations increases the probability of binding to the regulatory domain of protein kinase G (PKG) allowing for increased PKG-dependent phosphorlyation of proteins to occur. Although much is now known about the architecture of NO producing neurons in the locust there remains a major gap in our understanding of when and why NO is being produced in locusts.

One possibility is that NO is produced in response to stress and activation of its signalling pathway is involved in providing stress tolerance. Work from neuroblastoma cell lines and cardiac tissue from rats supports this hypothesis (Andoh et al. 2002; Van Cuong et al. 2006). In neuroblastoma cells preconditioning treatment increased the expression of neuronal NOS mRNA, NOS protein which then led to an increased production of NO; this was associated with oxidative stress tolerance (Andoh et al. 2002; Chiueh et al. 2005). In rat heart, increased activity of NO/cGMP/PKG protects ventricular myocytes from ischemia-reperfusion injury (Van Cuong et al. 2005). It is unknown what role, if any, NO has in generating stress tolerance in the locust. However in *Drosophila* two naturally occurring variants of the *foraging* (*For*) gene exists (Osborne et al. 1997). Rovers (For^R) have high PKG concentrations and move more when in the presence of food than sitters (For^S) which have reduced PKG concentrations. Interestingly, these

variants display altered behavioural responses to hypoxia. *Drosophila* carrying the *For*^{R} genotype leave feeding sites whereas *For*^{S} do not (Wingrove and O'Farrell, 1999). A notable difference between the two variants is reduced neuronal voltage-activated K^+ currents in *For*^{S}. Both peak and sustained currents were attenuated in sitter variants (Renger et al. 1999). This altered K^+ conductance is very similar to what is found in neuronal cell bodies of HS-preconditioned locusts (Ramirez et al. 1999; Wu et al. 2002).

Increased PKG activity has been shown to phosphorylate protein phosphatase 2A which then de-phosphorylates specific K^+ channels leading to increased K^+ conductance (Zhou et al 1996; White et al. 2002). Opposite to increased K^+ conductance, a decrease in K^+ conductance has been argued to reduce the likelihood of initiating heat-induced SD-like events in the locust (Robertson, 2004). One possibility is that reduced PKG activity reduces the efflux of K^+ to the extracellular space during stress thereby delaying the triggering of the SD-like event by reducing the rate at which $[K^+]_o$ can rise. For this to occur preconditioning treatments might subsequently attenuate NO production during stress thereby reducing PKG activity in the CNS and reducing K^+ conductance. This implies that lowered NO levels and decreased PKG activity would decrease the severity of SD-like events by reducing their duration. However in mammals NO levels in the affected tissue are increased following CSD (Read et al. 1997). Research from the CNS of rats suggests that increased basal NO levels, produced by endothelial NOS activity, decreases the likelihood of CSD (Petzold et al 2008). However, when selective neuronal NOS inhibitors are used the occurrence of KCl-induced SD is significantly reduced

whereas the duration of SD events are significantly longer (Urenjak and Obrenovitch, 2000). One must be mindful of the complex interaction of vascular supply of oxygen and the propensity to generate SD in mammals. Any role NO might have in regulating SD-like events in the locust would be dependent upon neuronally-derived NOS as insects do not possess the same vascular architecture of mammals.

1.7 Thesis overview

Two abiotic stresses that can profoundly influence nervous system function are temperature and hypoxia/anoxia. For animals to survive and reproduce, they must be able to properly interact with and respond to changing environmental conditions. In the context of my Ph.D. research I have been interested in understanding how the vCPG can be adaptively modified by preconditioning treatments. This thesis consists of four data chapters (three of which are published, the last is being prepared for resubmission) and they are presented in chronological order.

Using electrophysiological, biochemical, and pharmacological techniques to monitor changes in the CNS, I have been able to assess the role of various cellular signalling pathways in generating vCPG stress tolerance. Specifically, I have investigated the role of octopamine, a biogenic amine, in switching on protective adaptations that preserve neuronal function during heat stress. The role this amine has in generating CNS heat tolerance is investigated in the second chapter of my thesis. In the third chapter, I investigated whether differing PKG activities in the locust could regulate vCPG heat

tolerance. The fourth chapter investigates the similarity between heat-induced neuronal failure and SD phenomena in vertebrates. More precisely, we investigated if preconditioning treatment would confer tolerance to heat-induced SD-like events in the locust CNS. In the last chapter, I returned to the study of the NO/cGMP/PKG pathway and investigated whether NO is produced in the CNS during stress. Lastly I investigated if pharmacological manipulation of NO production and PKG activity could alter SD-like events occurring in the locust CNS.

Together, these four data chapters examine the involvement of the nitrergic and octopaminergic neuronal signalling pathways in providing stress tolerance.

Literature cited

Anderson T.R. and R.D. Andrew. Spreading depression: imaging and blockade in the rat neocortical brain slice. *J. Neurophysiol.* 88: 2713-2725 (2002).

Andoh, T. Chock, P.B. and C.C. Chiueh. Preconditioning-mediated neuroprotection: role of nitric oxide, cGMP, and new protein expression. *Ann. N.Y. Acad. Sci.* 962: 1-7 (2002).

Albrecht, F.O. The Anatomy of the migratory locust. University of London. The Athlone Press (1953).

Altner, H. Routil, C. and R. Loftus. The structure of bimodal chemo-, thermo-, and hygroreceptive sensilla on the antenna of Locusta migratoria. *Cell Tissue Res.* 215: 289-308 (1981).

Aitken, P.G. Jing, J. Young, J. Friedman, A. and Somjen, G.G. Spreading depression in human hippocampal tissue in vitro (Abstract). *Third IBRO Congr. Neurosci. Abs.* p. 329 (1991).

Aitken, P.G. Tombaugh, G.C. Turner, D.A. and G.G. Somjen. Similar propagation of SD and hypoxic SD-like depolarization in rat hippoccapis recorded optically and electrically. *J. Neurophysiol*. 80: 1514-1521 (1998).

Armstrong, G.A.B. and R.M Robertson. A role for octopamine in coordinating thermoprotection of an insect nervous system. *J. Therm. Biol.* 31: 149-158 (2006).

Armstrong, G.A.B. Shoemaker, K.L. Money, T.G.A. and R.M. Robertson. Octopamine mediates thermal preconditioning of the locust ventilatory central pattern generator via a cAMP/protein kinase A signaling pathway. *J. Neurosci.* 22: 12118-12126 (2006).

Bacon, J.P. Thompson, K.S.J. and M Stern. Identified octopaminergic neurons provide an arousal mechanism in the locust brain. *J. Neurophysiol.* 74: 2739-2743 (1995).

Balestrino, M. Young, J. and P. Aitken. Block of (Na^+,K^+)ATPase with ouabain induces spreading depression-like depolarization in hippocampal slices. *Brain Res.* 838: 37-44 (1999).

Balfanz, S. Strünker, T. Frings, S. and A. Baumann. A family of octopamine receptors that specifically induces cyclic AMP production or Ca^{2+} release in *Drosophila melanogaster*. *J. Neurochem*. 93: 440-451 (2005).

Barclay, J.W. and R.M. Robertson. Heat shock-induced thermoprotection of hindleg motor control in the locust. *J. Exp. Biol.* 203: 941-950 (2000).

Basarasky, T.A. Duffy, S.N. Andrew, R.D. and B.A. MacVicar. Imaging spreading depression and associate intracellular calcium waves in brain slices. *J. Neurosci.* 18: 7189-7199 (1998).

Baudoux, S. and M. Burrows. Synaptic activation of efferent neuromodulatory neurons in the locust S*chistocerca gregaria*. *J. Exp. Biol.* 201: 3339-3354 (1998).

Bellah, F.L. Fitch, G.K. and A.E. Kammer. A central action of octopamine on ventilation frequency in *Corydalus cornutus*. *J. Exp. Zool.* 231: 289-292 (1984).

Bicker, G. NO news from insect brains. *Trend Neurosci.* 21: 349-355 (1998).

Bicker, G. Sources and targets of nitric oxide signalling in insect nervous systems. *Cell Tissue Res.* 303: 137-146 (2001).

Bicker, G. STOP and GO with NO: nitric oxide as a regulator of cell motility in simple brains. *BioEssays* 27: 495-505 (2005).

Bicker, G. Pharmacological approaches to nitric oxide signalling during neural development of locusts and other model insects. *Arch. Insect Biochem. Physiol*. 64: 43-58 (2007).

Bischof, L.J. and E.E. Enan. Cloning, expression and functional analysis of an octopamine receptor from *Periplaneta americana*. *Insect. Biochem. Mol. Biol.* 34: 511-521 (2004).

Bodenheimer, F.S. and N. Segal. Die Vorzugstemperatur. *Z. angrew. Ent.* 15:490-500 (1929).

Bullerjahn, A. and H.-J. Pflüger. The distribution of putative nitric oxide releasing neurons in the locust abdominal nervous system: a comparison of NADPHd histochemistry and NOS-immunocytochemistry. *Zoology* 106: 3-17 (2003).

Burrows, M. The tracheal supply to the central nervous system of the locust. *Proc. R. Soc. Lond.* B 207:63-78 (1980).

Burrows, M. The Neurobiology of an Insect Brain. Oxford University Press, Oxford (1996).

Bustami, H.P. and R. Hustert. Typical ventilatory pattern of the intact locust is produced by the isolated CNS. *J. Insect. Physiol.* 49: 1285-1293 (2000).

Bräunig, P. and M. Burrows. Projections patterns of posterior dorsal unpaired median neurons of the locust subesophageal ganglion. *J. Comp. Neurol.* 478: 164-175 (2004).

Calabrese, V. Mancuso, C. Calvani, M. Rizzarelli, E. Butterfield, D.A. and A.M. Giuffrida Stella. Nitric oxide in the central nervous system: neuroprotection versus neurotoxicity. *Nat. Rev. Neurosci.* 8: 766-775 (2007).

Casey, T.M. Behavioral Mechanisms of Thermoregulation. Insect Thermoregulation. Wiley-Interscience. 80-114 (1981).

Chapman, R.F. The behaviour of nymphs of *Schistocerca gregaria* (Forskål) (Othoptera, Acrididae) in a temperature gradient, with special reference to temperature preference. *Behaviour* 24: 283-317 (1965).

Chiueh, C.C. Andoh, T. and P.B. Chock. Roles of thioredoxin in nitric oxide-dependent presonditioning-induced tolerance against MPTP neurotoxin. *Toxicol. App. Pharmacol.* 207 :S96-S102 (2005).

Collewijn, H. and A. Van Harreveld. Membrane potential of cerebral cortical cells during spreading depression and asphyxia. *Exp. Neurol.* 15: 425-436 (1966).

Czéh, G. Aitken, P.G. and G.G. Somjen. Membrane currents in CA1 pyramidal cells during spreading depression(SD) and SD-like hypoxic depolarization. *Brain Res.* 632: 195-208 (1993).

Czéh, G. and G.G. Somjen. Hypoxic failure of synaptic transmission in the isolated spinal cord, and the effects of divalent cations. *Brain Res.* 527: 224-233 (1990).

Davies, S.-A. Nitric oxide signalling in insects. *Insect Biochem. Mol. Biol.* 30:1123-1138 (2000).

Davenport, A.P. and P.D. Evans. Stress-induced changes in the octopamine levels of insect haemolymph. *Insect. Biochem.* 14: 135-143 (1984).

Duch, C. Mentel, T. and H.-J. Pflűger. Distribution and activation of different types of octopaminergic DUM neurons in the locust. *J. Comp. Neurol.* 403: 119-134 (1999).

Elphick, M.R. Green, I.C. and M. O'Shea. Nitric oxide synthesis and action in an invertebrate brain. *Brain Res.* 619: 344-346 (1993).

Evans, P.D. Multiple receptor types for octopamine in the locust. *J. Physiol.* 318: 99-122 (1981).

Evans, P.D. A modulatory octopaminergic neurone increases cyclic nucleotide levels in locust skeletal muscle. *J. Physiol.* 348: 325-340 (1984a).

Evans, P.D. The role of cyclic nucleotides and calcium in the mediation of the modulatory effects of octopamine on locust skeletal muscle. *J. Physiol.* 348, 325-340 (1984b).

Evans, P.D. Octopamine. Comprehensive Insect Physiology, Biochemistry, and Pharmacology, vol 11: Pharmacology. Oxford: Pergamon Press. 499-474 (1985).

Evans, P.D. and B. Maqueira. Insect octopamine receptors: a new classification scheme based on studies of clone *Drosophila* G-protein coupled receptors. *Invert. Neurosci.* 5: 111-118 (2005).

Evans, P.D. and C.M. Myers. Peptidergic and aminergic modulation of insect skeletal muscle. *J. Exp. Biol*. 124: 143-176 (1986).

Feder, M.E. and G.E. Hofmann. Heat-shock proteins, molecular chaperones and the stress response: evolutionary and ecological physiology. *Annu. Rev. Physiol.* 61: 243-282 (1999).

Gorji, A. Scheller, D. Straub, H. Tegtmeier, F. Köhling, R. Höhling, J.-M. Tuxhorn, I. Ebner, A. Wolf, P. Panneck, H.W. Oppel, F. Speckmann, E.-J. Spreading depression in human neocortical slices. *Brain Res.* 906: 74-83 (2001).

Goosey, M.W. and D.J. Candy. The D-octopamine content of the haemolymph of the locust, *Schistocerca Americana gregaria* and its elevation during flight. *Insect. Biochem.* 10: 393-397 (1980).

Guedes, R.C.A. Tsurudome, K. and N. Matsumoto. Spreading depression in vivo potentiates electrically-driven responses in frog optic tectum. *Brain Res.* 1036: 109-114 (2005).

Gunn, D.L. Perry, F.C. Symour, W.G. Telford, T.M. Wright, E.N. and D. Yeo. Behaviour of the desert locust (*Schistocerca gregaria* Forskål) in Kenya in relation to aircraft spraying. *Anti-Locust Bulletin* 3: 1-70 (1948).

Grafstein, B. Mechanism of spreading cortical depression. *J. Neurophysiol.* 19: 154-171 (1956).

Hadjikhani, N. Sanchez Del Rio, M. Wu, O. Schwartz, D. Bakker, D. Fischl, B.Kwong, K.K. Cutrer, F.M. Rosen, B.R. Tootell, R.B. Sorensen, A.G. and M.A. Moskowitz.

Mechanisms of migraine aura revealed by functional MRI in human visual cortex. *Proc. Natl. Acad. Sci.* 98: 4687-4692 (2001).

Hanke, W. and V.M. Fernandes de Lima. Central nervous tissue: and excitable medium. A study using the retinal spreading depression as a tool. *Phil. Trans. R. Soc. A* 366: 359-368 (2008).

Heinrich, B. and G.A. Bartholomew. An analysis of pre-flight warm-up in the sphinx moth, *Manduca Sexta*. *J. Exp. Biol.* 85:61-87 (1971).

Hofmann, F. Feil, R. Kleppisch, T. and J. Schlossmann. Function of cGMP-dependent protein kinases as revealed by gene deletion. *Physiol. Rev.* 86:1-23 (2006).

Hoyle, G. High blood potassium in insects in relation to nerve conduction. *Nature* 169: 281-282 (1952).

Hoyle, G. Evidence that insect dorsal unpaired median (DUM) neurons are octopaminergic. *J. Exp. Zool.* 193: 425-431 (1975).

Hoyle, G. D. and D. Dagan. Physiology characteristics and reflex activation of DUM (octopaminergic) neurons of locust metathoracic ganglion. *J. Neurobiol.* 9: 59-79 (1979).

Hull, C.D. and A. Van Harreveld. Absence of conduction of spreading depression through cortical region damaged by asphyxiation. *Am. J. Physiol.* 207: 921-924 (1964).

Jiang, C. Agulian, S. and G.G. Haddad. Cl^- and Na^+ homeostasis during anoxia in rat hypoglossal neruons: intracellular and extracellular *in vitro* studies. *J. Physiol.* 448: 697-705 (1992).

Joshi, I. and R.D. Andrew. Imaging anoxic depolarization during ischemia-like conditions in the mouse hemi-brain slice. *J. Neurophysiol.* 84, 414-424 (2001).

Kelty, J.D. Noseworthy, P.A. Feder, M.E. Robertson, R.M. and J.-M. Ramirez. Thermal preconditioning and heat-shock protein 72 preserve synaptic transmission during thermal stress. *J. Neurosci*. RC193:1-6 (2002).

Kiang, J.G. and G.C. Tsokos. Heat shock protein 70 KDa: molecular biology, biochemistry and physiology. *Pharmac. Ther*. 80: 183-201 (1998).

Klose, M. Armstrong, G. and R.M. Robertson. A role for the cytoskeleton in heat shock-mediated thermoprotection of locust neuromuscular junctions. *J. Neurobiol.* 60: 453-462 (2004).

Leitch, B., Judge, S. and R.M. Pitman. Octopaminergic modulation of synaptic Transmission between an identified sensory afferent and flight motoneuron in the locust. *J. Comp. Neurol.* 462: 55-70 (2003).

Lauritzen, M. Rice, M.E. Okada, and Y. Nicholson, C. Quisqualate, kainate and NMDA can inittiate spreading depression in the turtle cerebellum. *Brain Res.* 475: 317-327 (1988).

Leão, AAP. Spreading Depression of activity in the cerebral cortex. *J. Neurophysiol*. 7: 359-390 (1944).

Leão, AAP and R.S. Morrison. Propagation of spreading cortical depression. *J. Neurophysiol* 8: 33-45 (1945).

Lighton, J.R.B. Discontinuous ventilation in terrestrial insects. *Physiol. Zool.* 67:142-162 (1994).

Malamud, J.G. Miszin, A.P. and R.K. Josephson. The effects of octopamine on contraction kinetics and power output of the locust flight muscle. *J. Comp. Physiol.* 165: 827-835 (1988).

Mentel, T., Duch, C., Stypa, H., Wegener, G., Műller, U. and H.-J. Pflűger. Central modulatory neurons control fuel selection in flight muscle of migratory locust. *J. Neurosci.* 23: 1109-1113 (2003).

Moncada, S. Palmer, R.M. and E.A. Higgs. Nitric oxide: physiology, pathophysiology, and pharmacology. *Pharmacol. Rev.* 43: 109-142 (1991).

Money, T.G.A. Anstey, M.L. and R.M. Robertson. Heat stress-mediated plasticity in a locust looming-sensitive visual interneuron. *J. Neurophysiol*. 93: 1908-1919 (2005).

Money, T.G.A. De Carlo, C.A. and R.M. Robertson. Temperature-sensitive gating in a descending visual interneuron, DCMD. *J. Comp. Physiol.* A 192: 915-925 (2006).

Muller, U. The nitric oxide system in insects. *Prog. Neurobiol.* 51: 363-381 (1997).

Muller, U. and H. Hildebrandt. The nitric oxide cGMP system in the antennal lobe of *Apis mellifera* is implicated in integrative processing of chemosensory stimuli. *Eur. J. Neurosci.* 7: 2240-2248 (1995).

Müller, M. and K. Ballanyi. Dynamic recording of cell death in the in vitro dorsal vagal nucleus of rats in response to metabolic arrest. *J. Neurophysiol.* 89: 551-561 (2003).

Müller, M. and G.G. Somjen. Na^+ and K^+ concentrations, extra- and intracellular voltages, and the effect of TTX in hypoxic rat hippocampal slices. *J. Neurophysiol.* 83: 735-745 (2000).

Müller, M. and G.G. Somjen. Intrinsic optical singals in rat hippocampal slices during hypoxia-indueced spreading depression-like depolarization. *J. Neurophysiol.* 82: 1818-1831 (2001).

Nathanson, J.A. Octopamine receptors, adenosine 3'-,5'-monophosphate and neural control of firefly flashing. *Science* 203: 56-68 (1979).

Nicholson, C. Ten Bruggencate, G. Stöckle, H. and R. Steinberg. Calcium and potassium changes in extracellular microenvironement of cat cerebellar cortex. *J. Neurophysiol.* 41: 1026-1039 (1978).

Newland, P.L. and P. Yates. Nitrergic modulation of an oviposition digging rhythm in locusts. *J. Exp. Biol*. 210: 4448-4456 (2007).

Newman A.E.M. Foerster, M. Shoemaker, K.L. and R.M. Robertson. Stress-induced thermotolerance of ventilatory motor pattern generation in the locust, *Locusta migratoria*. *J. Insect Physiol.* 49: 1039-1047 (2003).

Obeidat, A.S. and R.D. Andrew. Spreading depression determines acute cellular damage in the hippocampal slice during oxygen/glucose deprivation. *Euro. J. Neurosci.* 10 3451-3461 (1998).

Obeidat, A.S. Jarvis, C.R. and R.D. Andrew. Glutamate does not mediate acute neuronal damage after spreading depression induced by O_2/glucose deprivation in the hippocampal slice. *J. Cereb. Blood Flow Metab.* 20: 412-422 (2000).

Orchard, I. Carlisle, J.A. Loughton, B.C. Gole, J.W.D. and R.G.H. Downer. In vitro studies on the effects of octopamine on locust fat body. *Gen. Comp. Endocrinol.* 48: 7-13 (1982).

Osborne, K.A. Robichon, A. Burgess, E. Butland, S. Shaw, R.A. Coulthard, A. Pereira, H.S. Greenspan, R.J. and M.B. Sokolowski. Natural behavior polymorphism due to a cGMP-dependent protein kinase of *Drosophila*. *Science* 277: 834- 836 (1997).

O'Shea, M. and P.D. Evans. Potentiation of neuromuscular transmission by octopaminergic neuron in the locust. *J. Exp. Biol.* 79: 169-190 (1979).

Ott, and S.R. and M. Burrows. Nitric oxide synthase in the thoracic ganglia of the locust: distribution in the neuropiles and morphology of neurones. *J. Comp. Neurol.* 395: 217-230 (1998).

Ott, and S.R. and M. Burrows. NADPH diaphorase histochemistry in the thoracic ganglia of locusts, crickets and cockroaches: species differences and the impact of fixation. *J. Comp. Neurol.* 410: 387-397 (1999).

Parsell, D.A. and S. Lindquist. The function of heat-shock proteins in stress tolerance: degradation and reactivation of damaged proteins. *Annu. Rev. Genet.* 27: 437-496 (1993).

Petzold, G.C. Haack, S. Halback, O.V.B.U. Priller, J. Lehmann, T.-N. Heinemann, U. Dirnagl, U. and J.P. Dreier. Nitric oxide modulates spreading depolarization threshold in the human and rodent cortex. *Stroke* 39: 1292-1299 (2008).

Prange, H.D. Temperature regulation by respiratory evaporation in grasshoppers. *J. Exp. Biol.* 154: 463-474 (1990).

Ramirez, J.M. Elsen, F.P. and R.M. Robertson. Long-term effects of prior heat shock on neuronal potassium currents recorded in a novel insect ganglion slice preparation. *J. Neurophysiol.* 81: 795-802 (1999).

Ramirez, J.M. and K.G. Pearson. Distribution of intersegmental interneurons that can reset the respiratory rhythm of the locusts. *J. Exp. Biol.* 141: 151-176. (1989a).

Ramirez, J.M. and K.G. Pearson. Alteration of the respiratory system at the onset of locust flight. I. Abdominal pumping. *J. Exp. Biol.* 142: 401-424 (1989b).

Ramirez, J.M. and K.G. Pearson. Octopaminergic modulation if interneurons in the flight system of the locust. *J. Neurophysiol.* 66: 1522- 1537 (1991).

Rast, G.F. Nitric oxide induces centrally generated motor patterns in the locust suboesophageal ganglion. *J. Exp. Biol.* 204: 3789-3801 (2001).

Read, S.J. Smith, M.I. Hunter, A.J. and A.A. Parsons. The dynamics of nitric oxide release measured directly and in real time following repeated waves of cortical spreading depression in the anaesthetized cat. *Neurosci. Lett.* 232: 127-130 (1999).

Renger, J.J. Yoa, W.D. Sokolowski, M.B. and C.F. Wu. Neuronal polymorphism among natural alleles of a cGMP-dependent kinase gene, *foraging*, in *Drosophila*. *J. Neurosci.* 19: RC28 (1999).

Robertson, R.M. Thermal stress and neural function: adaptive mechanisms in insect model systems. *J. Therm. Biol.* 29: 351-358 (2004).

Robertson, R.M. Kuhnert, C.T. and J.W. Dawson. Thermal avoidance during flight in the locust *Locusta migratoria*. *J. Exp. Biol.* 199: 1383- 1393 (1996).

Robertson, R.M. and Pearson, K.G. A preparation for the intracellular analysis of neuronal activity during flight in the locust. *J. Comp. Physiol.* 146: 311-320 (1982).

Robertson, R.M. Xu, H. Shoemaker, K.L. and K. Dawson-Scully. Exposure to heat shock affects thermosensitivity of the locust flight system. *J. Neurobiol.* 29: 367-383 (1996).

Rodgers, C.I. Armstrong, G.A.B. Shoemaker, K.L. LaBrie, J.D. Moyes, C.D. and R.M. Robertson. Stress preconditioning of spreading depression in the locust CNS. *PLoS ONE* 2:e1366 (2007).

Rodgers, C.I. Shoemaker, K.L. and R.M. Robertson. Photoperiod-induced plasticity of thermosensitivity and acquired thermotolerance in *Locusta migratoria*. *J. Exp. Biol.* 209: 4690-4700 (2006).

Roeder, T. A new octopamine receptor class in locust nervous tissue, the octopamine 3 (OA_3) receptor. *Life Sci.* 50, 21-28 (1992).

Roeder, T. Octopamine in invertebrates. *Prog. Neurobiol.* 59: 533-561 (1999).

Roeder, T. Tyramine and octopamine: ruling behavior and metabolism. *Annu. Rev. Entomol.* 50: 447-477 (2005).

Roeder, T. and M. Gewecke. Octopamine receptors in locust nervous tissue. *Biochem. Pharmac.* 39: 1793-1797 (1990).

Rounds, H.D. KCl-induced 'spreading depression' in the cockroach. *J. Insect Physiol.* 13: 869-872 (1966).

Sharp, F.R. Massa, S.M. and R.A. Swanson. Heat-shock protein protection. *Trends Neurosci.* 22: 97-99 (1999).

Smit, C.J.B. The behaviour of the brown locust in its solitary phase. *Tech. Commun. Dep. Agric. Tech. Serv. Pretoria.* 1:1-132 (1960).

Smith, J.M. Bradley, D.P. and M.F. James. Huang CL Physiological studies of cortical spreading depression. *Biol. Rev. Camb. Philos. Soc.* 81: 457-481 (2006).

Snow, R.W. Taylor, C.P. and F.E. Dudek. Electrophysiological and optical changes in slices of rat hippocampus during spreading depression. *J. Neurophysiol.* 50: 561-572 (1983).

Sombati, S. and G. Hoyle. Generation of specific behaviors in a locust by local release into neuropil of the natural neuromodulator octopamine. *J. Neurobiol.* 15: 481-506 (1984).

Somjen, G.G. Mechanisms of spreading depression and hypoxic spreading depression-like depolarization. *Physiol. Rev.* 81: 1065-1096 (2001).

Stevenson, P.A. and U. Spörhase-Eichmann. Localisation of octopaminergic neurons in insects. *Comp. Biochem. Physiol. B* 110: 203-215 (1995).

Stevenson, P.A. and W. Kutsch. Basic circuitry of an adult-specific motor program completed with embryogenesis. *Naturwissenschaften* 73: 741-743 (1986).

Streit, D.S. Ferreira F^{o}, C.R. and H. Martins-Ferreira. Spreading depression in isolated spinal cord. *J. Neurophysiol.* 74: 888-890 (1995).

Takano, T. Tian G.-F. Peng, W. Lou, N. Lovatt, D. Hansen, A.J. Kasischke, K.A. and M. Nedergaard. Cortical spreading depression causes and coincides with tissue hypoxia. *Nature Neurosci.* 10: 754-762 (2007).

Urenjak, J. and T.P. Obrenovitch. Pharmacological investigation into the involvement of nitric oxide in K^+-induced cortical spreading depression. *Naunyn Schmiedebergs Arch. Pharmacol.* 362: 137-144 (2000).

Uvarov, B. Grasshoppers and Locusts: A Handbook of General Acridology. Vol 2 University Press, Cambridge.

Van Cuong, D. Kim, N. Youm, J.B. Joo, H. Warda, M. Lee, J.-W. Park, W.S. Kim, T. Kang, S. Kim, H. and J. Han. Nitric oxide-cGMP-protein kinaseG signaling pathway induces anoxic preconditioning through activation of ATP-sensitive K^+ channels in rat hearts. *Am. J. Physiol. Heart Circ. Physiol.* 290: H1808-H1817 (2006).

Van Harreveld, A. and F.I. Khattab. Changes in cortical extracellular space during spreading depression investigated with the electron microscope. *J. Neurophysiol.* 30: 911-927 (1967).

Van Harreveld, A. Stamm, J.S. Christensen, E. Spreading depression in rabbit, cat and monkey. *Am. J. Physiol.* 184: 312-320 (1956).

Van Harreveld, A. Terres, G. and E.A. Dernburg. Cortical discontinuity and propagation of spreading depression. *Am. J. Physiol.* 184: 233-238 (1956).

Volkonsky, M.A. Sur la photo-akinèse des acridiens. *Archs Inst. Pasteur Algér.* 17:194-220 (1939).

Vyskočil, F. Kříž, N. and J. Bureš. Potassium-selective microelectrodes used for measuring the extracellular brain potassium during spreading and anoxic depolarization in rats. *Brain Res.* 39: 255-259 (1972).

Waloff, Z. Field studies on solitary and *transiens* desert locusts in the Red sea area. *Anti-Locust Bull* 40: 1-93 (1963).

Waloff, Z. and R.C. Rainey. Field studies on factors affecting the displacements of desert locust swarms in eastern Africa. *Anti-Locust Bull* 9: 1-50 (1953).

Watson, A.H.D. The dorsal unpaired median neurons of the locust metathoracic ganglion: neuronal structure and diversity, and synaptic integration. *J. Neurocytol.* 13: 303-327 (1984).

White, R.E. Han, G. Maunz, M. Dimitropoulou, C. El-Mowafy, A.M. Barlow, R.S. Catravas, J.D. Snead, C. Carrier, G.O. Zhu, S. and X. Yu. Endothelium-independent effect of estrogen on Ca^{2+}- activated K^{+} channels in human coronary artery smooth muscle cells. *Cardiovasc. Res.* 53: 650-661 (2002).

Whyard, S., Wyatt, G.R., and V.K. Walker. The heat shock response in *Locusta migratoria*. *J. Comp. Physiol. B.* 156: 813-817 (1986).

Wehner, R. Marsh, A.C. and S. Wehner. Desert ant on a thermal tightrope. *Nature* 357:586-587, (1992).

Wingrove, J.A. and P.H. O'Ferrell. Nitric oxide contributes to behavioral, cellular, and developmental responses to love oxygen in *Drosophila*. *Cell* 98: 105-114 (1999).

Wu, B.S. Lee, J.K. Thompson, K.M. Walker, V.K. Moyes, C.D. and R.M. Robertson. Anoxia induces thermotolerance in the locust flight system. *J. Exp. Biol.* 205: 815-827 (2002).

Wu, B.S. Walker, V.K. and R.M. Robertson. Heat shock-induced thermoprotection of action potentials in the locust flight system. *J. Neurobiol.* 49: 188-199 (2001).

Wu, J. and R.S. Fisher. Hyperthermic spreading depression in the immature rat hippocampal slice. *J. Neurophysiol*. 84: 1355-1360 (2000).

Xiao, C. Mileva-Seitz, V. Seroude, L. and R.M. Robertson. Targeting HSP70 to motoneurons protects locomotor activity from hyperthermia in *Drosophila*. *Develop. Neurobiol.* 67:438-455, (2007).

Zilberstein, Y. Fuchs, E. Hershtik, L. and A. Ayali. Neuromodulation for behavior in the locust frontal ganglion. *J. Comp. Physiol. A.* 190: 301-309 (2004).

Zhou, X.B. Schlossmann, J. Hofmann, F. Ruth, P. and M. Korth. Protein phosphatase 2A is essential for the activation of Ca^{2+}-activated K^{+} currents by cGMP-dependent protein kinase in tracheal smooth muscle and Chinese hamster ovary cells. *J. Biol. Chem.* 271: 19760-19767 (1996).

Chapter 2

Octopamine mediates thermal preconditioning of the locust ventilatory central pattern generator via a cAMP/protein kinase A signalling.

Gary A.B. Armstrong*, Kelly L. Shoemaker, Tomas G.A. Money and R. Meldrum Robertson.

Department of Biology, Queen's University, Kingston, Ont., Canada K7L 3N6.

* To whom correspondence should be sent: G.A.B. Armstrong, Department of Biology, Queen's University, Biosciences Complex, Kingston, Ontario, Canada K7L 3N6. Email (armstrog@biology.queensu.ca).

Citation: The Journal of Neuroscience 26:12118-12126 (2006).

2.1 Abstract

We investigated the role of biogenic amines in generating thermoprotection of the ventilatory motor pattern circuitry in *Locusta migratoria*. Levels of octopamine (OA) and dopamine (DA) in the metathoracic ganglion decreased during heat stress. We measured the thermosensitivity of central pattern generation in response to a ramped increase of temperature in semi-intact preparations. OA, DA, and tyramine (TA) were either bath applied or injected into the locust haemocoel 4-8 hours before testing. Neither TA nor DA modified the thermotolerance of ventilatory motor pattern generation. However, OA treatment by bath applications (10^{-4}M OA) or by injections into the haemocoel (2μg/10μl OA) mimicked heat shock preconditioning and improved the thermotolerance of the motor pattern by increasing the failure temperature and by decreasing the time taken to recover operation after a return to room temperature. Heat shock-induced thermoprotection was eradicated in locusts pre-injected with epinastine (OctβR antagonist). Neuropil injections of the cAMP agonist and PKA activator, Sp-cAMPs, both conferred thermoprotection in control locusts and rescued thermoprotection in epinastine-treated HS locusts. Similar injections of the PKA inhibitor Rp-cAMPs blocked the thermoprotective effect of bath-applied OA. Octopamine-mediated thermoprotection was also abolished with neuropil injections of cycloheximide or actinomycin D indicating a requirement for transcription and translation. We conclude that OA has a crucial role in triggering protein synthesis-dependent physiological adaptations to protect CNS function during heat stress by activating a cAMP/PKA pathway.

2.2 Introduction

Impaired CNS function during hyperthermia can have severe fitness consequences and animals have evolved several mechanisms to cope with heat stress. Unlike homeotherms, which can physiologically regulate body temperature during ambient temperature fluctuation, poikilotherms such as the locust (*Locusta migratoria*) must endure more extreme internal temperature changes. These animals are thus well suited for the investigation of physiological adaptations that have evolved to protect nervous systems from heat stress. Preconditioning locusts with a high (45°C) and prolonged (3hr) exposure to heat followed by a 1 hour recovery (heat shock treatment, HS) induces thermotolerance in particular tissues including the CNS (Robertson et al., 1996).

Abdominal ventilatory movements in locusts are controlled by a central pattern generator (CPG) located in the metathoracic ganglion (MTG; e.g. Bustami and Hustert, 2000). Cycle frequency increases with increasing temperature from about 1 Hz at room temperature to 2.5-3.0 Hz at 45°C. Motor pattern generation fails at high temperatures (Newman et al., 2003). Thermotolerance of the circuit can be improved by stress preconditioning using heat shock, anoxia or cold shock, and is mimicked by bath application of serotonin (Newman et al., 2003). At the moment of heat-induced rhythm failure there is an abrupt rise in extracellular potassium $[K^+]_o$ in the MTG from ~11mM to > 40mM; recovery of the rhythm is reliably associated with time-dependent restoration of the $[K^+]_o$ gradient with HS locusts showing more rapid recovery (Robertson, 2004).

The mechanisms that coordinate such HS-mediated thermotolerance are unknown and a possibility we examine here is that amines such as octopamine (OA) are involved.

Octopamine is an important invertebrate neurotransmitter (Nathanson, 1979), neuromodulator (Lange and Orchard, 1986) and neurohormone (Orchard 1982), generating an arousal response in invertebrates (Kravitz and Huber, 2003) similar to norepinephrine in vertebrates (Roeder 1999, 2005). In the insect CNS, OA is one of the most abundant amines, having a concentration much higher than tyramine (TA) and at least 2-3 times greater than dopamine (DA) (Evans, 1985). High concentrations of OA (170nM) have been reported in *L. migratoria* haemolymph (Orchard et al. 1981), along with similar concentrations (49nM) found in *Schistocerca americana gregaria* (Davenport and Evans, 1984). OA is known to modulate many motor patterns including foregut activity (Zilberstein et al. 2004), walking and flying (Sombati and Hoyle 1984) and ventilation (Bellah et al. 1984; Ramirez and Pearson, 1989). Levels of OA in locust haemolymph have been observed to increase after various stresses (e.g., heat, cold, mechanical and chemical stress) and in some instances as much as a 10-fold increase from original levels has been observed (Davenport and Evans 1984). In the insect CNS, β-adrenergic-like octopamine receptors (OctβRs) are coupled *via* G-proteins to adenylyl cyclase, giving rise to an increase in cAMP that results in modulation of motor patterns (Sombati and Hoyle, 1984; Bellah et al. 1984). Here we show that OA mediates HS-induced thermoprotective changes *via* a cAMP/PKA signalling pathway and protein synthesis.

2.3 Materials and Methods

Animals

Adult male locusts, *Locusta migratoria*, 4-6 weeks post-imaginal moult, were collected from a crowded colony maintained in the Biology Department at Queen's University. Animals were housed under a 12h:12h (light: dark) cycle. Light-time and dark-time cage temperatures were 25 ± 1°C and 21 ± 1°C respectively, and humidity was constant at 23 ± 1%. All animals were collected from the colony at the same time each morning, weighed and placed in a well ventilated 2L polyethylene container. Only animals that weighed 1.75 ± 0.25g were used for experimentation. All electrophysiological recordings were taken 4-8 hours after locusts were collected from the colony.

Heat Shock

Locusts designated for control (Con) and heat shock (HS) treatments were separated into different containers. HS animals were placed in a humid incubator for 3 hours at 45°C followed by a 1-5 hours recovery at room temperature (~21°C); Con animals were held at room temperature for 4-8 hours.

High Performance Liquid Chromatography (HPLC)

For both OA and DA assays animals were 3-5 weeks postimaginal moult at the time of treatment and dissection. Ganglia were collected at different times during HS treatment, ranging from 5 to 60 minutes after entering the incubator. Immediately following removal from the incubator the wings, legs and pronotum were removed from the animal,

and a dorsal midline incision was made. The gut and overlying tissues were dissected out and the MTG was quickly removed by cutting the connectives midway between the MTG and the abdominal ganglion (A4), and midway between the MTG and mesothoracic ganglion. All other nerve roots arising from the MTG were cut distally to prevent loss of ganglionic contents. The MTG was rinsed with cold standard locust saline, blotted dry on a clean lint-free wipe, and submerged in 100 µL of ice-cold 0.2 N perchloric acid (Sigma-Aldrich, Canada). Each dissection took approximately 5 minutes to complete.

Samples were sonicated individually for five to ten seconds using a probe sonicator (VirSonic 60, Virtis, Gardiner NY). Homogenized samples were then centrifuged at 15,000 rpm for 30 minutes at 4ºC. The supernatant was collected and frozen at -80ºC for no longer than one week. To prepare for HPLC, samples were thawed, and mixed with 100 µL mobile phase and were processed through a 0.22 µm centrifugal filter unit (Millipore, Canada) at 15,000 rpm for 11 minutes at 4ºC. Mobile phase consisted of 9% acetonitrile, 15% methanol, 5 mM citric acid, 75 mM sodium phosphate monobasic, and 2.1 mM sodium dodecyl sulfate, all dissolved in HPLC-grade water. pH was adjusted from 6.05 to 6.75 using concentrated sodium hydroxide.

Samples were manually injected onto an Inertsil C18 column (150A/OD52, 15 x 0.46 cm, 5 µm, CSC Chromatography Sciences, Montreal), and were detected electrochemically on a single-channel amperometric detector (Intro, VT-03 electrochemical flowcell, Antec Leyden) set at 0.75 V for both amines. Temperature was constant at 30ºC. Mobile phase

was first filtered and degassed through a 0.22 μM filter (Pall), and was pumped isocratically at 0.8 mL/min (Shimadzu LC-10ADVP pump). The putative peak of interest was initially identified on the basis of retention time in comparison to a known standard, and was further confirmed on the basis of changes in peak size and/or retention time in response to 1) changes in applied channel voltage; 2) percentage organics; and 3) pH. Integration of peaks was performed using a Shimadzu C-R5A Chromatopac Integrator, and calibration of peak size was conducted by injecting standards of known concentration. Fresh standards were run daily.

Semi-intact Preparation

A semi-intact preparation (Robertson and Pearson, 1982) was used to access the nervous system for electrophysiology. A dorsal midline incision was made from the 5th abdominal segment to the head. Animals were pinned ventral-side down and gut and overlying tissues were removed exposing the ventral nerve cord. Nerve 5 of the MTG was cut on both sides allowing saline and pharmacological agents to permeate the ganglion. A peristaltic pump (Peri-Star, World Precision Instruments, Sarasota, FL) superfused the thoracic and abdominal cavities with standard locust saline (147mM NaCl, 10mM KCl, 4mM $CaCl_2$, 3mM NaOH, 10mM HEPES buffer (pH=7.2)). Saline flow originated at the head-thorax junction and exited through an incision in the abdominal wall. Flow rate was constant at 5mL/min.

Electromyographic recording of the motor pattern

Motor patterns were recorded using an electromyographic (EMG) electrode made from 0.1mm diameter copper wire, insulated except at the tip, and positioned on the abdominal expiratory muscle 161 (Newman et al. 2003). Signals were amplified using a Model P15 Preamplifier (Grass Instruments, West Warwick, RI) and digitized using a Digidata 1200 (Axon Instruments Inc., Union City, CA). Data were analyzed using ClampFit 9.0 (Axon Instruments Inc., Union City, CA). Preparations were bathed for 1 hour with saline before starting the temperature ramp, allowing for any pharmacological treatments to have an effect and for the ventilatory rhythm to stabilize. Saline temperature was controlled by passing current through a Nichrome wire wrapped around an insulated glass pipette. Temperature was monitored using a thermocouple (BAT-12; Physitemp Instruments, Clifton, NJ) placed next to the MTG. Temperature was ramped up 5°C/minute starting at room temperature (~21°C) until failure of the motor pattern. At this time the heater was switched off permitting the saline temperature to return to ambient levels and allowing the motor pattern to recover.

Failure temperature (°C) and recovery time (s) were scored as the temperature at which all electrical activity from the muscle ceased and the length of time taken to recover motor pattern function. We also monitored the percentage of preparations that exhibited arrhythmias. We defined an arrhythmia as a ventilatory cycle with a burst duration 2 times longer than that of the preceding burst duration and a pause in the ventilatory rhythm for at least double the period of the preceding cycle. We also measured cycle frequency (Hz), burst duration (ms) and duty cycle (duration/period) of the motor pattern

during temperature ramps. Duty cycle was calculated by measuring the proportion of burst duration over the period of the rhythm. Data were plotted using SigmaPlot 8.0 (SPSS Inc., Chicago, IL).

Intracellular Recording

Intracellular recordings of ventilatory interneurons were made using sharp microelectrodes (1 M KAc, 40-60 MΩ) and amplified using a Model 1600 Neuroprobe Amplifier (A-M Systems Inc., Carlsborg, WA). Neurons were identified based on their phase relation to the EMG signal as either inspiratory (n=3) or expiratory (n=10). Of all impalements, 7 were successfully recorded throughout the temperature ramp until failure.

Pharmacology

Prior to testing the effects of temperature, OA and the OctβR antagonist epinastine (EP) were bath-applied in semi-intact preparations and the cycle frequency (Hz) of the ventilatory motor pattern was monitored. Drugs were dissolved in standard locust saline and superfused over the MTG for 20 min. OA-treated animals received 10^{-5}M, 10^{-4}M, and 10^{-3}M; whereas EP-treated locusts received bath applications of 10^{-6}M. Motor pattern changes were also monitored following an extended exposure (1hr) of 10^{-4}M of OA, DA, and tyramine (TA).

To examine if OA and other amines could generate thermotolerance in the CNS, short bath applications were applied to HS and Con locusts before the temperature ramp.

Concentrations of either 10^{-4}M or 10^{-3}M of OA were applied 20 minutes before thermotolerance testing. In a second set of experiments extended 1-hour treatments with 10^{-4}M of OA or TA were bath applied. Neurohormonal effects of OA and DA were investigated by injecting 2µg/10µl of OA, DA or EP into the haemocoel of intact locusts. Animals in the untreated comparison groups (HS and Con) received sham injections of standard locust saline. Locusts receiving injections of amines were superfused with standard locust saline for 1 hour in the semi-intact preparation and individuals receiving the 1 hour bath application of amines were given sham injections of saline prior to dissection. Injections were given 4-8 hours before testing thermotolerance.

We pharmacologically manipulated cAMP levels in the MTG by treating locusts with a 1 hour bath application of 10^{-5}M Forskolin (FOR), a potent activator of adenylyl cyclase. FOR was dissolved in 10µL of DMSO before dilution in standard locust saline. Sham injections also contained 10µL of DMSO.

To locally modulate activity of PKA we pressure-injected using a PicoSpritzer III (INTRACEL Inc., Shepreth, UK) small volumes (70nL) of either 10^{-4}M Sp-adenosine 3',5'-cyclic monophosphorothioate triethylammonium salt (Sp-cAMPs), an analog of cAMP and activator of PKA, or 10^{-4}M Rp-adenosine 3',5'-cyclic monophosphorothioate triethylammonium salt (Rp-cAMPs), a deactivator of PKA. Drugs were injected into the ventilatory neuropil every 5 or 10 minutes over 50 minutes. Ten minutes following the last injection we tested thermotolerance. Both Sp-cAMPs and Rp-cAMPs were first

dissolved in 10µL of DMSO, before dilution in standard locust saline. Sham injections of locust saline contained 10µL of DMSO.

To test if elements of the octopaminergic signalling pathway were interacting with the genome to confer thermoprotection, we arrested transcription and translation with 10^{-6}M actinomycin D (ACTD) and 10^{-6}M cycloheximide (CHX) respectively during a 1 hour bath application of 10^{-4}M OA (a treatment previously shown to induce thermotolerance). ACTD and CHX (70nL) were injected into the neuropil every 10 minutes (5 times over 50 minutes). 10 minutes following the final injection, we tested thermotolerance. ACTD and CHX were both dissolved in 10µL of ethanol before further dilution in standard locust saline. Sham injections of standard locust saline contained the same concentration of ethanol.

Potassium clearance

To test the ability to regulate $[K^+]_o$ we pressure-injected small volumes (150nL) of locust saline containing elevated levels of K^+ (147mM NaCl, 150mM KCl, 4mM $CaCl_2$, 3mM NaOH, 10mM HEPES buffer (pH=7.2)) into the ventilatory neuropil to arrest rhythm generation. We measured the length of time required to restore rhythm generation in Con, OA (1hr bath application 10^{-4}M), HS and EP-injected HS locusts.

Drugs

Chemicals were obtained from Sigma-Aldrich (Oakville, Canada). The OctβR antagonist EP was a generous gift of Boehringer Ingelheim Pharma GmbH & Co. KG (Biberach, Germany).

Statistical analyses

For HPLC

Animals were always run as matched pairs. That is, Con and HS animals were always dissected and processed by HPLC-ED together. All samples were ultimately calculated as "picograms per ganglion" using standard curves generated by injecting standards of known quantity. The samples were normalized to the Con of the pair. The graph of HPLC shows the Con value as 1 with no variability, while HS samples are described using the median and quartiles. Nonparametric statistics were applied as appropriate.

For Thermotolerance

Statistically significant differences between treatments were assessed by performing one-way or two-way repeated measures ANOVA (RM-ANOVA) followed by a multiple comparison (Tukey) test. Treatment groups tested for thermotolerance 4 to 8 hours after injections into the haemocoel were first grouped into one hour intervals (4, 5, 6, 7, and 8 hrs). A Pearson correlation test showed no significant differences between these groups and the data were pooled into one large group (4-8hrs). All data are reported as mean ± standard error. Data were analyzed using SigmaStat 3.1.1 (SPSS Inc. Chicago, IL).

2.4 Results

Heat shock depletes octopamine and dopamine in the metathoracic ganglion.

Octopamine and dopamine were resolved as well-defined peaks in HPLC chromatograms (Fig 2.1 A) with control levels of around 1.5 µg OA and 500 ng DA per MTG. We found a modest but significant decrease (Mann-Whitney, u = 245, n =15, $p = 0.056$) in the relative quantity of OA from 100 % to 90% after 15 minutes of heat shock (Fig 2.1 B). Levels returned to pre-HS values by 30 minutes. We also found a modest but significant decrease (Mann-Whitney, u = 245, n =14, $p = 0.056$) in the relative quantity of DA from 100 % to 92 % after 15 minutes of HS. Levels returned to 100 % by 30 minutes.

Octopamine, but not dopamine or tyramine, acutely increases ventilatory rhythm frequency.

To examine the excitatory neuromodulatory effects of OA on the ventilatory rhythm, various concentrations were superfused over the MTG. OA treatment did not disrupt rhythm generation (e.g. no arrhythmias or discontinuous ventilation, after 20 and 60 minutes). Exposure to 10^{-4} M OA and 10^{-3} M OA for 20 minutes significantly accelerated the rhythm (one-way RM-ANOVA, $F = 5.026$, df = 5, $p < 0.05$; Table 2.1). EP had no effect on rhythm generation (no arrhythmias or discontinuous ventilation) and had no effect on ventilatory rhythm frequency (Table 2.1). Following HS or 1 hr exposures to 10^{-4} M of OA, DA, TA, or 10^{-6} M EP there were no significant differences in ventilatory frequency (Table 2.1).

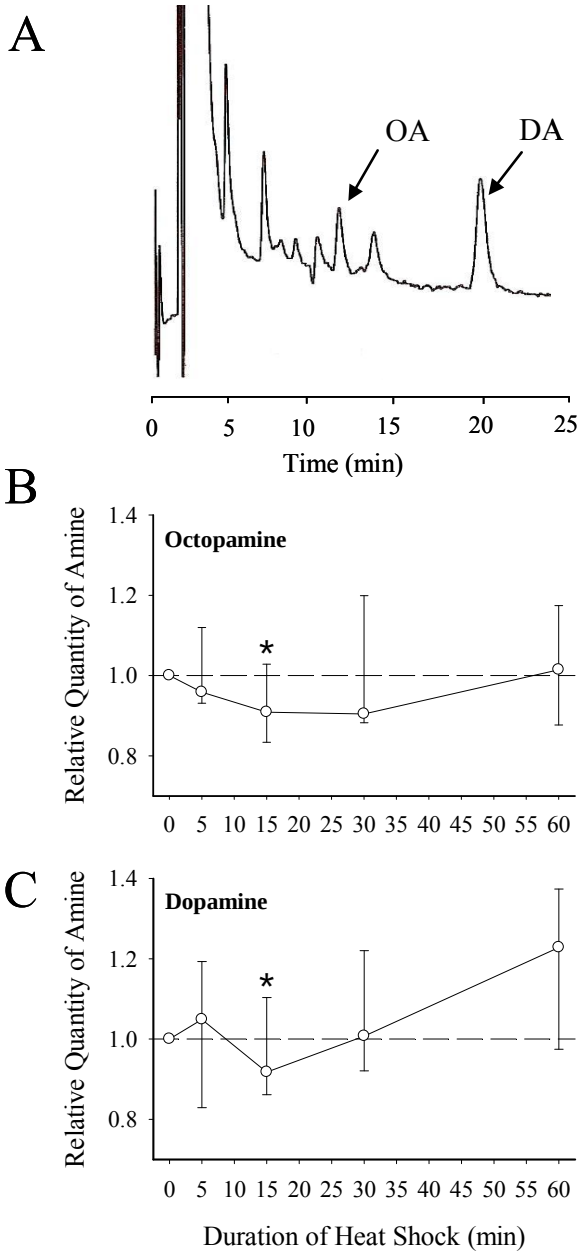
A
OA
DA
0 5 10 15 20 25
Time (min)
B
Octopamine
Relative Quantity of Amine
1.4
1.2
1.0
0.8
*
0 5 10 15 20 25 30 35 40 45 50 55 60
C
Dopamine
Relative Quantity of Amine
1.4
1.2
1.0
0.8
*
0 5 10 15 20 25 30 35 40 45 50 55 60
Duration of Heat Shock (min)

Figure 2.1

Figure 2.1. High performance liquid chromatography for octopamine and dopamine. A. Typical chromatogram of MTG tissue from a male locust, showing the octopamine peak at 11.27 minutes, and the dopamine peak at 19.89 minutes. See methods text for details of procedure. B. Relative levels of octopamine (OA) in the MTG different times after the start of heat shock (45°C). C. Relative levels of dopamine (DA) in the MTG different times after the start of heat shock. Note the significant transient decrease in ganglionic content of both amines after 15 minutes of HS. Levels recovered after 60 minutes. HS samples were run paired with Con samples allowing the HS level to be normalized to the Con in the pair. Data plotted as median and quartiles. The dashed line at 1 indicates no change relative to control and asterisks indicate significant difference from control. Sample sizes: OA, $n_{5\ min} = 8$, $n_{15\ min} = 14$, $n_{30\ min} = 7$, $n_{60\ min} = 9$. DA, $n_{5\ min} = 8$, $n_{15\ min} = 14$, $n_{30\ min} = 7$, $n_{60\ min} = 7$.

Table 2.1. Aminergic- and EP-induced changes in motor pattern frequency after various exposure lengths.

	Frequency (Hz)	
Treatment	20 min exposure	60 min exposure
Con	0.99 ± 0.05 (21)	0.96 ± 0.05 (21)
HS	1.07 ± 0.04 (17)	1.02 ± 0.06 (15)
DA 10^{-4}M	Not tested	0.85 ± 0.09 (10)
TA 10^{-4}M	Not tested	0.92 ± 0.08 (10)
OA 10^{-5}M	1.14 ± 0.08 (8)	Not tested
OA 10^{-4}M	1.21 ± 0.06 (8) *	1.09 ± 0.06 (13)
OA 10^{-3}M	1.28 ± 0.06 (8) *	Not tested
EP 10^{-6}M	0.89 ± 0.06 (10)	0.90 ± 0.05 (10)

Values are mean ± SE. (n)
Asterisk indicate significant differences from Con ($P < 0.05$).

HS and octopamine increase the upper thermal limit for pattern generation.

Ventilatory motor pattern frequency increased from about 1Hz to 3Hz as thoracic temperature was ramped from 20ºC to failure (~38-45ºC) (Fig 2.2A,B and Fig 2.3A). During the temperature ramp the duration of expiratory bursts recorded from muscle 161 decreased from 250-350ms to ≤ 100ms prior to pattern failure (Fig 2.2 A,C and Fig 2.3 B) whereas duty cycle did not change (Fig 2.2 A,D and Fig 2.3 C). Below the point of failure there were no significant differences in motor pattern frequency, expiratory burst duration or duty cycle between Con, HS, and OA injected animals as temperature was raised. However, the prevalence of arrhythmias at elevated temperatures was greater in Con and epinastine-injected HS locusts (EP-HS) (65% and 60%) and lower in HS and OA-injected animals (40% and 25%) suggesting a rhythm-stabilizing effect of OA and HS treatments at high temperatures (Fig 2.4 B). Also HS and OA preparations continued to operate at higher temperatures than Con preparations (Fig 2.2) as indicated by the extension of the temperature relationships into the 40-45°C bin (Fig 2.3).

To confirm that failure of pattern generation measured at the periphery was not a result of axonal conduction failure in the nerve roots, or the failure of neuromuscular transmission, we recorded intracellularly from pattern generating interneurons in the MTG during temperature ramps (Fig 2.5). Identification was made on the basis of membrane potential oscillation in phase with the ventilatory EMG, supporting high frequency bursts of action potentials, and an ability to modify the rhythm when stimulated (data not shown). For 7 of 7 such recordings central failure was exactly coincident with failure of the EMG

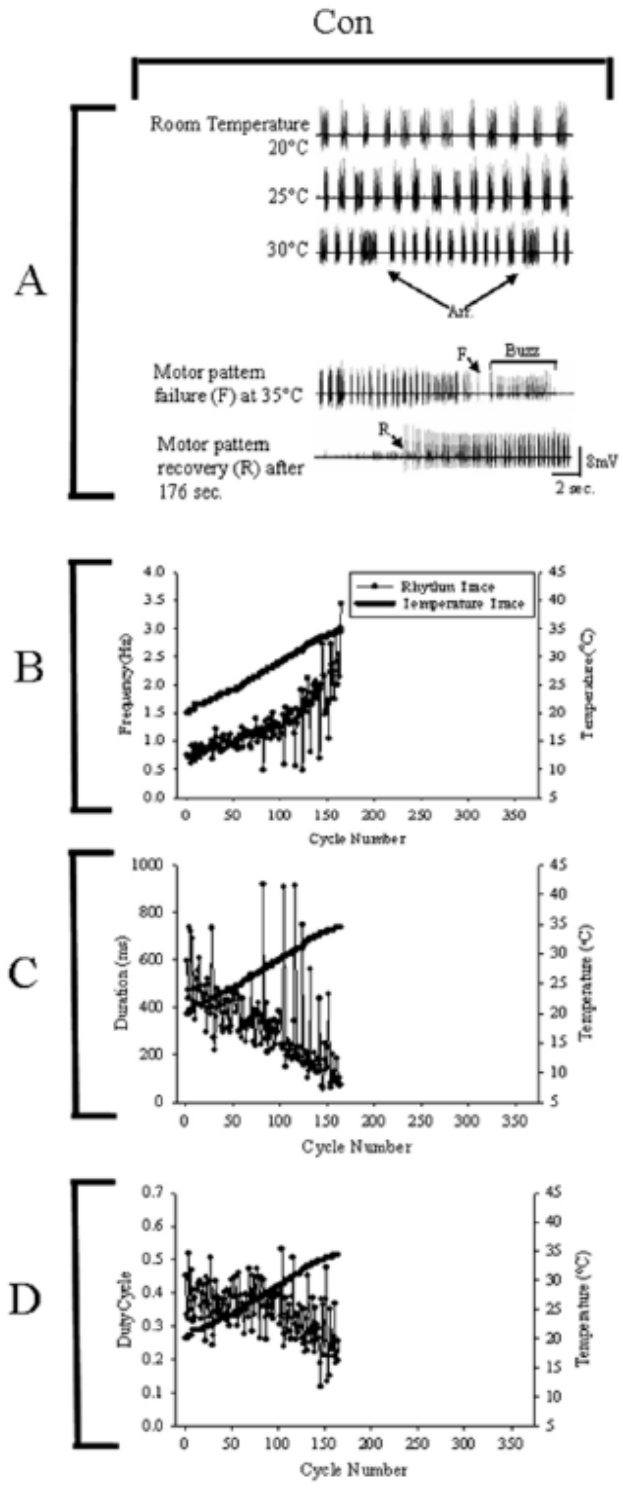
Con
A
Room Temperature
20°C
25°C
30°C
Air.
Buzz
F
Motor pattern
failure (F) at 35°C
R
Motor pattern
recovery (R) after
176 sec.
8mV
2 sec.
B
Rhythm Imce
Temperature Imce
Frequency(Hz)
Temperature(°C)
Cycle Number
C
Duration (ms)
Temperature (°C)
Cycle Number
D
DutyCycle
Temperature (°C)
Cycle Number

Figure 2.2

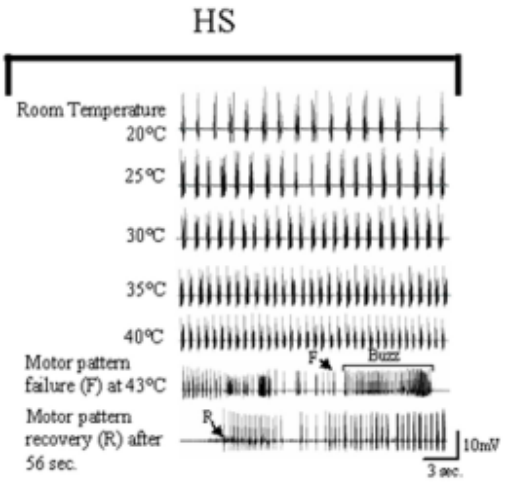
HS
Room Temperature
20°C
25°C
30°C
35°C
40°C
Motor pattern
failure (F) at 43°C
F
Buzz
Motor pattern
recovery (R) after
56 sec.
R
10mV
3 sec.

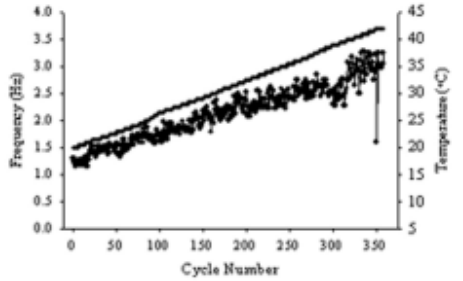
Frequency (Hz)
Temperature (°C)
Cycle Number

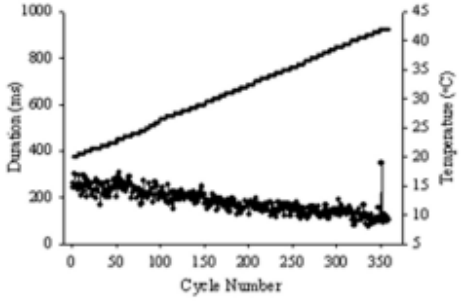
Duration (ms)
Temperature (°C)
Cycle Number

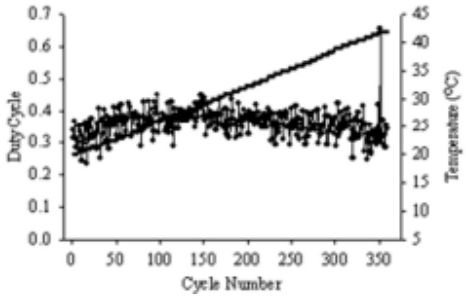
Duty Cycle
Temperature (°C)
Cycle Number

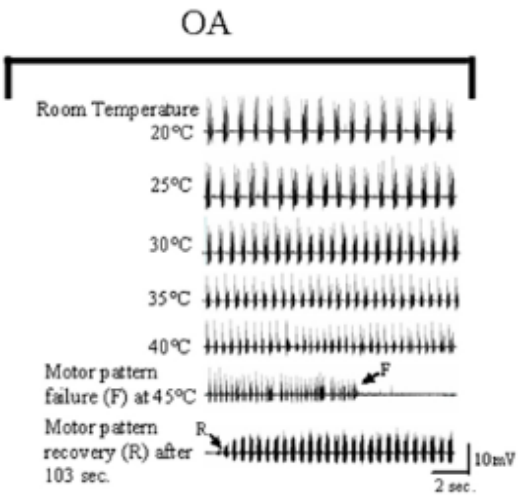
OA
Room Temperature
20°C
25°C
30°C
35°C
40°C
Motor pattern
failure (F) at 45°C
F
Motor pattern
recovery (R) after
103 sec.
R
10mV
2 sec.

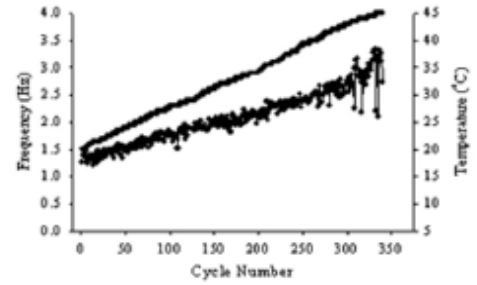
Frequency (Hz)
Temperature (°C)
Cycle Number

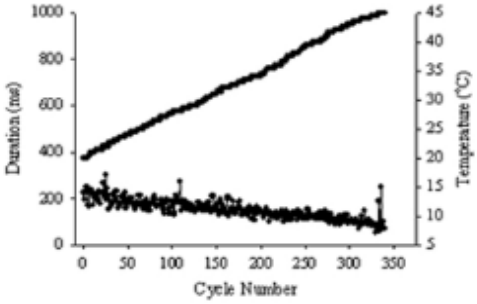
Duration (ms)
Temperature (°C)
Cycle Number

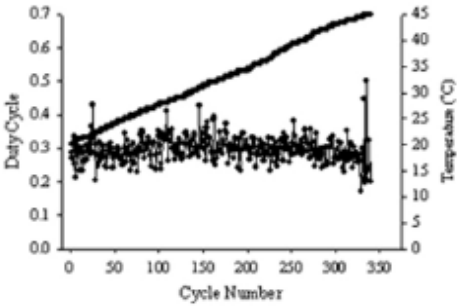
Duty Cycle
Temperature (°C)
Cycle Number

Figure. 2.2. Ventilatory motor pattern activity in control (Con, left column), heat shock-treated (HS, middle column) and octopamine-injected animals (OA, right column) during temperature ramps (5°C/min until failure). A. Electromyographic traces of the motor pattern at different temperatures, at failure (F) and at recovery (R). Arrhythmias (Arr.) characterized by a long burst duration and a subsequent increase in cycle period become more frequent as temperature increases. Failure is often followed by a burst of unpatterned electrical activity (Buzz, not present in OA locust). B. Instantaneous rhythm frequency plotted against cycle number during the temperature ramp. C. Expiratory burst duration plotted against cycle number during the temperature ramp. D. Duty cycle plotted against cycle number during the temperature ramp. Arrhythmias in Con preparations are evident as single cycle decreases in motor pattern frequency and increases in expiratory burst duration and duty cycle.

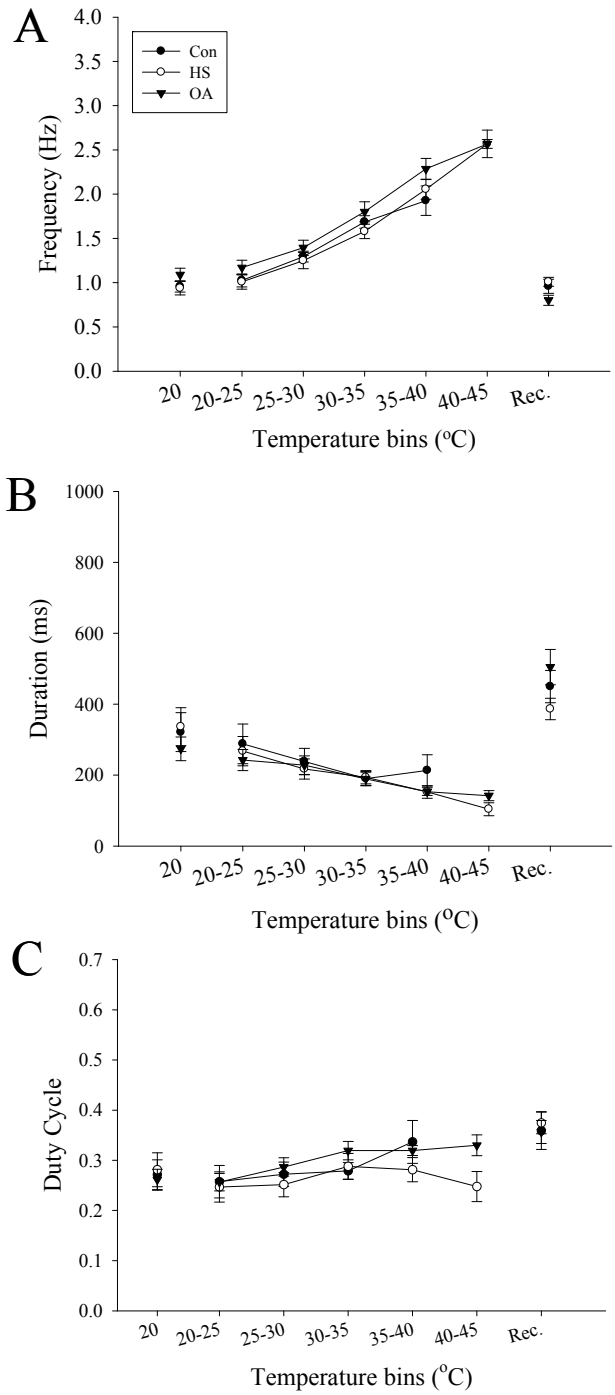
A
Con
HS
OA
Frequency (Hz)
4.0
3.5
3.0
2.5
2.0
1.5
1.0
0.5
0.0
20
20-25
25-30
30-35
35-40
40-45
Rec.
Temperature bins (°C)
B
Duration (ms)
1000
800
600
400
200
0
20
20-25
25-30
30-35
35-40
40-45
Rec.
Temperature bins (°C)
C
Duty Cycle
0.7
0.6
0.5
0.4
0.3
0.2
0.1
0.0
20
20-25
25-30
30-35
35-40
40-45
Rec.
Temperature bins (°C)

Figure 2.3

Figure. 2.3. Motor pattern parameters during temperature ramps in Con, HS and OA preparations. A. Relationship between motor pattern frequency and temperature. Frequency increases as temperature is raised. B. Expiratory burst duration decreases as temperature is raised. D. Duty cycle remains unchanged by the rise in temperature. Values for each parameter were averaged within each 5°C temperature bin and plotted as mean ± standard error. Note that HS and OA relationships have values at 40-45°C whereas Con relationships terminate at 35-40°C. Values before and after the temperature ramp are presented as 20°C and Rec. Sample sizes: Con, n=13; HS, n=10; OA, n=11. Error bars represent mean ± standard error.

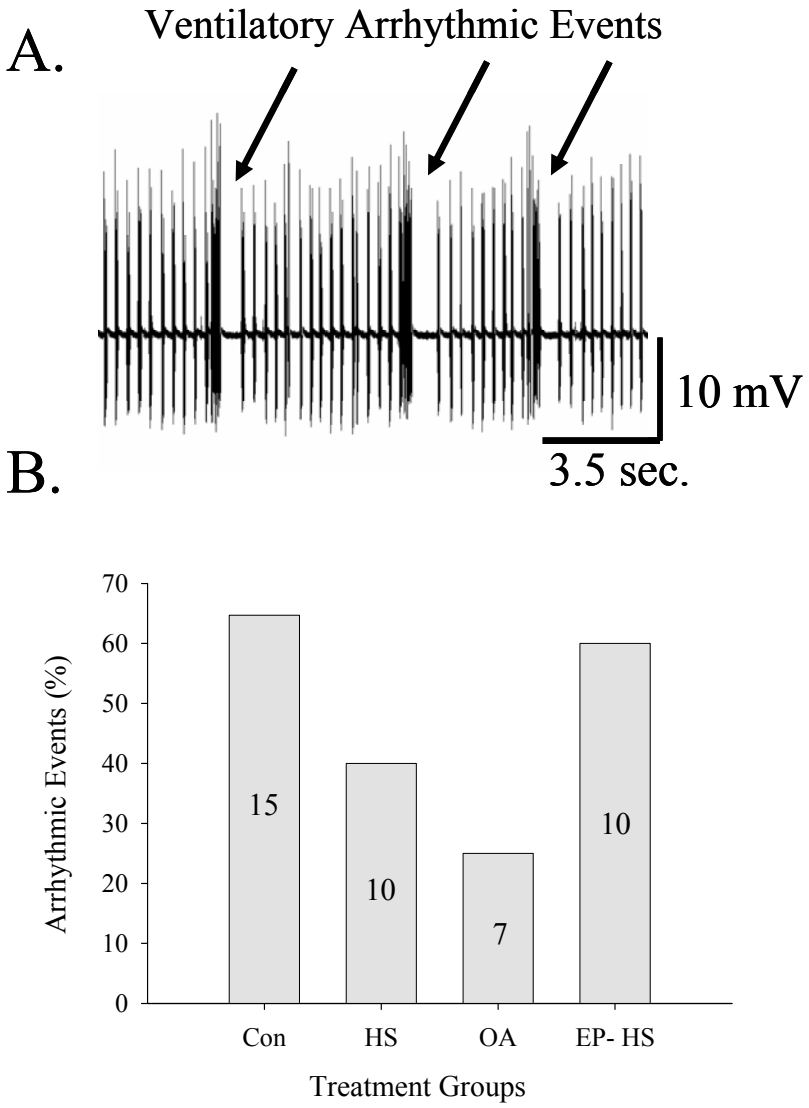

Figure 2.4. Frequency of occurrence of ventilatory arrhythmias. A. Electromyographic trace of expiratory muscle 161 with three successive arrhythmias (Arr.). B. The frequency of occurrence (%) of locusts having at least 1 arrhythmic event in Con, HS, OA and EP-HS preparations. Note fewer arrhythmias in HS and OA compared with Con and EP-HS locusts.

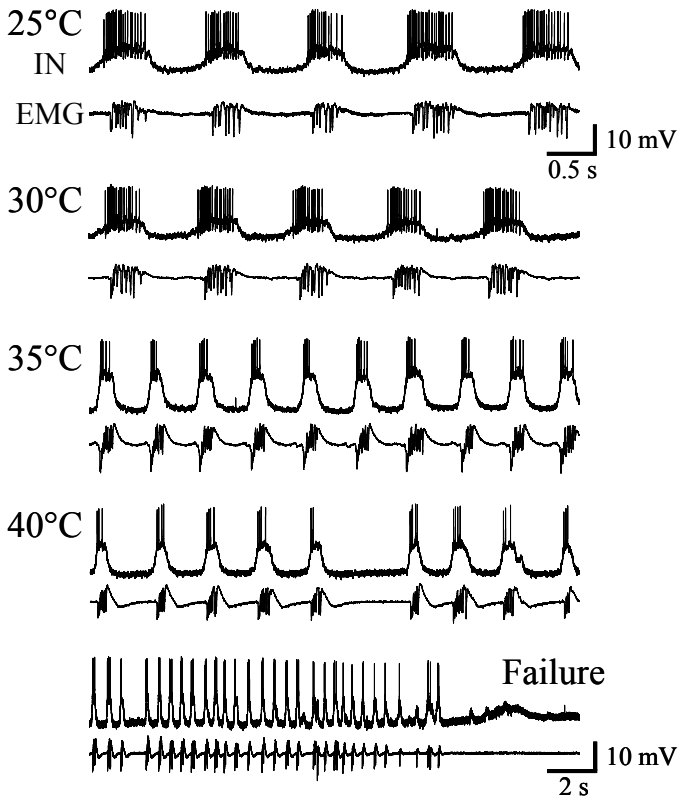

Figure 2.5. Failure of central pattern generation. Intracellular recording of a ventilatory interneuron (top trace) and EMG of expiratory muscle 161 (bottom trace) during a temperature ramp to failure. The rhythm frequency increases with temperature, with fewer interneuronal spikes per cycle. Note the arrhythmia at 40°C, and that failure monitored electromyographically was coincident with failure of the CPG. Lowest panel has different time scale.

recording (Fig 2.5). For 5 of the 7 recordings failure was associated with subsequent depolarization of the neuron.

Neurohormonal effects of octopamine mediate ventilatory thermotolerance

To test if acute OA treatment could generate thermotolerance, short bath applications of 20 minutes were given and compared with Con and HS preparations. The temperature at which the ventilatory motor pattern failed was significantly increased by HS treatment but was unaffected by short 20 minute bath applications of OA at both 10^{-4}M and 10^{-3}M (Fig 2.6 A, 10^{-3}M data not shown; one-way RM-ANOVA, $F = 6.775$, df = 12, $p = 0.007$). HS animals recovered ventilation significantly faster than Con animals (one-way RM-ANOVA, $F = 5.281$, df = 12, $p = 0.015$) but recovery time in OA-treated (both concentrations) animals and Con were not different from one another (Fig 2.6 B, data for 10^{-3}M not shown). Similar OA treatment on HS preparations had no significant effect (data not shown).

Extended (1h) bath applications of 10^{-4}M OA induced thermotolerance of the neural circuitry coordinating ventilation similar to a HS treatment whereas 10^{-4}M TA did not (Fig 2.6 C,D). Failure temperatures for OA and HS groups were significantly higher than Con and TA (one-way RM-ANOVA, $F = 7.416$, df = 3. $p = 0.001$; Tukey test $p = 0.05$; Fig 2.6 C). The length of time taken to recover motor pattern function was also

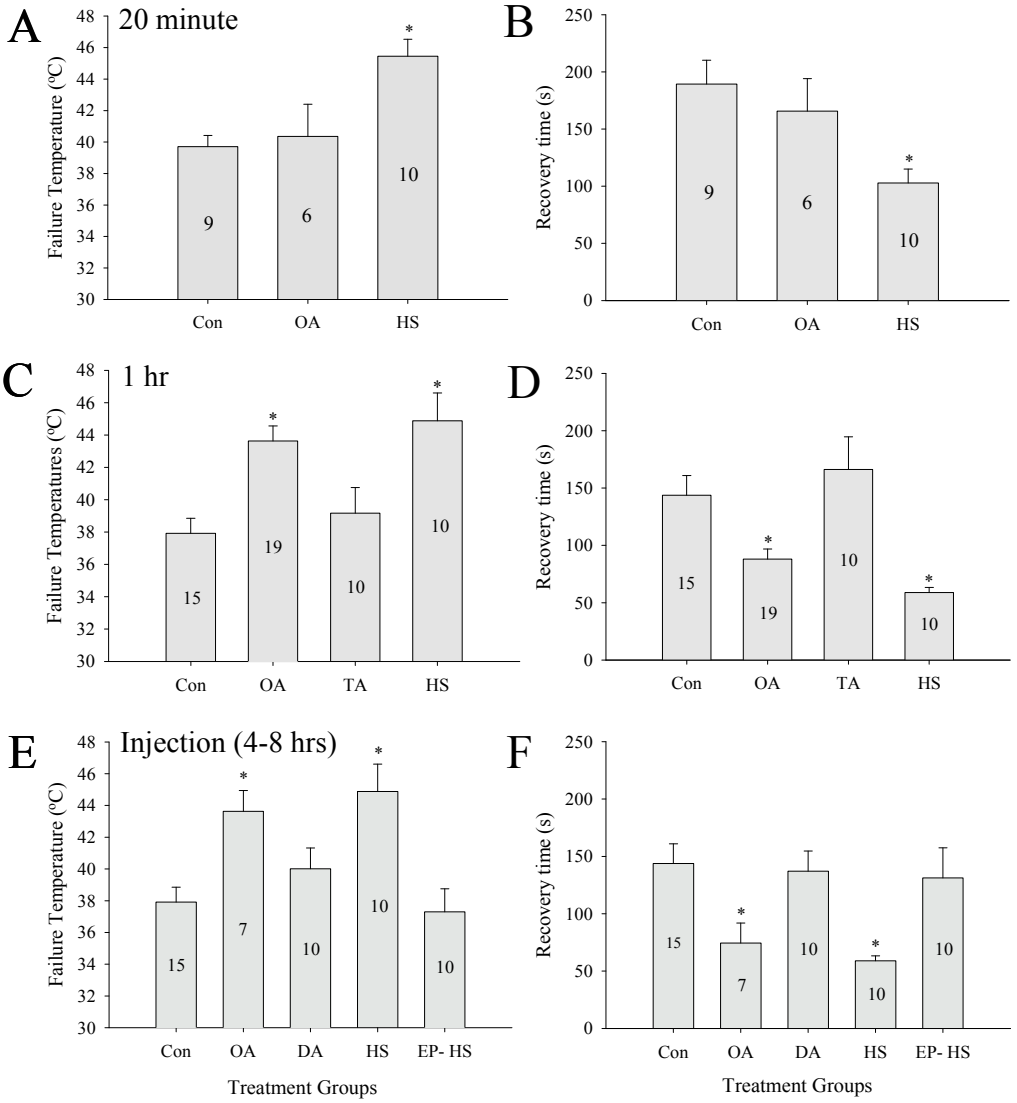
A
20 minute
Failure Temperature (ºC)
B
Recovery time (s)
C
1 hr
Failure Temperatures (ºC)
D
Recovery time (s)
E
Injection (4-8 hrs)
Failure Temperature (ºC)
F
Recovery time (s)
Con
OA
TA
DA
HS
EP- HS
Treatment Groups

Figure 2.6

Figure 2.6. Ventilatory thermotolerance measured by failure temperature (A,C,E) and recovery time (B,D,F). A & B. Thermotolerance induced by HS but not by 20 minute bath applications of 10^{-4}M octopamine (OA). C & D. Thermotolerance induced by HS and by 1 hr bath application of 10^{-4}M OA but not by 1 hr bath application of 10^{-4}M tyramine (TA). E & F. Thermotolerance induced by HS, and by injection of OA (2μg/10μl) into the haemocoel of intact animals 4-8 hours prior to testing. Similar injections of dopamine (DA) were ineffective. Injections of epinastine (EP) to block OctβRs abolished the effect of HS (HS-EP). Con and HS animals received sham injections of the same volume of locust saline. Numbers in the bars indicate sample sizes. Asterisks indicate significant differences from Con ($P < 0.05$). Error bars represent mean ± standard error.

significantly shorter in HS and OA compared with Con and TA groups (one-way RM-ANOVA, $F = 8.854$, df = 3, $p = 0.001$; Tukey test $p < 0.05$; Fig 2.6 D).

To test longer exposures to amines, injections (2µg/µl) of OA, DA or EP into the haemocoel were made 4-8 hours before thermotolerance testing. There were significant differences in the level of thermotolerance (failure temperature, one-way RM-ANOVA, $F = 4.430$, df = 4, $p = 0.004$; recovery time, one-way RM-ANOVA, $F = 6.059$, df = 4, $p = 0.001$). We found HS failure temperatures to be significantly higher (Tukey test, $p < 0.05$) than all groups except for OA-injected animals (Fig 2.6 E). Furthermore, failure temperatures for OA-injected animals were significantly higher than Con and epinastine-injected HS locusts (EP-HS) (Tukey test, $p = 0.01$; Fig 2.6 E). No significant differences in failure temperatures were found between Con, DA, and EP-HS groups. Recovery time was significantly different between groups (one-way RM-ANOVA, $F = 6.059$, df = 4, $p = 0.001$; Fig 2.6 F). Both HS- and OA-injected locusts recovered ventilation significantly faster than Con, EP-HS and DA groups (Tukey test, $p = 0.05$). In separate experiments EP was injected into control locusts. These animals had failure temperatures and recovery times of 40.7 ± 2.1°C and 183 ± 38s and were not significantly different from the sham-injected Con group. We also tested to see if recovery of thermoprotection could be achieved in EP-injected control animals with a bath application of 10^{-4}M of OA for 1 hour. We found no increase in failure temperature; it was slightly lower than controls (36.2 ± 1.8°C vs. 37.4 ± 1.0°C), suggesting a persistent block of OctβRs by EP.

Recovery time was significantly increased in EP-injected control animals when compared to the control group (234 ± 48s vs. 143 ± 22s, *t*-test, $p = 0.05$).

Octopamine-mediated thermotolerance depends on the cAMP/PKA pathway.

Upon elevating cAMP levels with a 1 hour bath application of 10^{-5}M FOR we found a significant difference in failure temperature between treatments (one-way RM-ANOVA, $F = 5.162$, df = 2, $p = 0.015$; Fig 2.7 A). HS- and FOR-treated locusts had significantly higher failure temperatures than the Con group (Tukey Test, $p < 0.010$). Furthermore, significant differences were found in recovery time (one-way RM-ANOVA, $F = 7.107$, df = 2, $p = 0.004$; Fig 2.7 B). Following FOR treatment we found motor pattern recovery time to be significantly shorter than controls (Tukey Test $p = 0.005$).

Neuropil injections of Sp-cAMPs (PKA agonist) or Rp-cAMPs (PKA antagonist) led to significant differences in both failure temperatures (one-way RM-ANOVA, $F = 5.590$, df = 3, $p = 0.003$; Fig 2.8 A) and recovery times (one-way RM-ANOVA, $F = 5.846$, df = 3, $p = 0.002$; Fig 2.8 B) of the motor pattern. Following injections of Sp-cAMPs, the ventilatory neural circuitry had significantly higher failure temperatures (Tukey Test, $p = 0.011$) and shorter recovery times (Tukey Test, $p = 0.061$) than controls (Fig 2.8 A,B). Furthermore, by bath applying OA while injecting Rp-cAMPs into the neuropil we observed a significant reduction in the level of thermoprotection conferred by OA (Fig 2.8 A,B). Failure temperatures were significantly increased (Tukey Test, $p = 0.093$) and recovery times were significantly increased (Tukey Test, $p = 0.022$) when compared to

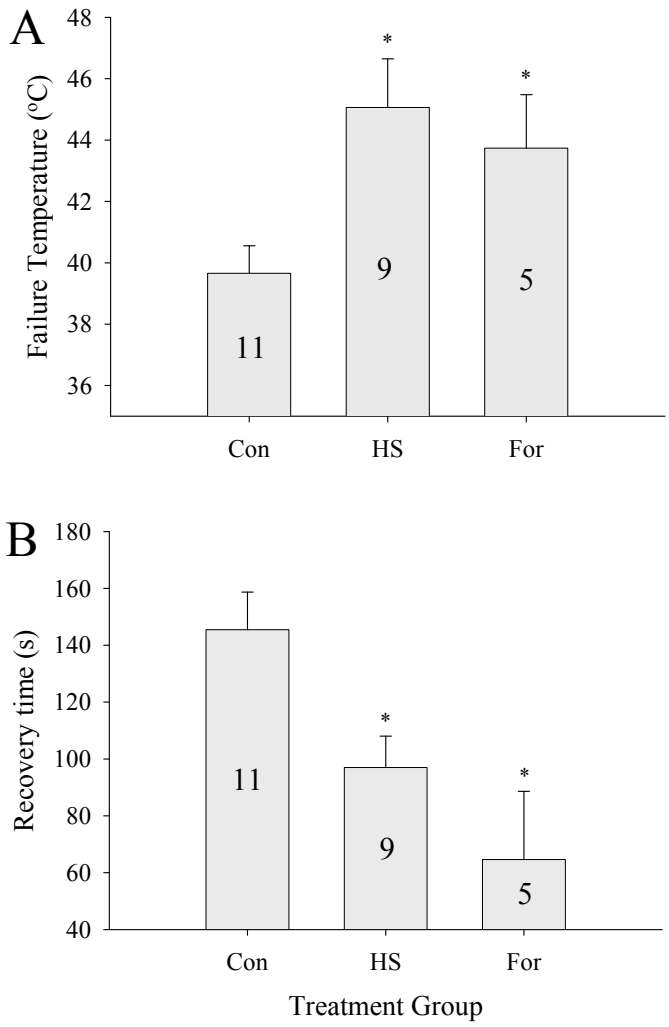

Figure 2.7. Activation of adenylyl cyclase via bath application (1hr) of 10^{-5}M forskolin (For) mimics HS. A. Failure temperature. B. Recovery time. Numbers in the bars indicate sample sizes. Asterisks indicate significant differences from Con ($P < 0.05$). Error bars represent mean ± standard error.

OA-treated locusts. Failure temperatures and recovery times of locusts injected with saline into the neuropil while concurrently giving a 1 hour bath application of 10^{-4}M OA and locusts which received injections of Sp-cAMPs were not significantly different from one another (failure temperature, Tukey Test, $p = 0.697$; recovery time, Tukey Test, $p = 0.938$). In addition, we found that thermoprotection could be rescued in EP-HS locusts by bypassing the receptor and directly activating the pathway with Sp-cAMPs (Fig 8 C,D). Failure temperatures in these animals were significantly higher than those of HS locusts treated with epinastine (Tukey Test, $p = 0.037$). Recovery time was reduced in these animals when compared to EP-HS locusts (Tukey Test, $p = 0.126$).

Octopamine-mediated thermotolerance requires protein synthesis.

We examined the effects of blocking transcription and translation during bath application of OA. Locusts which receive neuropil injections of ACTD while being bathed in OA had significantly reduced failure temperatures (Tukey Test, $p = 0.032$) and took a significantly longer time to recover (Tukey Test, $p = 0.10$) following heat-induced failure of the CPG (Fig 2.9 A,B) than OA-treated animals. Similarly, locusts which received neuropil injections of CHX while being bathed in OA had reduced failure temperatures (Tukey Test, $p = 0.009$) and took longer to recover (Tukey Test, $p = 0.08$) than locusts treated with OA (Fig 2.9 A,B).

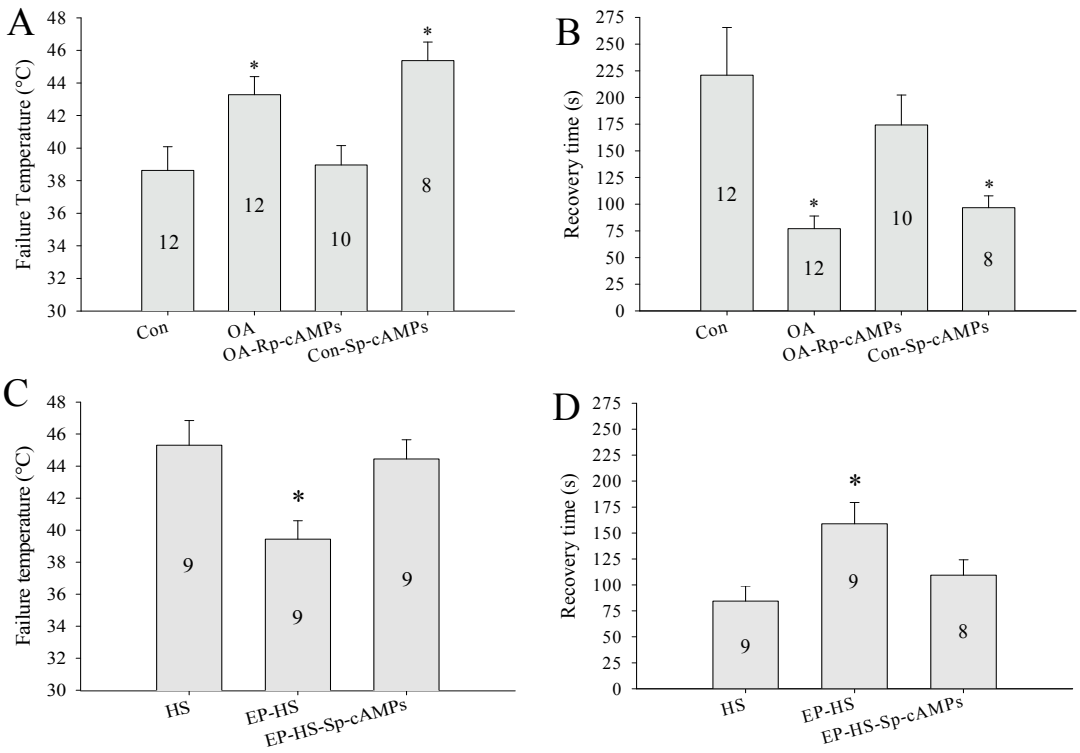

Figure 2.8. Activating the PKA pathway mimics HS. A & B. Thermotolerance induced via injections (70nl) of the cAMP analog Sp-cAMPs into the ventilatory neuropil over 1 hour (Con-Sp-cAMPs). Thermotolerance induced by 1 hr bath application of 10^{-4}M octopamine (OA) was abolished via injections of Rp-cAMPs (OA-Rp-cAMPs). Con and OA preparations received sham injections of locust saline. C & D. Thermotolerance was recovered in HS locusts treated with the OctβRs antagonist epinastine by neuropil injection of Sp-cAMPs. Numbers in the bars indicate sample sizes for each group. Asterisks indicate significant differences from Con and OA-Rp-cAMPs in A and B, and HS in C and D ($P < 0.05$). Error bars represent mean ± standard error.

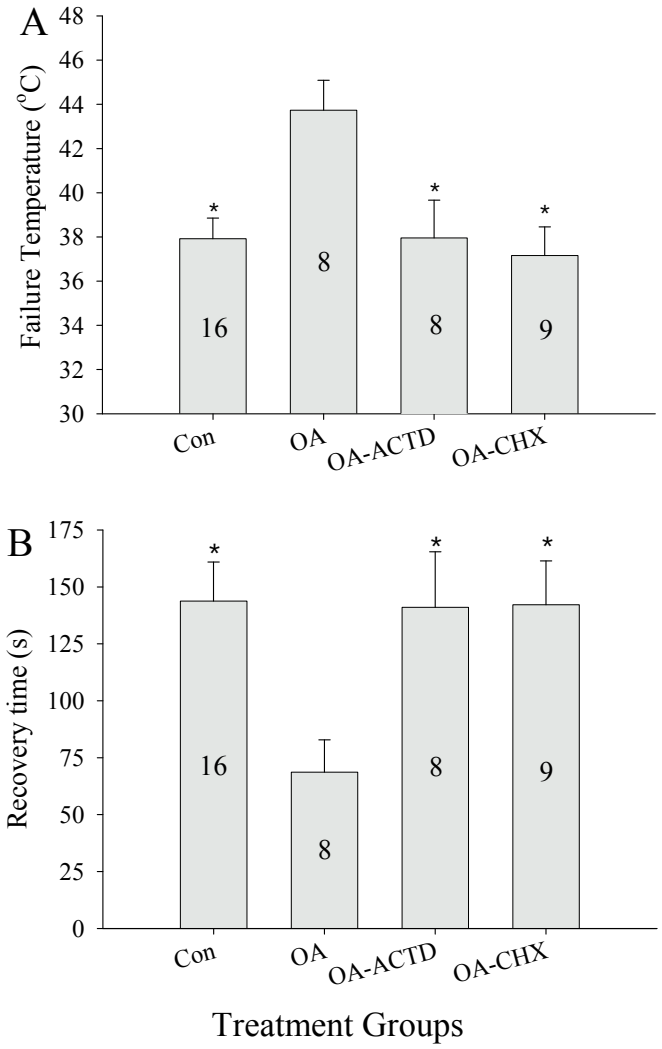

Figure 2.9. Octopamine-mediated thermotolerance is dependent upon protein synthesis. Injections of actinomycin D (OA-ACTD) a transcription inhibitor, or cycloheximide (OA-CHX) a translation inhibitor, into the ventilatory neuropil abolished the effect of bath application of 10^{-4}M OA for 1 hour (OA). A. Failure temperature. B. Recovery time. Con and OA preparations received sham injections. Numbers in the bars indicate sample sizes. Asterisks indicate significant differences from OA-treated animals ($P < 0.05$). Error bars represent mean ± standard error.

Octopamine and HS both increase motor pattern recovery rates following injection of K^+ into the ventilatory neuropil.

Hyperthermic failure of motor pattern generation is coincident with a rapid rise in extracellular [K^+] and recovery is reliably correlated with clearance of this load (Robertson, 2004). We measured the length of time taken to re-establish motor pattern operation following injections of locust saline containing high levels of K^+ (150mM vs. 10mM). In all experiments motor pattern operation was arrested by this treatment. The length of time taken to recover motor pattern operation following injections was significantly different between groups (RM-ANOVA, $F = 6.768$, df = 3, $P = 0.001$). OA- and HS-treated locusts were able to recover motor pattern function significantly faster than Con and EP-HS- treated locusts (Tukey test, $P < 0.08$; Fig 2.10).

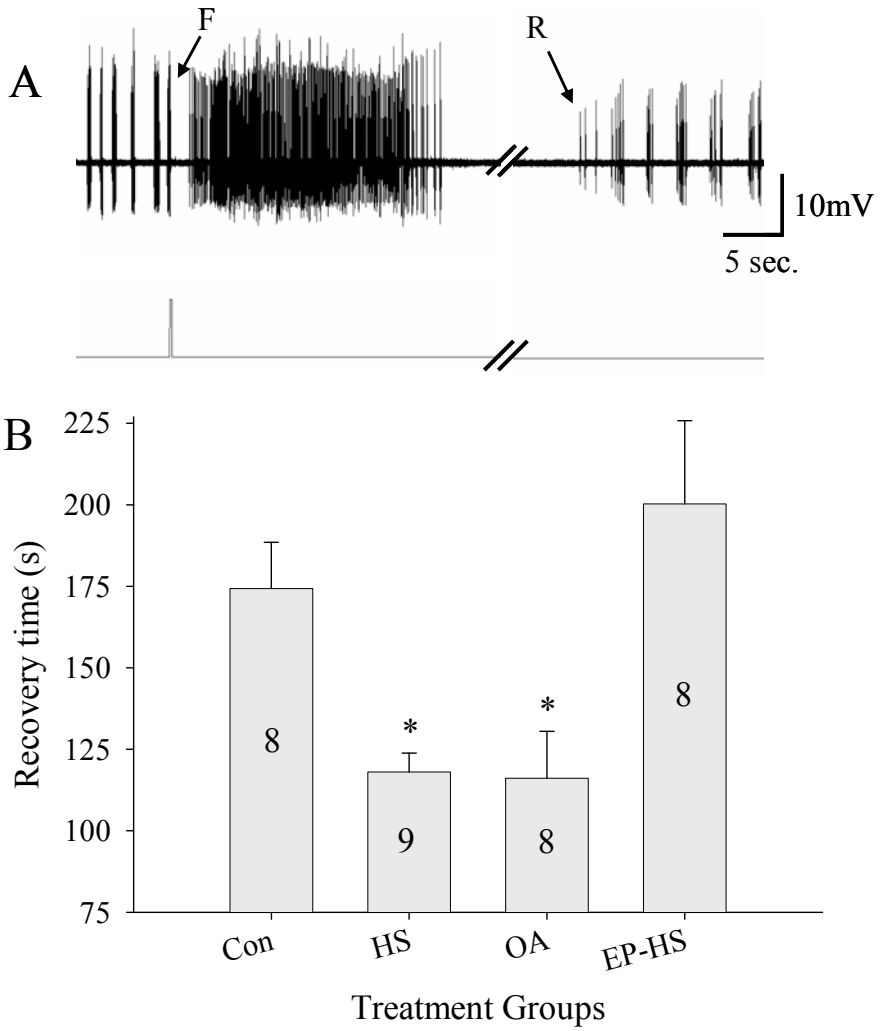

Figure 2.10. Octopamine treatment and HS increases speed of motor pattern recovery following K^+ injection. A. EMG of activity in expiratory muscle 161 (upper trace) following injection of saline containing high K^+ (150mM vs. 10mM) into the ventilatory neuropil (timing indicated in lower trace). Note termination of ventilatory rhythm generation (F) associated with a burst of unpatterned activity and subsequent recovery (R). B. Recovery time was shorter in HS and OA animals. Epinastine abolished the effect of HS (EP-HS). Numbers in the bars indicate sample sizes. Asterisks indicate significant differences from Con and EP-HS groups ($P < 0.05$). Error bars represent mean ± standard error.

2.5 Discussion

In its semi-arid habitat of Asia and Africa, *L. migratoria* is exposed to an average air temperature of 32°C with temperatures reaching 55°C during the hottest periods of the day (Uvarov, 1977). Excess heat gained through metabolism, substrate conduction and radiant energy from the sun drives internal temperatures of the locust well above ambient levels (Uvarov, 1966). In response to these harsh challenges, locusts have evolved physiological mechanisms to cope with extreme temperatures. HS preconditioning confers subsequent protection of the locust nervous system from hyperthermic stress (e.g. Robertson et al. 1996; Barclay and Robertson, 2000). We demonstrate here that octopamine (OA) is the crucial endogenous ligand that signals neural tissue to switch on protective physiological adaptations that provide thermotolerance.

We used ventilation, a vital motor activity controlled by neural circuitry in the MTG as our model system for investigating the thermoprotection of circuit function. The ventilatory CPG, like all insect neural circuits, is sensitive to temperature change, and as body temperature rises, neural activity increases. Ventilatory rhythm frequency increases and expiratory burst duration decreases as temperature of the MTG rises, whereas duty cycle remains stable throughout temperature change. At some point during a temperature ramp thermal stress exceeds the physiological mechanisms that allow ventilatory rhythm generation to operate and ventilation fails. In our semi-intact preparation ventilatory motor pattern operation failed at 38-40°C in control animals and 44-45°C in HS preconditioned animals. Locusts treated with OA had failure temperatures between 43

and 44°C, whereas neither DA (40°C) nor TA (39°C) generated thermoprotection. In addition to extension of the upper thermal limit, recovery of CPG function following temperature-induced failure was more than twice as fast in animals that had received HS or OA treatment. The most conclusive evidence we have that OA is signalling neural tissue to switch on a thermoprotective response during HS treatment is that blocking effects of endogenous OA with epinastine, a highly selective and potent antagonist of locust OctβRs (Roeder et al., 1998), abolished the protective changes which are normally acquired during HS.

Using HPLC to measure ganglionic OA concentrations during heat stress we observed a modest drop in content of OA after 15 minutes before returning to normal levels after 30 minutes. Although this drop in OA is likely a result of OA being released into peripheral and central sites such as the ventilatory neuropil we cannot rule out the possibility that during heat stress there is a reduction in OA synthesis or increase in its metabolism. We confirmed the direct excitatory actions of OA on the ventilatory CPG (Sombati and Hoyle, 1984, Ramirez and Pearson, 1989). Exposures to short (20min) bath applications of OA resulted in increased motor pattern frequency. Furthermore, treatment with epinastine was sufficient to block the excitatory effects of OA on the ventilatory rhythm. In locusts, haemolymph OA concentrations more than double after exposures to heat stress (Davenport and Evans, 1984). The source of increased haemolymph OA is probably from ganglionic OA-immunoreactive dorsal unpaired median (DUM) and ventral unpaired median (VUM) neurons of the ventral ganglia (Stevenson and Spörhase-

Echmann, 1995; Duch et al. 1999; Bräunig and Burrows, 2004). The vast majority of these neurons have peripheral release sites although central release sites for OA in the MTG have been reported (Watson, 1984). We suggest that these central release sites modulated the ventilatory CPG during times of stress.

In the insect CNS OctβRs are coupled to adenylyl cyclase (Maqueira et al. 2005; Evans and Maqueira, 2005). Following activation of these receptors $[cAMP]_i$ rises in the CNS and epinastine blocks this rise in $[cAMP]_i$ (Roeder et al. 1998). Increased adenylyl cyclase activity following a 1 hour forskolin application increased motor pattern thermotolerance in our experiments. To further confirm the role cAMP plays in protecting the CNS we used a pressure injection system to deliver nanolitres of an agonist or antagonist directly into the ventilatory neuropil over a 1 hour period. Injections of the membrane-permeable cAMP analog and protein kinase A (PKA) activator, Sp-cAMPs (Wang et al. 1991), protected the ventilatory CPG. Failure temperatures were 6°C higher and the CPG recovered its function 2 minutes faster than in control preparations. In addition, injections of Sp-cAMPs into epinastine-treated HS locusts restored thermoprotection even though OctβRs were blocked. Using the potent competitive inhibitor of cAMP-PKA mediated effects, Rp-cAMPs (Botelho et al. 1988; Wang 1991; Widmer et al. 2005), we were able to abolish the thermoprotective effects of OA treatment. Thus we have shown that raising cAMP levels and activating PKA mimics the effects of a prior HS, whereas reducing cAMP/PKA-mediated effects attenuates the ability of the circuit to cope with thermal stress.

Increased intracellular levels of cAMP have been noted to regulate K^+ channel activity (Goldsmith and Abrams, 1992; Yuan et al. 2002). We have shown that decreased K^+ channel activity has protective effects (Wu et al. 2001) and after HS whole-cell patch-clamp recordings from neurons of the MTG show reduced K^+ currents (Ramirez et al. 1999). The reduction in K^+ currents may be mediated by OA, which is known to reduce resting K^+ conductance in locusts (Walther and Zittlau 1998). K^+ channel down-regulation may delay the build up in $[K^+]_o$ at high temperatures but another crucial step in protecting the CNS would be the ability to clear excess extracellular potassium. Thus modulation of the Na^+/K^+ATPase pump and/or $K^+/Na^+/2Cl^-$ cotransporter activity could be involved in HS-mediated thermotolerance. OA stimulates the activity of the Na^+/K^+ATPase pump in locust muscle tissue (Walther and Zittlau, 1998) and regulates glia-specific pumps on the sheath of the thoracic ganglia which have been shown to regulate potassium permeability in cockroaches (Schofield and Treherne, 1985). Increased pump activity in neurons and glia following OA and HS treatments may account for the increase in motor pattern recovery rates following injections of high K^+ saline. It is interesting to note that HS and OA-treated animals have fewer instances of arrhythmias than Con and Ep-HS locust. The presence of hyperthermic arrhythmias could be attributed to neurons and glia which are just beginning to lose their ability to maintain ionic gradients. The increased prevalence of ventilatory arrhythmias seen in animals which do not possess the physiological mechanisms to cope with thermal stress could be a result of poor $[K^+]_o$ handling at high temperatures.

Although ion channel and membrane pump regulation may play a major role in maintaining electrochemical homeostasis during times of increased stress, the plastic changes in potassium handling occurring after HS rely on a process which requires time to generate. We did not see a protective effect following 20 minute bath applications of OA. Thus it seems unlikely that the acute neuromodulatory effects of OA, which modulate channel and pump activity, play a role in generating a thermoprotected circuit. An alternative possibility is that 1hour bath applications of OA or injections into the haemocoel trigger the up-regulation of heat shock proteins, notably HSP70 (requiring a similar length of time to be transcribed and translated; Whyard et al. 1986), which in turn protect the operation of K^+ channels and the Na^+/K^+ATPase (Burdon and Cutmore, 1982; Armstead and Hecker, 2005; Riordan et al. 2005) at high temperatures.

Although it has been postulated that OA may indirectly interact with the genome and increase synthesis of specific proteins (Roeder, 2005; Armstrong and Robertson, 2006) little evidence has been provided that this is the case. In this report we show that the thermoprotective effects of OA treatment rely upon gene transcription and translation. There are two plausible pathways for OA to interact with the genome and increase HSP levels. One mechanism would be through a cAMP-CREB pathway (Roeder, 2005; Armstrong and Robertson, 2006). However the primary induction pathway for HSPs is via heat shock transcription factor (HSF) binding to heat shock element (HSE) and it is more reasonable to assume that cAMP and PKA might help promote HSF binding to

DNA. Previous reports support this claim and Ohnishi et al. (1998, 1999) have shown that protein kinase inhibitors (staurosporine, H7 and combinations of calphostin and H89) suppressed heat-induced activation of HSF and HSP72 production.

HS preconditioning offers a protective change in the ability to handle subsequent thermal stress. The mechanisms for coordinating these changes following HS have remained elusive. We show here that a coordinated change in CNS physiology resulting in improved thermotolerance after HS preconditioning is mediated by octopamine activating a cAMP/PKA pathway and requires protein synthesis.

2.6 References

Armstead, W.M. and J.G. Hecker. Heat shock protein modulation of K_{ATP} and K_{Ca} channel cerbrovasodilation after brain injury. *Am. J. Physiol. Heart. Circ. Physiol.* 289: H1184-H1190 (2005).

Armstrong, G.A.B. and R.M. Robertson. A role for octopamine in coordinating thermoprotection of an insect nervous system. *J. Therm. Biol.* 31: 149-158 (2006).

Barclay, J.W. and R.M. Robertson. Heat shock-induced thermoprotection of hindleg motor control in the locust. *J. Exp. Biol.* 203: 941-950 (2000).

Bellah, K.L. Fitch, G.K. and A.E. Kammer. A central action of octopamine on ventilation frequency in *Corydalus cornutus*. *J. Exp. Zool.* 231: 289-292 (1984).

Botelho, L.H.P. Rothermel, J.D. Coombs, R.V. and B. Jastorff. cAMP analog antagonist of cAMP action. *Meth. Enzymol.* 159: 159-172 (1988).

Bräunig, P. and M. Burrows. Projection patterns of posterior dorsal unpaired median neurons of the locust subesophageal ganglion. *J. Comp. Neurol.* 478: 164-175 (2004).

Burdon, R.H. and C.M.M Cutmore. Human heat shock gene expression and the modulation of plasma membrane Na^+,K^+-ATPase activity. *FEBS Lett.* 140: 45-48 (1982).

Chapman, R.F. A field study of the potassium concentration in the bloods of the red locust *Nomadacris septemfasciata* (serv.), in relation to its activity. *Anim. Behav.* 6: 60-61 (1958).

Chentsova, N.A. Gruntenko, N.E. Bogomolova, E.V. Adonyeva, N.V. Karpova, E.K. and I.Y. Rauschenback. Stress response in *Drosophila melanogaster* strain *inactive* with decreased tyramine and octopamine contents. *J. Comp. Physiol.* B 172: 643-650 (2002).

Davenport, A.P. and P.D. Evans. Stress-induced changes in the octopamine levels of insect haemolymph. *Insect. Biochem.* 14: 135-143 (1984).

Duch, C. Mentel, T. and H.-J. Pflüger. Distribution and activation of different types of octopaminergic DUM neurons in the locust. *J. Comp. Neurol.* 403: 119-134 (1999).

Evans, P.D. Octopamine. In: Comprehensive Insect Physiology, Biochemistry, and Pharmacology, Vol. 11: Pharmacology, pp474-499. Oxford: Pergamon Press. (1985).

Evans, P.D. and B. Maqueira. Insect octopamine receptors: a new classification scheme based on studies of cloned *Drosophila* G-protein coupled receptors. *Invert. Neurosci.* 5: 111-118 (2005).

Goldsmith, B.A. and T.W. Abrams. cAMP modulates multiple K^+ currents, increasing spike duration and excitability in *Aplysia* sensory neurons. *Proc. Natl. Acad. Sci.* 89: 11481-11485 (1992).

Hirashima, A. Sukhanova, M.J. and I.Y. Rauschenback. Biogenic amines in *Drosophila virilis* under stress conditions. *Biosci. Biotechnol. Biochem.* 64: 2625-2630 (2000).

Kravitz, E.A. and R. Huber. Aggression in invertebrates. *Curr. Opin. Neurobiol.* 13:736-743 (2003).

Lange, A.E. and I. Orchard. Identified octopaminergic neurons modulate contractions of locust visceral muscle via adenosine 3',5'-monphosphate (cyclic AMP). *Brain Res.* 363: 340-349 (1986).

Maqueira, B. Chatwin, H. and P.D. Evans. Identification and characterization of a novel family of *Drosophila* β-adrenergic-like octopamine G-protein coupled receptors. *J. Neurochem.* 94: 547-560 (2005).

Nathanson, J.A. Octopamine receptors, adenosine 3',5'-monophosphate, and neural control of firefly flashing. *Science* 28: 254-268 (1979).

Newman, A.E.M. Foerster, M. Shoemaker, K.L. and R.M. Robertson. Stress-induced thermotolerance of ventilatory motor pattern generation in the locust, *Locusta migratoria*. *J. Insect Physiol.* 49:1039-1047 (2003).

Ohnishi, K. Wang, X. Takahashi, A. Matsumoto, H. Aoki, H. and T. Ohnishi. Effects of protein kinase inhibitors on heat-induced *hsp*72 gene expression in a human glioblastoma cell line. *Cell Signal.* 10: 259-264 (1998).

Ohnishi, K. Wang, X. Takahashi, A. Matsumoto, H. and T. Ohnishi. The protein kinase inhibitor, H-7, suppresses heat induced activation of heat shock transcription factor 1. *Mol. Cell Biochem.* 197: 129-135 (1999).

Orchard, I. Octopamine in insects: neurotransmitter, neurohormone, and neuromodulator. *Can. J. Zool.* 60: 659-669 (1982).

Orchard, I. Loughton, B.G. and R.A. Webb. Octopamine and short-term hyperlipaemia in the locust. *Gen. Comp. Endocr.* 45: 175-180 (1981).

Ramirez, J.-M. Elsen, F.P. and R.M. Robertson. Long-term effects of prior heat shock on neuronal potassium currents recorded in a novel insect ganglion slice preparation. *J. Neurophysiol.* 81: 795-802 (1999).

Ramirez, J.M. and K.G. Pearson. Alteration of the respiratory system at the onset of locust flight. *J. Exp. Biol.* 142: 401-424 (1989).

Rauschenback, I.Y. Serova, L.I. Timochina, I.S. Chentsova, N.A. and L.V. Shumnaja. Analysis of differences in dopamine content between two lines of *Drosophila virilis* in response to heat stress. *J. Insect Physiol.* 39: 761-767 (1993).

Riordan, M. Sreedharan, R. Wang, S. Thulin, G. Mann, A. Stankewich, M. Van Why, S. Kashgarian, M. and N.I. Siegel. HSP70 binding modulates detachment of NA-K-ATPase following energy deprivation in renal epithelial cells. *Am. J. Physiol. Renal. Physiol.* 288: F1236-F1242 (2005).

Robertson, R.M. Thermal stress and neural function: adaptive mechanisms in insect model systems. *J. Therm. Biol.* 29:351-358 (2004).

Robertson, R.M. and K.G. Pearson. A preparation for the intracellular analysis of neural activity during flight in the locust. *J. Comp. Physiol.* 146: 311-320 (1982).

Robertson, R.M. Xu, H. Shoemaker, K.L. and K. Dawson-Scully. Exposure to heat shock affects thermosensitivity of the locust flight system. *J. Neurobiol.* 29: 367-383 (1996).

Roeder, T. Tyramine and octopamine: ruling behavior and metabolism. *Annu. Rev. Entomol.* 50: 447-477 (2005).

Roeder, T. Degen, J. and M. Gewecke. Epinastine, a highly specific antagonist of insect neuronal octopamine receptors. *Eur. J. Pharmacol.* 349: 171-177 (1998).

Schofield, P.K. and J.E. Treherne. Octopamine reduces potassium permeability of the glia that form the insect blood-brain barrier. *Brain Res.* 360: 244-348 (1985).

Sombati, S. and G. Hoyle. Generation of specific behaviors in a locust by local release into neuropil of the natural neuromodulator octopamine. *J. Neurobiol.* 15: 481-506 (1984).

Somjen, G.G. Mechanisms of spreading depression and hypoxia spreading depression-like depolarizations. *Physiol. Rev.* 81: 1065-1096 (2001).

Stevenson, P.A. and U. Spörhase-Echmann. Localization of octopaminergic neurons in insects. *Comp. Biochem. Physiol.* B 110: 203-215 (1995).

Uvarov, B. Grasshoppers and Locusts, a handbook of general acridology, Vol 1. Cambridge, UK: Cambridge UP. (1966).

Uvarov, B. Grasshoppers and Locusts, a handbook of general acridology, Vol 2. Centre of Overseas Pest Research, London. (1977).

Walther, C. and K.E. Zittlau. Resting membrane properties of locust muscle and their modulation II. Actions of the biogenic amine octopamine. *J. Neurophysiol.* 80: 785-797 (1998).

Wang, L.-Y. Salter, M.W. and J.F. MacDonald. Regulation of kainite receptors by cAMP-dependent protein kinase and phosphatases. *Science* 253: 1132-1135 (1991).

Watson, A.H.D. The dorsal unpaired median neurons of the locust metathoracic ganglion: neuronal structures and diversity, and synaptic integration. *J. Neurocytol.* 13: 303-327 (1984).

Whyard, S. Wyatt, G.R. and V.K. Walker. The heat shock response in *Locusta migratoria*. *J. Comp. Physiol.* B 156: 813-817 (1986).

Widmer, A. Höger, U. Meisner, S. French, A.S. and P.H. Torkkeli. Spider peripheral mechanosensory neurons are directly innervated and modulated by octopaminergic efferents. *J. Neurosci.* 25: 1588-1598 (2005).

Wu, B.S. Walker, V.K. and R.M. Robertson. Heat shock-induced thermoprotection of action potentials in the locust flight system. *J. Neurobiol.* 49: 188-199 (2001).

Yuan, L.-L. Adams, J.P. Swank, M. Sweatt, J.D. and D. Johnston. Protein kinase modulation of dendritic K^+ channels in hippocampus involves a mitogen-activated protein kinase pathway. *J. Neurosci.* 22: 4860-4868 (2002).

Zilberstein, Y. Fuchs, E. Hershtik, L. and A. Ayali. Neuromodulation for behavior in the locust frontal ganglion. *J. Comp. Physiol. A.* 190: 301-309 (2004).

Chapter 3

Natural variation in the thermotolerance of neural function and behavior due to a cGMP dependent protein kinase.

Ken Dawson-Scully[1], Gary A.B. Armstrong[2], Clement Kent[1], R. Meldrum Robertson[2], and Marla B. Sokolowski[1*]

[1] University of Toronto, Department of Biology, Mississauga, Ontario, L5L-1C6 Canada.

[2] Queen's University, Department of Biology, Kingston, Ontario, K7L-3N6 Canada.

[*] To whom correspondence should be addressed. E-mail: msokolow@utm.utoronto.ca

Citation: PLoS ONE 2:e773 (2007).

3.1 Abstract

Although it is acknowledged that genetic variation contributes to individual differences in thermotolerance, the specific genes and pathways involved and how they are modulated by the environment remains poorly understood. We link natural variation in the thermotolerance of neural function and behavior in *Drosophila melanogaster* to the *foraging* gene *(for,* which encodes a cGMP dependent protein kinase (PKG)) as well as to its downstream target, protein phosphatase 2A (PP2A). Genetic and pharmacological manipulations revealed that reduced PKG (or PP2A) activity caused increased thermotolerance of synaptic transmission at the larval neuromuscular junction. Like synaptic transmission, feeding movements were preserved at higher temperatures in larvae with lower PKG levels. In a comparative assay, pharmacological manipulations altering thermotolerance in a central circuit of *Locusta migratoria* demonstrated conservation of this neuroprotective pathway. In this circuit, either the inhibition of PKG or PP2A induced robust thermotolerance of neural function. We suggest that PKG and therefore the polymorphism associated with the allelic variation in *for* may provide populations with natural variation in heat stress tolerance. *for*'s function in behavior is conserved across most organisms, including ants, bees, nematodes, and mammals. PKG's role in thermotolerance may also apply to these and other species. Natural variation in thermotolerance arising from genes involved in the PKG pathway could impact the evolution of thermotolerance in natural populations.

3.2 Introduction

Exposure to extreme ambient temperatures will result in the eventual failure of normal neural functioning. This is most evident in poikilothermic organisms that have evolved numerous adaptations to temperature stress (Guschina and Harwood, 2006; Rinehart et al. 2006) including cellular homeoviscosity (Hazel, 1995), heat shock responses (Newman et al. 2003), evaporative heat loss (Bressin and Willmer, 2000) and a suite of behavioral strategies (Spiewok and Schmolz, 2006). At extremely high but sub-lethal temperatures, neural failure occurs through a string of events that start with motor pattern arrhythmicity which leads to spreading depression and eventual synaptic transmission failure. In humans, high internal body temperatures can lead to seizures, respiratory distress, cognitive dysfunction, brain damage or death (Glazer, 2005; Bouchama and Knochel, 2005). Because neural output failure occurs before permanent thermal damage (Tryba and Ramirez, 2004), there exists a potential for the recovery of circuit function upon return to normal temperatures. Yet, little is known about the substrates responsible for thermotolerance of the nervous system to stresses such as hyperthermia. Here we investigate natural variation in endogenous protection mechanisms exhibited by insects and discover a novel pathway that acts to increase the thermotolerance of the nervous system.

In nature, *Drosophila melanogaster* larvae spend their lives feeding and moving through fermenting fruit which can reach temperatures ranging from 10-50°C (Feder, 1997). Natural allelic variation in the *foraging (for)* gene, which encodes a cGMP dependent

protein kinase (PKG) results in rover (for^R) or sitter (for^s) larval foraging behaviors (Osborne et al. 1997). Rovers move more than sitters when feeding, and have higher PKG transcript levels and activities (de Belle and Sokolowski, 1989). However, it remains unclear how levels of PKG modulate neural function to influence behavior. Here we demonstrate for the first time that natural allelic variation in *for* influences levels of heat stress tolerance.

Two separate findings suggested a potential relationship between *for*-PKG and thermotolerance of neural function during hyperthermia (Renger et al. 1999; Ramirez et al. 1999). First, reduced PKG activity in sitters is associated with more transient (less conductance) neuronal K^+ currents than rovers, and pharmacological inhibition of PKG substantially reduces K^+ conductances (Renger et al. 1999). Second, in locusts, similar transient and reduced K^+ currents have been associated with heat shock-mediated protection of neural function, including induced thermotolerance of synaptic transmission (Ramirez et al. 1999) and central pattern generation (Newman et al. 2003). Thus, our hypothesis is that PKG, as a regulator of neuronal thermotolerance, could mediate protection against heat-induced neural trauma in *Drosophila melanogaster* and *Locusta migratoria*. Our results suggest a conserved function of the PKG pathway in thermotolerance.

3.3 Results and Discussion

Thermotolerance of behavior correlates with reduction of PKG.

To determine if *Drosophila for* variants have different levels of thermotolerance, we developed a behavioral assay that allowed us to increase temperature systematically and record the temperature at which larval mouth hook movements failed. Larval mouth hooks are critical for growth and survival because they are used to feed and move (Sokolowski, 1982). Mouth hook movements are easily visible in our preparation (see methods). When we increased temperature linearly at 5°C/min (starting from 22°C) the natural rover variant, for^R, exhibited mouth hook movement failure (see methods) at a significantly lower temperature than the natural sitter for^s (~2°C lower; Figure 3.1A.). Similarly, for^{s2}, the sitter mutant generated on a rover genetic background exhibited significantly higher failure temperatures than for^s and for^R suggesting that sitters with their lower PKG levels have increased thermotolerance (Osborne et al. 1997). Finally, because the for^R and for^{s2} strains share a common genetic background, our results demonstrate that the rover/sitter differences in thermotolerance are specific and localizable to *for*.

Thermotolerance of synaptic transmission via reduced PKG or PP2A inhibition.

To investigate the neural underpinnings of differences in thermotolerance between the *for* variants, we assayed evoked excitatory junction potentials (EJPs) at larval muscle 6. We

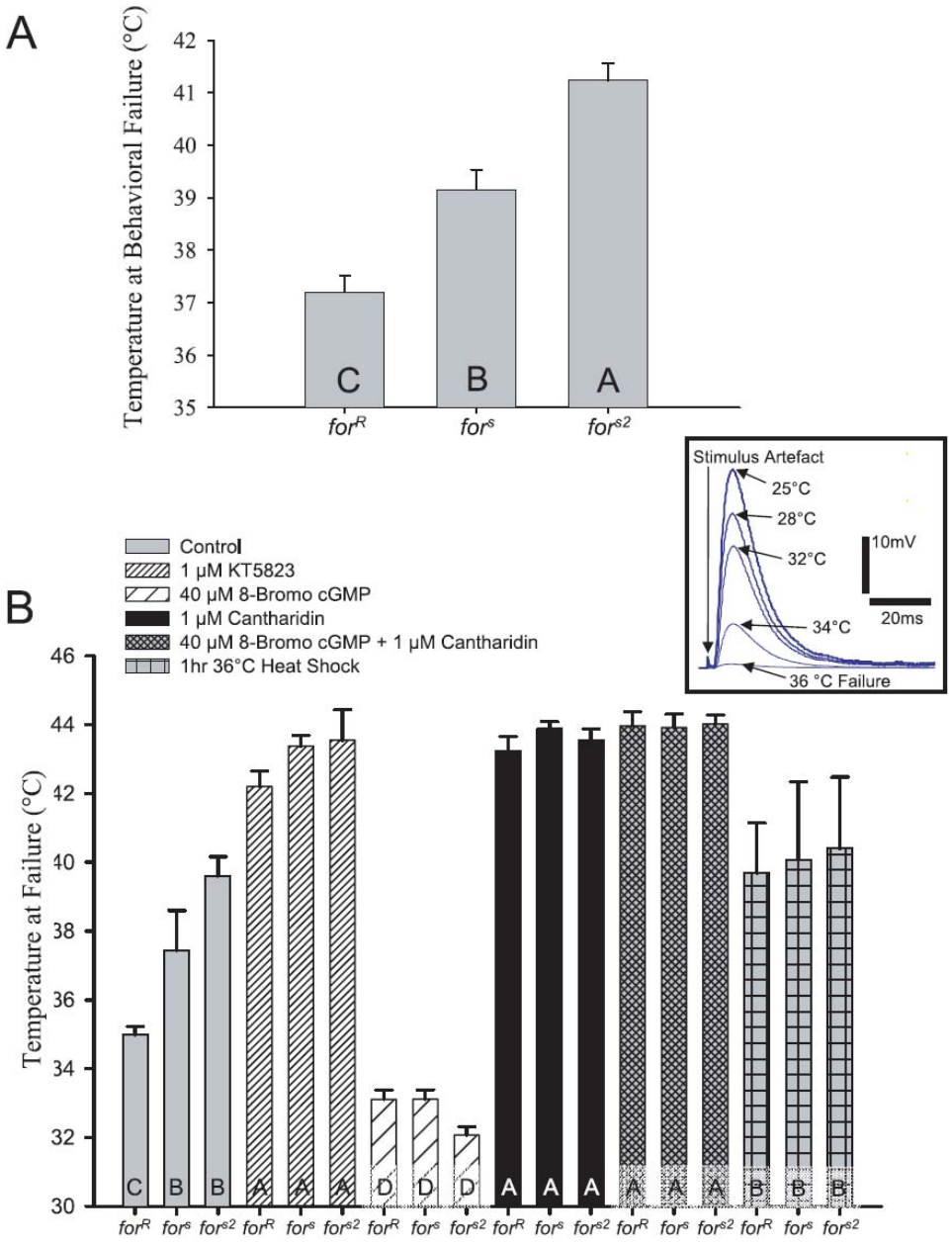
A
Temperature at Behavioral Failure (°C)
42
41
40
39
38
37
36
35
C
B
A
for^R
for^s
for^s2
Stimulus Artefact
25°C
28°C
32°C
34°C
36 °C Failure
10mV
20ms
B
Control
1 µM KT5823
40 µM 8-Bromo cGMP
1 µM Cantharidin
40 µM 8-Bromo cGMP + 1 µM Cantharidin
1hr 36°C Heat Shock
Temperature at Failure (°C)
46
44
42
40
38
36
34
32
30
C B B A A A D D D A A A A A A B B B
for^R for^s for^s2 for^R for^s for^s2 for^R for^s for^s2 for^R for^s for^s2 for^R for^s for^s2 for^R for^s for^s2

Figure 3.1

Figure 3.1. Hyperthermic failure of both behavior and NMJ synaptic transmission in 3rd instar *for*^{R}, *for*^{s} and *for*^{s2} *Drosophila melanogaster* larvae. (A) Temperature at behavioral failure of mouth hook movement significantly differed between larvae with different *for* genotypes, *for*^{R} failed at 37.2°C±0.3 (N=30), *for*^{s} failed at 39.2°C±10.4 (N=30) and *for*^{s2} failed at 41.2°C±0.3 (N=30). Significant differences were found across groups (Kruskal-Wallis on ranks, $H_{(2,90)}$=37.617, p<0.001) where letters (A, B, C) denote significant differences using a post-hoc test (Tukey, p<0.05). (B) Hyperthermic failure of evoked excitatory junction potential (EJP) failure (see inset) at the NMJ N>5 for all genotype and treatment combinations. Decreased thermotolerance of evoked synaptic transmission correlated with genotype (*for*^{s2}>*for*^{s}>*for*^{R} for thermotolerance), where significant differences were found across treatment groups (Two Way ANOVA, $F_{(5,118)}$=175.20, p<0.001). The involvement of PKG activity in thermotolerance was confirmed using pharmacological agents to activate PKG (40 µM 8-Bromo cGMP), inhibit PKG (1 µM KT5823) or inhibit a PKG phosphorylation target PP2A (1 µM Cantharidin). A combination of 8-Bromo cGMP and Cantharidin was also used, demonstrating that Cantharidin likely acts downstream of PKG activation. The three genotypes did not differ after being treated with a prior heat shock of 36°C for 1 hour and a 30 minute recovery. Letters in histogram bars represent statistical groupings using a post-hoc test, whereby bars with different letters are significantly different (Tukey, p<0.05). Error bars represent SEM.

increased temperature at a rate of 5°C/min (starting from 22°C) and found that synaptic transmission in *for*^{s} and *for*^{s2} failed (response less than 1 mV) at significantly higher temperatures than in *for*^{R}, suggesting that lower PKG activity leads to increased thermoprotection (Figure 3.1B). In order to confirm this, we used pharmacological manipulations of the PKG pathway. We pretreated dissected larval preparations with combinations of the cell-permeable PKG-specific inhibitor KT5823 and the PKG activator 8-Bromo-cGMP. Pharmacological inhibition of PKG significantly increased the temperature of synaptic failure in forR, fors, and fors2 larvae; in this case, failure for all three strains was not observed until ~42°C (Figure 3.1B). In contrast, activation of PKG via 8-bromo-cGMP significantly decreased thermotolerance (failure was observed at ~33°C) of synaptic transmission compared to non-treated controls in all for strains (Figure 3.1B).

To explore what might act downstream of PKG in thermotolerance, we looked for potential candidate molecules known to be intermediaries of both PKG and K^+ channels. Interestingly, PKG is known to phosphorylate protein phosphatase 2A (PP2A) leading to the de-phosphorylation of specific K^+ channels and an increase in channel conductance (Zhou et al. 1996; White et al. 2002). We found that the PP2A-specific inhibitor Cantharidin increased the thermotolerance of synaptic transmission as strongly as did the PKG inhibitor (Figure 3.1B). To test if PP2A inhibition acted within the PKG pathway we simultaneously applied both the PKG activator (8-Bromo-cGMP) and the PP2A inhibitor (Cantharidin) to the preparation. We found that the decrease in thermotolerance

found by increasing PKG activity with 8-Bromo-cGMP was abolished when PP2A was inhibited, suggesting PP2A acts downstream of PKG. Thus, both genetic and pharmacological analyses demonstrate that there is a negative relationship between PKG activity and the thermotolerance of neuromuscular transmission in *D. melanogaster* larvae. These results paralleled those found for mouth hook movements (Figure 3.1A), our behavioral measure of thermotolerance.

PKG inhibition and PP2A inhibition induce rapid thermotolerance of neural circuitry. To determine if the thermoprotective consequences of PKG manipulations are conserved and also apply to central circuitry and motor pattern generation, we measured its effects on thermotolerance in an established model system used to study thermotolerance, the ventilatory motor pattern generator of the locust, *Locusta migratoria* (Newman et al. 2003). Locusts that have undergone a prior heat shock exhibit a robust ~10°C increase to the thermotolerance of neural function during hyperthermia (Newman et al. 2003; Dawson-Scully and Robertson, 1998) as well as a reduction in neuronal whole cell potassium currents (Ramirez et al.1999). This suggests that PKG-mediated K^+ current reductions in this model could cause significant changes in thermal protection. We observed thermoprotection and rapid recovery of the circuit when we pressure-injected KT5823 into the neural circuit for ventilation ten minutes prior to increasing the temperature (Figure 3.2B). Our initial trials of the induction of thermotolerance in this circuit via PKG inhibition demonstrated magnitudes of response equal to the data on previously published heat shock pretreated locusts (Newman et al. 2003; Dawson-Scully

and Robertson, 1998). Thus, for comparison, we examined neural output failure (observable loss of firing pattern > 2sec) from both control (C, no heat shock) and heat-shocked (HS) locusts with a combination of pharmacological treatments similar to those used in the *Drosophila* preparation [combinations of cell-permeable PKG-specific inhibitor (KT5823), PKG activator (8-Bromo-cGMP), PP2A inhibitor (Cantharidin)].

In three separate experiments, a prior heat shock induced a significant increase in thermotolerance of the ventilatory motor pattern generator increasing the tolerance of the circuit by ~8°C (Figure 3.2B i-iii). Untreated controls (no pharmacological manipulation, no heat shock) also took approximately twice the time for the circuit to recover when compared to untreated heat shocked animals (Figure 3.2C i-iii). These results are similar to prior reports on the effect of a HS pretreatment on central circuitry during hyperthermia (Newman et al. 2003). Thermotolerance was significantly increased in control animals by the application of the PKG inhibitor KT5823 (Figure 3.2Bi) and the PP2A inhibitor Cantharidin (Figure 3.2Bii), extending the thermotolerance of the neural circuit by ~8°C. Further, recovery time of the circuit was also significantly decreased (~70%) in KT5823-treated animals (Figure 3.2Ci) and Cantharidin-treated animals (Figure 3.2Cii) compared with untreated controls. Interestingly, there were no significant differences between untreated HS preparations and animals treated with either PKG or PP2A inhibitors except for the recovery time of Cantharidin treated HS animals. Therefore, PKG or PP2A inhibition increases the thermotolerance of neural function in this locust central circuit and this response was as equally pronounced as a prior

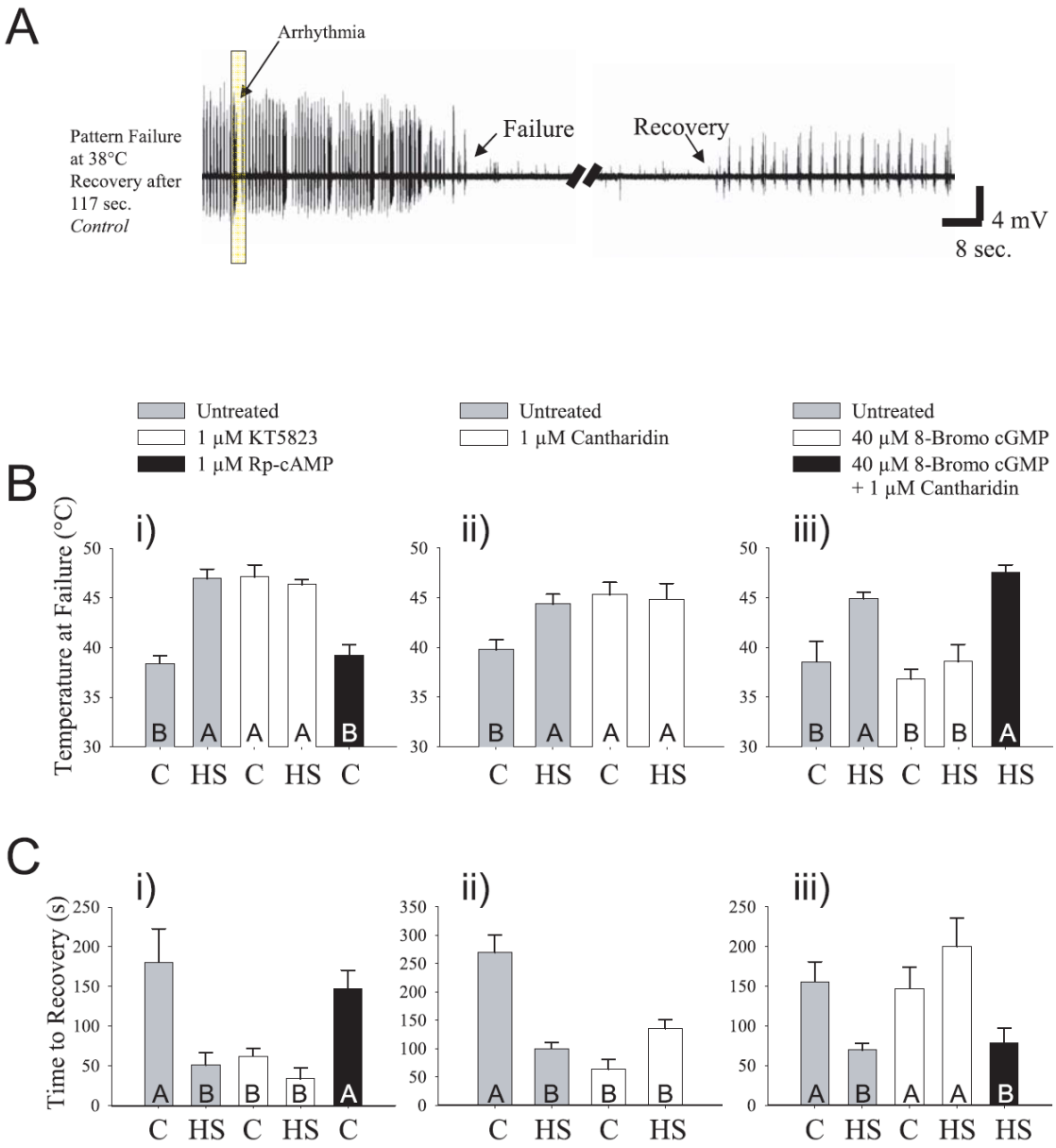
A
Arrhythmia
Pattern Failure
at 38°C
Recovery after
117 sec.
Control
Failure
Recovery
4 mV
8 sec.
B
Untreated
1 µM KT5823
1 µM Rp-cAMP
Untreated
1 µM Cantharidin
Untreated
40 µM 8-Bromo cGMP
40 µM 8-Bromo cGMP
+ 1 µM Cantharidin
Temperature at Failure (°C)
i)
ii)
iii)
C HS C HS C
C HS C HS
C HS C HS HS
C
Time to Recovery (s)
i)
ii)
iii)
C HS C HS C
C HS C HS
C HS C HS HS

Figure 3.2

Figure 3.2. Hyperthermic failure of locust ventilatory motor pattern generation. (A) Sample traces of the ventilatory rhythm recorded from an abdominal expiratory muscle in a control locust. Note the ventilatory arrhythmias prior to failure. At failure, temperature was allowed to return to room temperature and time to recovery was recorded. Note that the ventilatory motor pattern after recovery is at a lower frequency just prior to failure because the temperature is lower. (B) Three separate experiments were performed to examine the pharmacological effects of i) PKG and PKA inhibitors ii) PP2A inhibitor and iii) PKG activator and PKG activator coupled with the PP2A inhibitor. (B i) Reduction in PKG activity (1 μM KT5823) increased the thermotolerance of neural function as strongly as a prior heat shock treatment during hyperthermia, whereas PKA inhibition (1μM Rp-cAMP) had no effect. Significant treatment effects were found (ANOVA $F_{(4,31)}$=18.71, $p<0.001$; N>4 for all treatments) where letters (A, B, C) denote significant differences using a post-hoc test (Tukey, $p<0.05$). (B ii) Reduction of PP2A activity (1μM Cantharidin) also increased the thermotolerance of neural function during hyperthermia where significant treatment effects were found (ANOVA $F_{(3,31)}$=4.60, $p<0.001$; N>6 for all treatments). (B iii) Activation of PKG using 40 μM 8-Bromo cGMP did not increase the thermotolerance of the circuit, but abolished the protective effects of heat shock preconditioning. Moreover, the PP2A inhibitor Cantharidin counteracted the effect of 8-Bromo cGMP in HS animals thereby inducing maximal thermotolerance. Significant treatment effects were found (ANOVA $F_{(4,41)}$=9.60, $p<0.001$; N>6 for all treatments). (C) Recovery time of the motor pattern upon return to

room temperature showed corresponding differences in the same treatment groups (short recovery times associated with high failure temperatures in B). Here too significant differences were found across treatments: i) ANOVA $F_{(4,31)}=7.62$, $p<0.001$, $N>4$; ii) ANOVA $F_{(3,32)}=19.65$, $p<0.001$, $N>6$; iii) ANOVA $F_{(4,41)}=4.78$, $p<0.001$, $N>6$, Letters in histogram bars represent statistical groupings whereby bars with different letters are significantly different using a post-hoc test (Tukey, $p<0.05$). Error bars represent SEM.

conditioning heat shock. We found the same pattern in the thermotolerance of synaptic transmission at the NMJ of *Drosophila* larvae. for^{R}, for^{s}, and for^{s2} did not differ in thermotolerance when exposed to a prior heat shock of 36°C for 1 hr with a 30 min recovery (Figure 3.1B). In order to determine if the observed thermoprotective effects are specific to the inhibition of PKG, we examined the effects of inhibition of protein kinase A (PKA) Rp-cAMP. Rp-cAMP produced no significant differences in failure temperature or recovery time compared to untreated controls (Figures 3.2Bi,Ci). Interestingly, previous work has shown that PKA influences thermotolerance of neural function in an opposite fashion to PKG and in a much slower time scale (1 hr vs. several min) (Armstrong et al. 2006).

To examine the rapidity of the effect of pharmacological manipulation on thermotolerance we developed an acute treatment with the PKG inhibitor KT5823. When the temperature ramp reached 30°C (approximately three minutes before failure), we pressure-injected 25nL of 1μM KT5823 into previously untreated animals and observed an extremely rapid and equally pronounced thermal protection of the circuit when compared to data shown in Figure 3.2A (not shown). This showed that unlike a heat shock conditioning, the protective effect of PKG and PP2A inhibition can be induced rapidly.

PKG activator 8-bromo-cGMP abolishes thermoprotective effect of a prior heat shock.

To obtain a better understanding of how the protective effect of a heat shock pre-treatment interacts with the PKG pathway, we examined the effect of the PKG activator 8-Bromo cGMP on previously heat shocked locusts. Initially we found that there was no significant difference in failure temperature or recovery time of the circuit in non-heat shocked animals with and without 8-Bromo cGMP (Figures 3.2B, C). However, HS-mediated thermotolerance was abolished with the addition of 8-Bromo cGMP. Compared with untreated HS animals, simultaneous applications of both the PKG activator and the PP2A inhibitor in HS animals resulted in maximal thermotolerance in failure temperature and reduced times to recovery. These results coupled with the *Drosophila* larval experiments (see above) indicated that PP2A likely acts downstream from PKG and interacts with the same pathway affected by heat shock preconditioning.

PKG and PP2A inhibition abolish arrhythmic events arising from heat stress. Arrhythmias (pattern interruptions) in the ventilatory motor pattern indicate stress-induced transient malfunction of the pattern generating mechanisms. We found that either a prior heat shock or inhibition of PKG or PP2A reduced the number of arrhythmias observed during hyperthermia (not shown). Locusts that did not receive a pharmacological treatment or a heat shock had the highest prevalence of arrhythmias observed across all preparations during temperature increases (60%). However, 8-bromo-cGMP-treated control (50%) and 8-bromo-cGMP-treated heat shock (40%) preparations were also high compared to all other treatments. Finally, non-heat shocked animals exposed to PKG inhibitor exhibited the lowest occurrence of arrhythmias

(12.5%). Thus, both PKG and PP2A inhibition not only protect synaptic transmission between synapses, but their inhibition also protects the delicate coordination of neural circuitry during hyperthermic stress. Inhibition of these enzymes did not alter neural temporal properties.

Little is known about the genes and pathways that contribute to nervous system function under thermal stress despite their obvious importance to the survival of organisms. We identify two molecules, cGMP-dependent protein kinase (PKG) and protein phosphatase 2A (PP2A) that rapidly and dramatically extend the thermal operating range of neural function. By decreasing PKG or PP2A activity we increased the thermotolerance of synaptic transmission at the NMJ of *Drosophila* larvae and the thermotolerance of the ventilatory motor pattern in adult *Locusta*. Similarly, activation of PKG via 8-Bromo cGMP decreased the thermotolerance of synaptic transmission at the NMJ of *Drosophila* larvae and abolished the thermotolerance conferred via a prior heat shock in adult *Locusta*.

Surprisingly, in spite of the numerous investigations into the roles of HSPs, little is known about their mechanisms of action in nervous tissue. Specifically, it is not known whether signaling pathways such as PKG and PP2A act in conjunction with the HS response pathway to protect neural function (Dawson-Scully and Robertson, 1998; Karunanithi et al. 1999). However, as mentioned previously, our ability to abolish the protective effects of a prior HS through the application of cGMP in *Locusta* suggests that

PKG may interact with the HS response pathway. One possible model is that PKG-PP2A interacts with a stress inducible heat shock protein such as HSP27. HSP27 is a chaperone from the small HSP family known to confer protection from starvation, hyperthermia and oxidative stress and to play a role in *Drosophila* lifespan (Wang et al. 2004). In order for HSP27 to act as a chaperone, it requires dephosphorylation by PP2A (Cairns et al. 1994). We have shown pharmacologically that a decrease in PP2A rapidly induces thermotolerance of neural function (Figures 3.1 & 3.2). Thus, it is feasible that the previously reported slower time course (3 to 4 hr) of protection to neural function resulting from a prior HS (Newman et al. 2003; Ramirez et al.1999; Dawson-Scully and Robertson, 1998; Whyard et al. 1986) may be due to upregulated HSP27 which uses a large proportion of the available intracellular active PP2A, thereby mimicking PP2A inhibition. Whether PKG-PP2A directly interacts with heat shock response pathways remains to be determined.

The hyperthermic temperatures used in our experiments are ecologically relevant. Fermenting fruit, a main habitat of *D. melanogaster* larvae, can range in temperature from 10-50°C in nature and temperatures at the higher end are lethal for *D. melanogaster* larvae (Feder, 1997). Thus, the rover/sitter differences in thermotolerance and behavior should have fitness consequences in nature. Sitter larvae are expected to have higher survivorship while foraging in fruit under hyperthermic conditions. In fact, *D. melanogaster* larvae collected from a desert site in Tunisia behaved as sitters whereas those collected 1500m away in an oasis site behaved more rover-like (Sokolowski and

Carton, 1990). Rovers may avoid temperature stress within the fruit because of their greater tendency to leave their food (de Belle and Sokolowski, 1987). To what extent, the observed ~2°C differences in the upper temperature limit for larval mouth hook movement behavior in rovers and sitters reflects fitness differences in nature remains to be determined. Interestingly, a 2°C increase in seasonal environmental temperatures in the poikilothermic common eelpout, *Zoarces viviparous,* has dramatic effects on survival in the wild (Pörtner and Knust, 2007). Similarly, the survivorship of rover and sitter larvae in nature could vary depending on how hyperthermic conditions vary in space and time.

We found similar functions for PKG and PP2A in rapid thermoprotection of the nervous systems of both *D. melanogaster* and *L. migratoria.* This suggests a conserved role for these molecules in thermotolerance in response to environmental stress. Whether or not our findings can be extended to mammalian models remains to be determined. If so, manipulations of the PKG pathway could be used to rapidly treat neural failure during hyperthermic and febrile episodes in mammals, including humans.

3.4 Materials and Methods

D. melanogaster Experiments:

Animals: We used foraging 3rd instar (96 ± 2 hr) *Drosophila melanogaster* larvae reared on a yeast-sugar-agar medium at 24±1°C under 12L:12D light cycle with lights on at 0800 hr. We used a rover strain homozygous for the for^R allele, and two sitter strains homozygous for for^s and for^{s2}. The wild type-derived rover (for^R) and sitter (for^s) strains are natural allelic variants of the *for* gene which is located on chromosome-2. To control for genetic background they have co-isogenic third chromosomes (originating from the rover strain) and shared X-chromosomes. The for^{s2} strain is a sitter mutant generated on a rover for^R genetic background (Pereira and Sokolowski, 1993) such that for^{s2} differs from for^R only in their alleles at *for*. for^s and for^{s2} larvae have significantly lower PKG enzyme activity than for^R (Osborne et al. 1997). N indicates the number of animals while n indicates the number of trials. Both are reported in the figure legends.

Behavior:

Drosophila larvae were secured to a glass dish in 2 ml of Schneider's Insect Medium (Sigma) using a blunt magnetic placed pin distal to the CNS. Preparations were heated on a Peltier plate (5°C/min) from 22°C. We measured the persistence of rhythmic mouth hook movement. The frequency of mouth hook movements increased (>3Hz) with increasing temperature until abrupt failure. Failure of mouth hook movement was considered to have occurred when mouth hook movements stopped for at least 30 sec. The temperature at the beginning of this 30 sec period was recorded as the failure

temperature. Pauses in mouth hook movement occur occasionally although no difference in pausing was observed between rovers and sitters. The temperature was controlled by a single switch (on/off) and no other settings are manipulated. Prior to each experiment the ramping of temperature was recorded for several runs to verify its accuracy. We found it to be highly consistent.

Electrophysiology:

Drosophila larvae were dissected and pinned on a glass dish in Schneider's Insect Medium (Sigma); internal organs and the central nervous systems were removed to reveal the segmental muscles and their corresponding nerves. Segmental nerves in segments 3 or 4 were stimulated using a suction electrode and the corresponding excitatory junction potential (EJP) was recorded from muscle 6 with a glass intracellular electrode filled with 3M KCl (40-80 MΩ). The preparation was superfused with HL-6 saline (Macleod et al. 2002) with 1 mM $[Ca^{2+}]_e$ and heated at a rate of approximately 5°C/min from room temperature (~20°C) to synaptic failure (Figure 3.1B inset). Pharmacological treatments of preparations included one or a combination of the following agents (all chemicals obtained from Sigma): 1 μM KT5823 (Calbiochem; PKG-specific inhibitor; a relatively specific PKG inhibitor (Grider, 1993) that competes for the ATP binding site on the kinase (Kase et al. 1987)), 40 μM 8-bromo-guanosine 3',5'-cyclic monophosphate (VWR; 8-bromo-cGMP; cGMP analogue), 1 μM Cantharidin (Calbiochem; PP2A-specific inhibitor; a cell permeable terpenoid that binds to PP2A at the "Cantharidin binding site" to inhibit its action (Li and Casida, 1992)) and 1 μM Rp-cAMP (PKA inhibitor;

competitive with cAMP at PKA binding sites (Rothermel and Parker Botelho, 1998)). Preparations were bathed with the compound(s) of interest for 5 min prior to heating. KT5823, 8-Bromo-cGMP, and Cantharidin were dissolved in DMSO, resulting in a 0.2% (v/v) DMSO concentration in the saline during treatment. 0.2% (v/v) DMSO in physiological saline was used as a control for the solvent's effects on synaptic transmission, and no differences were observed.

Cantharidin (Specificity: PP2A>PP1>>PP2B) is an inhibitor of protein phosphatase 2A (IC_{50} = 40 nM) and it can inhibit protein phosphatase 1 at higher concentrations (IC_{50} = 473 nM). To rule out possible effects of protein phosphatase 1 inhibitiion, we measured the temperature of failure of synaptic transmission in for^R at the NMJ using a low 100 nM concentration of Cantharidin (Li et al. 1993; Li and Casida, 1992; Graziano et al. 1988). This concentration is known to specifically inhibit PP2A. We found that synaptic transmission at the NMJ in for^R treated with 100 nM Cantharidin failed at 42.7°C +/- 0.33, whereas for^R treated with 1 μM Cantharidin failed at 43.2°C +/- 0.42; no significant differences were found between the high and low Cantharidin treatments (Student's t-test, t=1.045, df=11, P=0.319).

L. migratoria Experiments:

Animals: Male locusts aged 4-6 weeks were obtained from a crowded colony (12:12 photoperiod; 25±1°C daytime temperature) maintained in the Department of Biology at

Queen's University. Heat shocked (HS) animals were held for 3 hr in a 2L plastic container in a humid incubator at 45°C and allowed 1 hr for recovery. Control animals were held at room temperature for 4 hr prior to experiments. Animals were dissected and pinned on a cork board; overlying tissue was removed exposing the dorsal surface of the metathoracic ganglion.

Electrophysiology

Ventilatory motor patterns were monitored using a copper electromyographic (EMG) electrode positioned on expiratory muscle 161 in the second abdominal segment. Standard locust saline was superfused through thoracic and abdominal cavities and heated at a rate of 5°C/min until motor pattern failure at which point saline was allowed to return to room temperature. Pressure injections (32±13.5 nL, 10psi, 150ms) into the ventilatory neuropil were made with glass microelectrodes filled with either 1μM KT5823 (using DMSO) in standard locust saline or locust saline alone (sham pressure-injections contained DMSO) 10 min before the temperature ramp (pre-treated) or during the temperature ramp at 30°C (acutely treated; ~3 min before failure in controls).

Statistics

Statistical analyses used One-Way and Two-Way ANOVA (F is reported) and One-Way ANOVA on ranks (H is reported; Kruskal Wallis) followed by a post-hoc Tukey Multiple Comparison test. Figures show significant differences using letter designations, where A

is the highest mean, B indicates the next highest mean, etc. Data points with different letters show significant differences ($P<0.05$).

3.5 References

Armstrong, G.A. Shoemaker, K.L. Money, T.G. and R.M. Robertson. Octopamine mediates thermal preconditioning of the locust ventilatory central pattern generator via a cAMP/protein kinase A signaling pathway. *J. Neurosci.* 26:12118-12126 (2006).

Bouchama, A. anf J.P. Knochel. Heat Stroke. *N. Engl. J. Med.* 346: 1978 -1988 (2002).

Bressin, S. and P.G. Willmer. Estimation of thermal constants: the importance of using equilibrium temperature rather than ambient temperature demonstrated with hoverflies (Diptera, Syrphidae, genus Eristalis) *J. Exp Biol.* 203: 2511- 2517 (2000).

Cairns, J. Qin, S. Philp, R. Tan, Y.H. and G.R. Guy. Dephosphorylation of the small heat shock protein Hsp27 in vivo by protein phosphatase 2A. *J. Biol. Chem.* 269: 9176 - 9183 (1994).

Dawson-Scully, K. and R.M. Robertson. Heat shock protects synaptic transmission in flight motor circuitry of locusts. *Neuroreport* 9: 2589-2593 (1998).

de Belle, J.S. and M.B. Sokolowski. Heredity of rover/sitter: alternative foraging strategies of *Drosophila melanogaster*. *Heredity* 59: 73-83 (1987).

de Belle, J.S. and M.B. Sokolowski. Genetic localization of foraging (fog): a major gene for larval behavior in drosophila melanogaster. *Genetics* 123: 157-163 (1989).

Feder, M.E. Necrotic fruit: a novel model system for thermal biologists. (1997) *J. Therm. Biol.* 22**:** 1-9 (1997).

Glazer, J.L. Management of heatstroke and heat exhaustion. *Am. Fam. Physician*.71: 2133-2140 (2005).

Graziano, M.J. Pessah, I.N. Matsuzawa, M. and J.E. Casida. Partial characterization of specific cantharidin binding sites in mouse tissues. *Mol. Pharmacol.* 6: 706-712 (1988).

Grider, J.R. Interplay of VIP and nitric oxide in regulation of the descending relaxation phase of peristalsis. *Am. J. Physiol.* 264: G334-G340 (1993).

Guschina, I and J. Harwood. Mechanisms of temperature adaptation in poikilotherms. *FEBS Lett.* 580: 5477-5483 (2006).

Hazel, J.R. Thermal adaptation in biological membranes: is homeoviscous adaptation the explanation? *Annu. Rev. Physiol.* 57: 19-42 (1995).

Karunanithi, S. Barclay, J.W. Robertson, R.M. Brown, I.R. and H.L. Atwood. Neuroprotection at *Drosophila* synapses conferred by prior heat shock. *J. Neurosci.* 19: 4360- 4369 (1999).

Kase, H. Iwahashi, K. Nakanishi, S. Matsuda, Y. Yamada, K. Takahashi, M. Murakata, C. Sato, A. and M. Kaneko. (1987). K-252 compounds, novel and potent inhibitors of protein kinase C and cyclic nucleotide-dependent protein kinases. *Biochem. Biophys. Res. Comm.* 142: 436–440 (1987).

Li, Y.M. and J.E. Casida. Cantharidin-binding protein : identification as protein phosphatase 2A. *Proc. Natl. Acad. Sci.* 89: 11867-11870 (1992).

Li, Y.M. Mackintosh, C. and J.E. Casida. Protein phosphatase 2A and its [3H]cantharidin/[3H]endothall thioanhydride binding site. Inhibitor specificity of cantharidin and ATP analogues. *Biochem. Pharmacol.* 46: 1435-1443 (1993).

Macleod, G.T. Hegstrom-Wojtowicz, M. Charlton, M.P. and H.L. Atwood. Fast cacium signals in Drosophila motor neuron terminals. *J. Neurophysiol.* 88: 2659-2663 (2002).

Newman, A.E.M. Foerster, M. Shoemaker, K.L. and R.M. Robertson. Stress-induced thermotolerance of ventilatory motor pattern generation in the locust, *Locusta migratoria*. *J. Insect Physiol.* 49:1039-1047 (2003).

Osborne, K.A. Robichon, A. Burgess, E. Butland, S. Shaw, R.A. Coulthard, A. Pereira, H.S. Greenspan, R.J. and M.B. Sokolowski. Natural behavior polymorphism due to a cGMP-dependent protein kinase of *Drosophila*. *Science* 277: 834- 836 (1997).

Pereira, H.S. and M.B. Sokolowski. Mutations in the larval foraging gene affect adult locomotory behavior after feeding in drosophila melanogaster. *Proc. Natl. Acad. Sci.* 90: 5044-5046 (1993).

Pörtner, H.O. and R. Knust. Climate change affects marine fishes through the oxygen limitation of thermal tolerance. *Science* 315: 95-97 (2007).

Ramirez, J.M. Elsen, F.P. and R.M. Robertson. Long-term effects of prior heat shock on neuronal potassium currents recorded in a novel insect ganglion slice preparation. *J. Neurophysiol.* 81: 795-802 (1999).

Renger, J.J. Yoa, W.D. Sokolowski, M.B. and C.F. Wu. Neuronal polymorphism among natural alleles of a cGMP-dependent kinase gene, *Foraging*, in *Drosophila*. *J. Neurosci.* 19: RC28 (1999).

Rinehart, J.P. Hayward, S. Elnitsky, M.A. Sandro, L. Lee, R. Jr. and D.J. Denlinger. Continuous up-regulation of heat shock proteins in larvae, but not adults, of polar insects. *Proc. Natl. Acad. Sci.* 103: 14223-14227 (2006).

Rothermel, J.D. and L.H. Parker Botelho. A mechanistic and kinetic analysis of the interactions of the diastereoisomers of adenosine 3',5'-(cyclic)phosphorothioate with purified cyclic AMP-dependent protein kinase. *Biochem. J.* 251: 757–762 (1988).

Sokolowski, M.B. and Y. Carton. Microgeographic variation in *Drosophila melanogaster* larval behavior. *J. Insect Behav.* 2: 829-833 (1990).

Sokolowski, M.B. *Drosophila* larval foraging behaviour: digging. (1982) *Animal Behav.* 30: 1252-1253 (1982).

Spiewok, S. and E. Schmolz. Changes in temperature and light alter the flight speed of hornets (*Vespa crabro* L.). *Physiol. Biochem. Zool.* 79: 188-193 (2006).

Tryba, A.K. and J.-M. Ramirez. Hyperthermia modulates respiratory pacemaker bursting properties. *J. Neurophysiol.* 92: 2844-2852 (2004).

Wang, H.D. Kazemi-Esfarjani, P. and S. Benzer. Multiple-stress analysis for isolation of *Drosophila* longevity genes. *Proc. Natl. Acad. Sci.* 101: 12610-12614 (2004).

White, R.E. Han, G. Maunz, M. Dimitropoulou, C. El-Mowafy, A.M. Barlow, R.S. Catravas, J.D. Snead, C. Carrier, G.O. Zhu, S. and X.Yu. Endothelium-independent effect of estrogen on Ca^{2+}-activated K^{+} channels in human coronary artery smooth muscle cells. *Cardiovasc Res.* 53: 650-661 (2002).

Whyard, S., Wyatt, G.R., and V.K. Walker. The heat shock response in *Locusta migratoria*. *J. Comp. Physiol. B.* 156: 813-817 (1986).

Zhou, X.B. Schlossmann, J. Hofmann, F. Ruth, P. and M. Korth. Protein phosphatase 2A is essential for the activation of Ca^{2+}-activated K^{+} currents by cGMP-dependent protein kinase in tracheal smooth muscle and Chinese hamster ovary cells. *J. Biol. Chem.* 271: 19760-19767 (1996).

Chapter 4

Stress Preconditioning of Spreading Depression in the Locust CNS.

Corinne I. Rodgers, Gary A. B. Armstrong, Kelly L. Shoemaker, John D. LaBrie, Christopher D. Moyes, and R. Meldrum Robertson

Queen's University, Department of Biology, Kingston, Ontario, Canada K7L 3N6

Citation: PLoS ONE 2:e1366 (2007).

4.1 Abstract

Cortical spreading depression (CSD) is closely associated with important pathologies including stroke, seizures and migraine. The mechanisms underlying SD in its various forms are still incompletely understood. Here we describe SD-like events in an invertebrate model, the ventilatory central pattern generator (CPG) of locusts. Using K^+ -sensitive microelectrodes, we measured extracellular K^+ concentration ($[K^+]_o$) in the metathoracic neuropile of the CPG while monitoring CPG output electromyographically from muscle 161 in the second abdominal segment to investigate the role K^+ in failure of neural circuit operation induced by various stressors. Failure of ventilation in response to different stressors (hyperthermia, anoxia, ATP depletion, Na^+/K^+ ATPase impairment, K^+ injection) was associated with a disturbance of CNS ion homeostasis that shares the characteristics of CSD and SD-like events in vertebrates. Hyperthermic failure was preconditioned by prior heat shock (3h, 45°C) and induced-thermotolerance was associated with an increase in the rate of clearance of extracellular K^+ that was not linked to changes in ATP levels or total Na^+/K^+ ATPase activity. Our findings suggest that SD-like events in locusts are adaptive to terminate neural network operation and conserve energy during stress and that they can be preconditioned by experience. We propose that they share mechanisms with CSD in mammals suggesting a common evolutionary origin.

4.2 Introduction

Neural function under stressful conditions is contingent upon maintaining ion gradients across cell membranes, which are essential for neuronal signaling. Hyperthermic failure of neural operation is associated with a loss of ion homeostasis and a major redistribution of ions, including K^+ (Wu and Fisher, 2000; Robertson, 2004a). This pattern of ionic disturbance, monitored by an abrupt rise in extracellular potassium ($[K^+]_o$) and depression of electrical activity, shares many characteristics of cortical spreading depression (CSD (Leão, 1944)). In mammalian tissue CSD has been associated with several important pathologies including stroke, seizures and migraine (Somjen, 2001; Somjen, 2002; Smith et al. 2006). In an insect model system, the onset of hyperthermic failure can be preconditioned by prior stress (Newman et al. 2003). Preconditioning resulting in ischaemic tolerance is considered an evolutionarily conserved phenomenon of cerebral plasticity, evident in invertebrates and vertebrates including humans (Gidday, 2006). Here we characterize stress-induced neural depression of ventilatory central pattern generation in the migratory locust to determine its similarity to CSD and we tested the role of the Na^+/K^+ ATPase in mediating the preconditioning effects of prior heat shock (HS) on hyperthermic neural failure.

Ventilation in locusts is under the control of a reliable central pattern generator (CPG) located in the metathoracic ganglion (MTG) (Huster, 1975; Bustami and Hustert, 2000) which is sensitive to several forms of stress including changes of internal CO_2 (Gulinson and Harrison, 1996; Henderson et al. 1998), pH (Snyder et al. 1980) and temperature

(Banks et al. 1975; Lighton and Lovegrove, 1990; Henderson et al. 1998; Newman et al. 2003). In particular, increased temperature elevates the cycle frequency of the ventilatory motor pattern from 1 cycle/s at room temperature to 3 cycles/s just prior to hyperthermic failure at 38-40 °C (Newman et al. 2003). A subsequent return to room temperature permits recovery of pattern generation within 2 to 3 minutes. Several important neural properties are protected by prior HS (for review, see refs: Robertson, 2004a; Robertson, 2004b). HS-mediated thermoprotection of the ventilatory CPG results in an increase in the failure temperature and a decrease in the time taken to recover, and can be mimicked by octopamine acting through a cAMP signaling pathway (Armstrong et al. 2006). Given that circulating octopamine increases after heat stress in locusts (Davenport and Evans, 1984), that octopamine reduces K^+ conductances and increases activity of the Na^+/K^+ ATPase (Walther and Zittlau, 1998) and that HS reduces whole cell K^+ currents in locust metathoracic neurons (Ramirez et al. 1999), we hypothesized that HS preconditioning acts by stabilizing K^+ homeostasis.

We compared the dynamics of $[K^+]_o$ during failure of motor pattern generation induced by different stressors (hyperthermia, anoxia, ATP depletion, K^+ injection) and used ouabain (a specific Na^+/K^+ ATPase toxin) both to induce repetitive, propagating waves of ionic disturbance and to test the role of the Na^+/K^+ ATPase in HS-mediated thermoprotection. We demonstrate that the surges of $[K^+]_o$ associated with cessation of ventilatory motor patterning represent SD-like phenomena whose occurrence can be interpreted as an adaptive response to conserve energy in the locust, rather than the

culmination of cellular collapse. Using TTX and TEA we show that SD-like behaviour is not activity-dependent and that some part of the $[K^+]_o$ surge is via TEA-sensitive K^+ channels. Finally we show that the hyperthermic SD-like event can be preconditioned by a prior HS acting to increase the rate of $[K^+]_o$ clearance, and that the effect of HS is not obviously mediated by the Na^+/K^+ ATPase.

4.3 Results

Stress-induced failure of the ventilatory motor pattern correlates with a sharp rise in extracellular potassium.

Ventilatory motor pattern activity and extracellular potassium ion concentrations in the MTG were measured during treatment with various cellular stressors in order to establish a relationship between stress-induced circuit failure and an extracellular build-up of potassium ions (Figures 4.1 and 4.2). Hyperthermic failure of the ventilatory CPG was reliably associated with an abrupt increase in $[K^+]_o$, which occurred in 100% of CON preparations (Figure 4.1A) and of all preparations irrespective of preconditioning or pharmacological treatment ($N_{total} = 85$). When the temperature was allowed to return to baseline levels, $[K^+]_o$ remained elevated before gradually decreasing (Figure 4.1A). Post-stress recovery of the ventilatory central pattern generator correlated with restoration of $[K^+]_o$ to initial levels (Figure 4.1A). In addition, abrupt surges in $[K^+]_o$ were reliably triggered by ATP depletion using 10^{-3}M sodium azide (NaN_3) and anoxia (100% N_2) (Figure 1B and C). Peak $[K^+]_o$ reached during surges induced by hyperthermia (52 ± 2 mM), NaN_3 (85 ± 2 mM) and anoxia (79 ± 3 mM) were different (one-way ANOVA, $P < 0.001$, $F_{(2,38)} = 43.634$). The peak $[K^+]_o$ induced by hyperthermia was lower than the $[K^+]_o$ peaks induced by NaN_3 and anoxia (*post hoc* Tukey tests, $P < 0.05$). The recovered motor pattern was robust but not identical to the pre-stress motor pattern (see e.g. Figure 4.1Ci and ii).

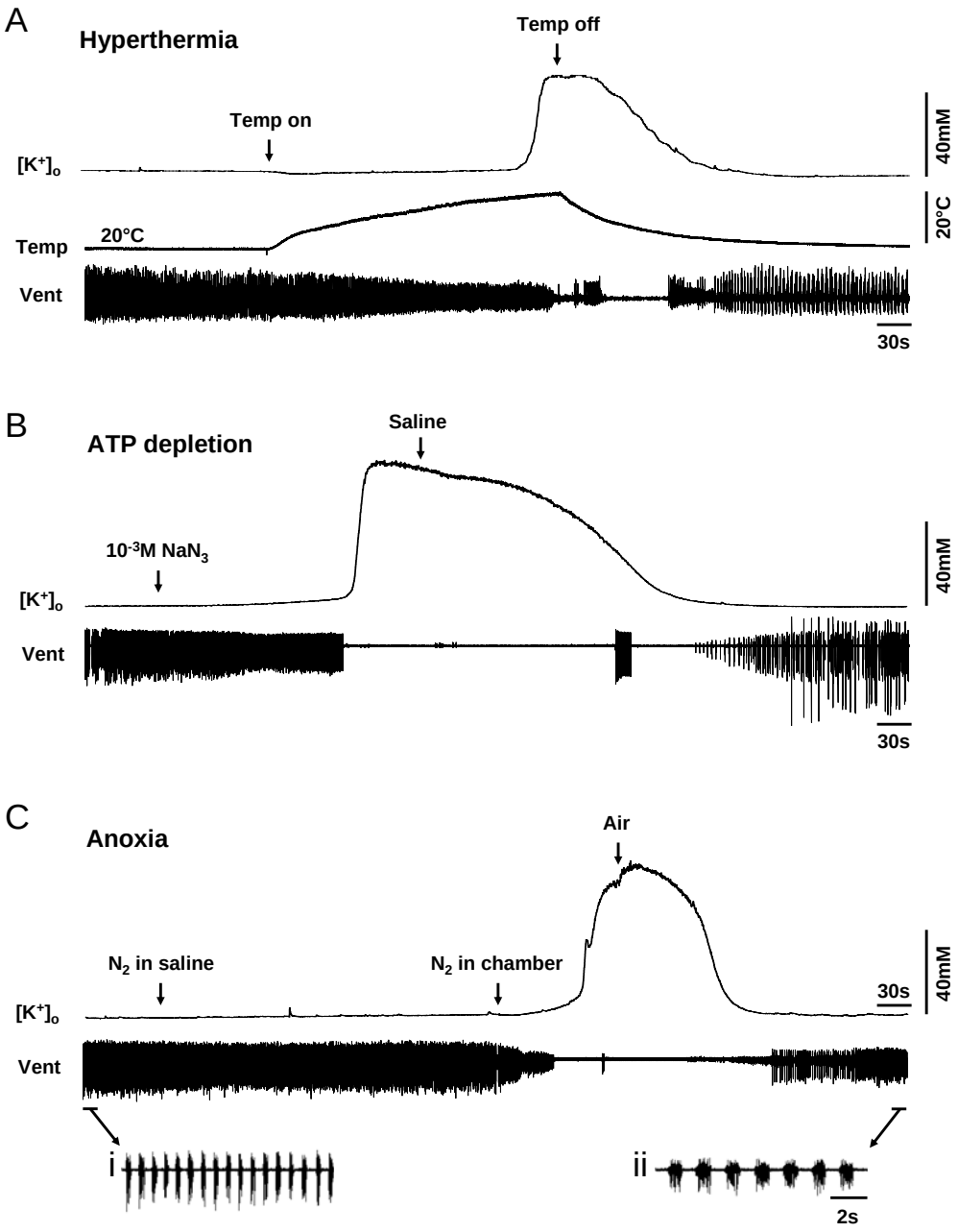
A
Hyperthermia
Temp off
Temp on
[K+]o
40mM
20°C
Temp
20°C
Vent
30s
B
ATP depletion
Saline
10-3M NaN3
[K+]o
40mM
Vent
30s
C
Anoxia
Air
N2 in saline
N2 in chamber
30s
[K+]o
40mM
Vent
i
ii
2s

Figure 4.1

Figure 4.1. Stress-induced motor pattern failure is associated with surges of $[K^+]_o$. Simultaneous recordings of the ventilatory motor pattern (Vent), the temperature of the superfusing saline at the MTG (Temp in **A**) and the extracellular potassium concentration ($[K^+]_o$). **A.** An abrupt increase in $[K^+]_o$ was reliably associated with heat-induced failure of the ventilatory motor pattern, which occurred in 100% of preparations (N=17). $[K^+]_o$ was restored to normal baseline levels if heat was removed and this was associated with recovery of ventilatory motor patterning. **B.** 10^{-3}M NaN_3 was bath-applied until 1 minute post-failure (N=6). $[K^+]_o$ gradually decreased and the motor pattern recovered upon superfusion of standard locust saline. **C.** N_2 was bubbled into the superfusing saline for 5 minutes, then blown over the preparation until 1 minute post-failure (N=18). Re-oxygenation resulted in $[K^+]_o$ clearance and recovery of the motor pattern. **i** and **ii** show expansions of the motor pattern trace pre- and post-stress to show more clearly the ventilatory motor pattern. In **B** and **C** the temperature was constant at room temperature (~22ºC).

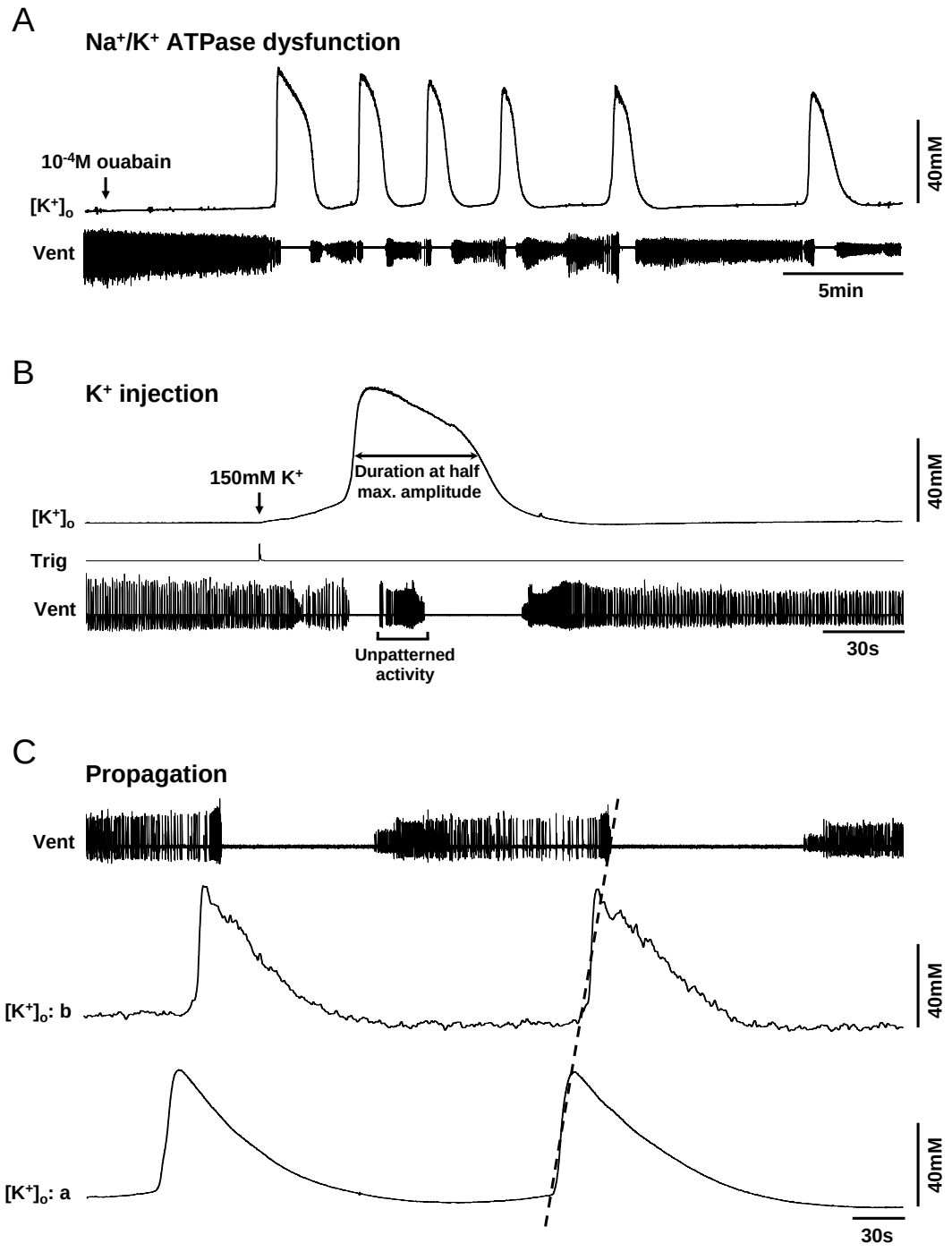
A
Na+/K+ ATPase dysfunction
10-4M ouabain
[K+]o
Vent
40mM
5min
B
K+ injection
150mM K+
Duration at half max. amplitude
[K+]o
Trig
Vent
40mM
Unpatterned activity
30s
C
Propagation
Vent
[K+]o: b
40mM
[K+]o: a
40mM
30s

Figure 4.2

Figure 4.2. Characteristics of $[K^+]_o$ surges. Simultaneous recordings of the ventilatory motor pattern (Vent), a monitor of pressure-injection of a bolus of K^+ within the MTG (Trig in **B**) and the extracellular potassium concentration ($[K^+]_o$). **A.** Continuous bath application of 10^{-4}M ouabain elicited multiple surges in $[K^+]_o$ (N=13). In the experiment shown here it took 434 seconds for 10^{-4}M ouabain to penetrate the MTG and induce failure of motor pattern generation. **B.** A 35nl pressure-injection of locust saline containing a 15-fold higher $[K^+]$ (150mM compared to 10mM) into the MTG neuropile was sufficient to bring $[K^+]_o$ to threshold and induce an abrupt surge (N=18). **C.** Two K^+ -sensitive microelectrodes were inserted in different regions of the MTG (**a** and **b**) to illustrate propagation (dotted line). In this experiment the propagation speed was 1.9 mm/min.

Abrupt surges in $[K^+]_o$ were reliably triggered by Na^+/K^+ ATPase inhibition using 10^{-4}M ouabain and by locally increased $[K^+]_o$ within the ganglion (Figure 4.2). Continuous bath application of 10^{-4}M ouabain elicited multiple surges in $[K^+]_o$ where the rise and fall of $[K^+]_o$ was associated with failure and recovery of the ventilatory motor pattern, respectively (Figure 4.2A). The time from ouabain application to the midpoint of the initial $[K^+]_o$ increase was 557 ± 43 seconds. The average $[K^+]_o$ surge period from the first to the second surge was 217 ± 16 seconds. $[K^+]_o$ increased to a mean peak of 63 ± 5 mM during the initial surge induced by 10^{-4}M ouabain and subsequently returned to a mean baseline level of 10 ± 0.2 mM. $[K^+]_o$ clearance always coincided with recovery of motor pattern generation, however the ventilatory rhythm frequency and duration became more variable following each $[K^+]_o$ surge (Figure 4.2A). A 35nl injection of locust saline containing a 15-fold higher $[K^+]$ (150mM compared to 10mM) was sufficient to bring $[K^+]_o$ to threshold for induction of an abrupt surge (Figures 4.2B and 4.S1). The peak $[K^+]_o$ reached during surges induced by K^+ injection was 63 ± 8 mM. The average duration of the $[K^+]_o$ surge, measured at half the maximum amplitude, was 64 ± 9 seconds. It was of interest to determine if the repetitive ionic disturbance is localized to one area in the MTG, or if, similar to CSD, there is propagation across different areas of the locust nervous system. To investigate this we measured $[K^+]_o$ simultaneously at two different locations in the MTG ~0.4 to 0.6mm apart (Figure 4.2C). Abrupt surges in $[K^+]_o$ generated by injection of high $[K^+]$ saline into the extracellular space spread locally to other areas of the MTG at a speed of 2.4 ± 0.04 mm/min (Figure 4.2C), but did not

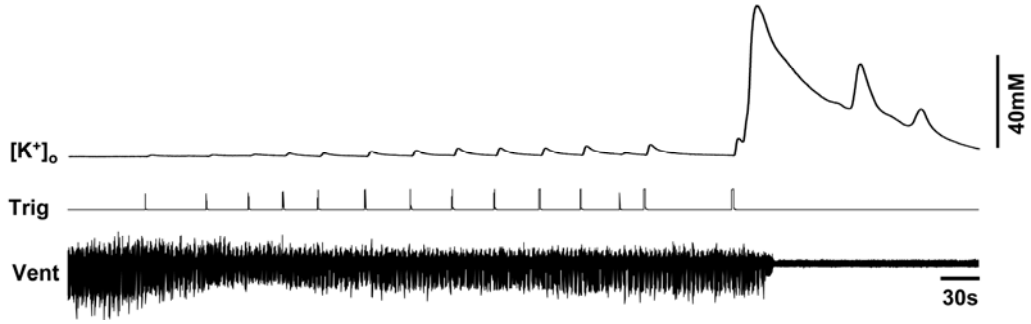

Figure 4.S1. Gradual increases in the volume of K^+ injected triggered a tissue response. Simultaneous recordings of the ventilatory motor pattern (Vent), pressure-injection of a bolus of K^+ within the MTG (Trig) and the extracellular potassium concentration ($[K^+]_o$). Injection of very small volumes of high K^+ saline triggered a tissue response, however ignition of the all-or-none $[K^+]_o$ event occurred only when a threshold was reached.

propagate through the connectives to the mesothoracic ganglion and vice versa (N=3; data not shown).

The hyperthermic $[K^+]_o$ event does not represent complete collapse of the K^+ gradient.

To determine if the peak $[K^+]_o$ represented complete collapse of the $[K^+]_o$ gradient during hyperthermia, temperature was increased beyond failure of the motor pattern until a second $[K^+]_o$ plateau was reached at ~60ºC (100 ± 7 mM; Figure 4.3A). The motor pattern did not recover upon return to room temperature and $[K^+]_o$ remained elevated. Hyperthermia following anoxic arrest of the motor pattern eliminated the hyperthermic $[K^+]_o$ event and only the second plateau (113 ± 6 mM) was evident without recovery (Figure 4.3B) suggesting that these different stressors converge on the same tissue response. There was no difference in the ultimate $[K^+]_o$ at ~60°C between the two treatment groups (hyperthermia alone and anoxia-induced failure of the motor pattern prior to hyperthermia) (*t*-test, $t = -1.370$, $P = 0.185$, d.f. = 21).

The hyperthermic $[K^+]_o$ event is delayed by Na^+ channel block and diminished by K^+ channel block.

We used voltage-gated Na^+ and K^+ channel blockers (TTX and TEA, respectively) to determine if the hyperthermic SD-like event in the locust is dependent on neural activity and if K^+ efflux is at least in part via TEA-sensitive K^+ channels. Bath application of 10^{-6}M TTX quickly abolished electrical activity from ventilatory muscle 161 while $[K^+]_o$ remained stable at ~10mM for 15 minutes prior to the temperature ramp (Figure 4.4A).

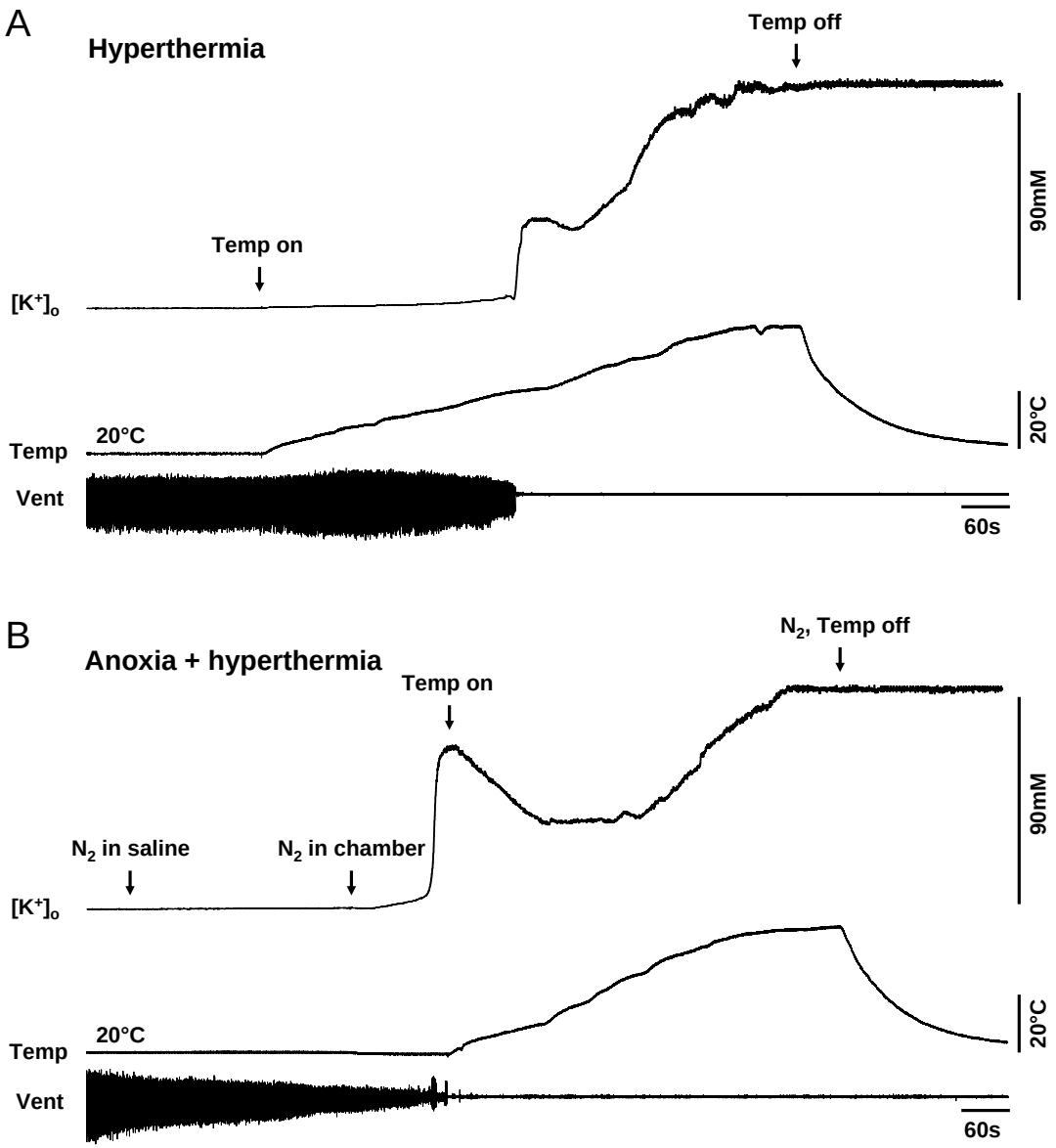
A
Hyperthermia
Temp off
Temp on
90mM
[K+]o
20°C
Temp
Vent
60s
B
Anoxia + hyperthermia
N2, Temp off
Temp on
N2 in saline
N2 in chamber
90mM
[K+]o
20°C
Temp
Vent
60s

Figure 4.3

Figure 4.3. The hyperthermic $[K^+]_o$ event is not representative of complete collapse of the K^+ gradient. **A.** During a continuous increase of temperature $[K^+]_o$ increased sharply at ~40°C coincident with motor pattern failure and continued to rise until a second plateau was reached at ~60°C. When the heater was turned off $[K^+]_o$ remained elevated and motor pattern generation failed to recover (N=11). **B.** Only the second plateau was evident during temperature increase to ~60ºC following prior anoxic arrest of motor pattern generation. When the N_2 was turned off and internal temperature returned to room temperature $[K^+]_o$ remained elevated and motor pattern generation failed to recover (N=12).

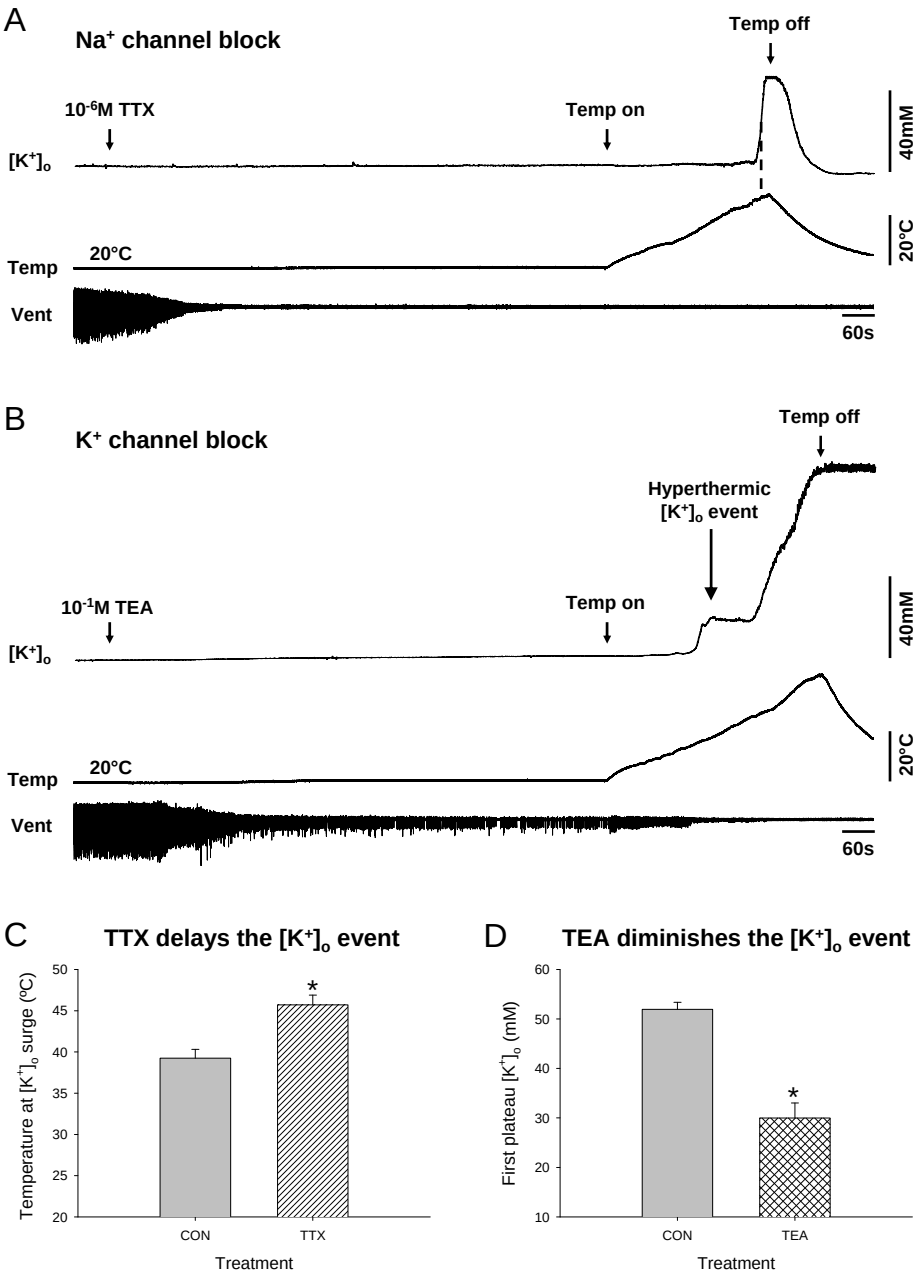

Figure 4

Figure 4.4

Figure 4.4. The hyperthermic $[K^+]_o$ event is delayed by blocking Na^+ channels and neural activity using TTX and is diminished by blocking K^+ channels using TEA. **A.** 10^{-6}M TTX abolished electrical activity within minutes while $[K^+]_o$ remained stable. The abrupt rise in $[K^+]_o$ was not significantly diminished by TTX. The hyperthermic $[K^+]_o$ event occurred at a significantly higher temperature (measured at dotted line) in the absence of electrical activity (46 ± 1°C) compared to CON locusts (39 ± 1°C) (**C**) (N_{CON} = 17; N_{TTX} = 15). **B.** 10^{-1}M TEA significantly reduced the hyperthermic $[K^+]_o$ event (N_{CON} = 17; N_{TEA} = 6) (**D**). $[K^+]_o$ increased with continued temperature increase to ~60°C.

However, occurrence of the hyperthermic $[K^+]_o$ event was TTX-resistant; there was no difference in the peak $[K^+]_o$ level between CON and TTX locusts (52 ± 2 mM and 50 ± 4 mM respectively; *t*-test, $t = 0.334$, $P = 0.741$, d.f. = 30). The abrupt rise in $[K^+]_o$ was delayed in TTX-treated locusts, occurring at higher temperatures during the continuous ramp increase than in CON locusts (46 ± 1 °C versus 39 ± 1 °C; *t*-test, $t = -4.541$, $P < 0.001$, d.f. = 30) (Figure 4.4C). Due to the effectiveness of the sheath enclosing the contents of the MTG, bath application of a high concentration of TEA (10^{-1}M) was required to successfully abolish motor pattern generation, although electrical activity was still detected from muscle 161. The hyperthermic $[K^+]_o$ event occurred at 38.9 ± 0.6 °C in locusts treated with 10^{-1}M TEA compared to 39.3 ± 0.9 °C (no significant difference) in CON locusts (Figure 4.4B) but was reduced in amplitude (30 ± 3 mM versus 52 ± 2 mM; *t*-test, $t = 5.429$, $P < 0.001$, d.f. = 21) (Figure 4.4D). With continued temperature increase to ~60°C $[K^+]_o$ reached a higher second plateau in TEA-treated locusts (109 ± 9 mM) that was not different from the second plateau in CON locusts (*t*-test, $t = -0.755$, $P = 0.462$, d.f. = 15).

Initiation of $[K^+]_o$ surges are not correlated with ATP levels within the ganglion.

Cell energetics may play a role in the initiation of, and recovery from, the $[K^+]_o$ event induced by various cellular stressors. ATP levels in the MTG taken from locusts subjected to hyperthermia before and after heat shock preconditioning (CON and HS), 10^{-4}M ouabain, 10^{-3}M sodium azide, and anoxia (100% N_2) were compared prior to stress, at failure and at subsequent recovery of the motor pattern (Figure 4.5A).

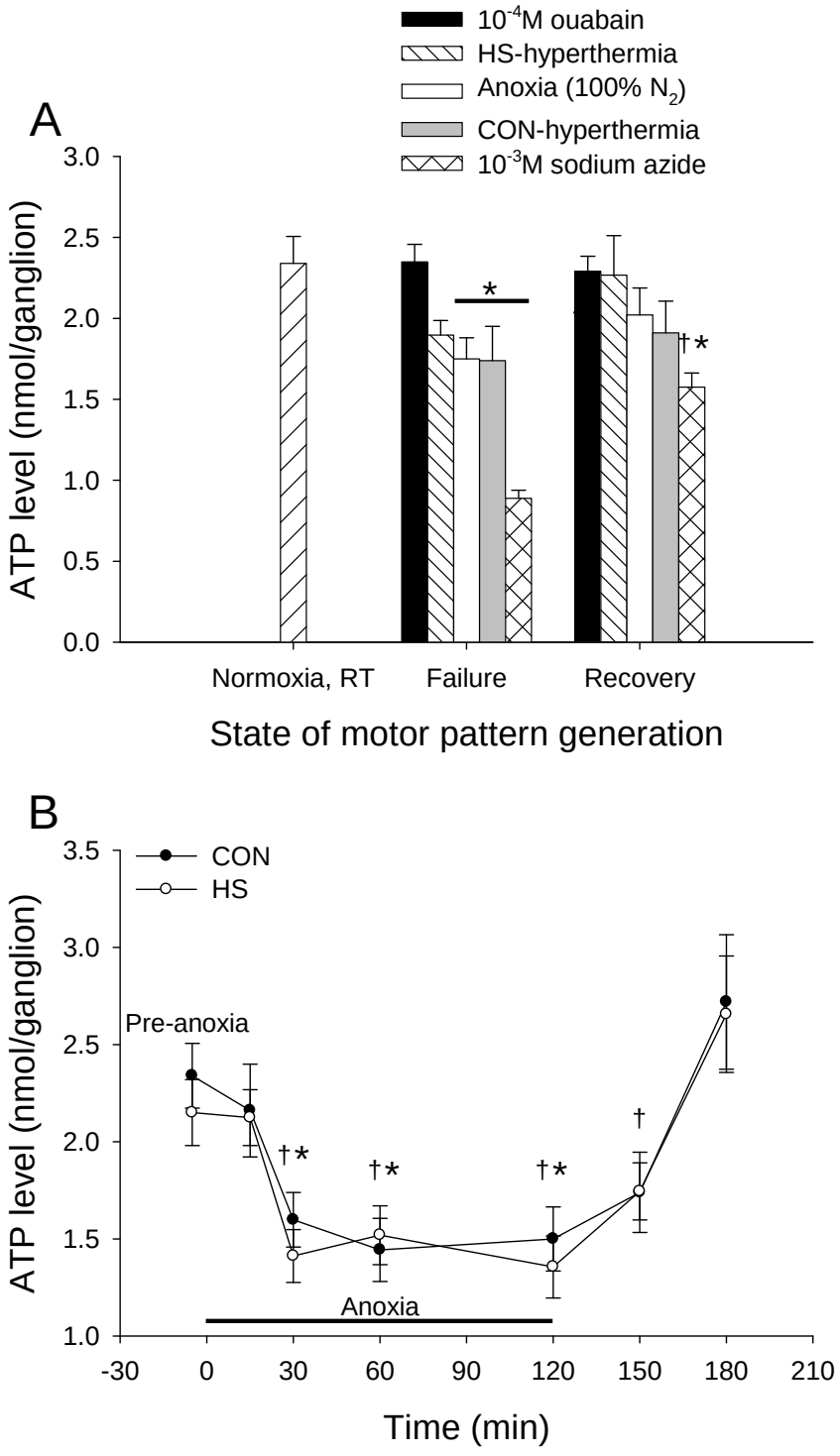
A
10-4M ouabain
HS-hyperthermia
Anoxia (100% N2)
CON-hyperthermia
10-3M sodium azide
ATP level (nmol/ganglion)
3.0
2.5
2.0
1.5
1.0
0.5
0.0
*
†*
Normoxia, RT
Failure
Recovery
State of motor pattern generation
B
CON
HS
ATP level (nmol/ganglion)
3.5
3.0
2.5
2.0
1.5
1.0
Pre-anoxia
†*
†*
†*
†
Anoxia
-30
0
30
60
90
120
150
180
210
Time (min)

Figure 4.5

Figure 4.5. Failure and recovery of the CPG are not dependent on MTG ATP and HS preconditioning does not confer protection by improving ATP availability. **A.** ATP levels did not differ from the pre-stress level (Normoxia at room temperature; N=16) in locusts treated with 10^{-4}M ouabain or hyperthermia (HS) at failure or recovery, or in all other groups at recovery following stress-induced failure with the exception of NaN_3-treated locusts. There was a main effect of treatment driven by significant differences among groups within failure and recovery (not indicated by symbols). There was no effect of HS pre-treatment on ATP levels at failure or recovery of motor pattern generation. Asterisks indicate significant differences from the pre-stress level and daggers indicate significantly different ATP levels at failure and recovery in ganglia of NaN_3-treated locusts. Sample sizes (failure, recovery): $N_{Ouabain}$=10,11; $N_{HS\text{-}hyperthermia}$=8,8; N_{Anoxia}=9,8; $N_{CON\text{-}hyperthermia}$=7,7; $N_{Sodium\ azide}$=8,9. **B.** CON and HS locusts did not have significantly different ATP levels during anoxia-induced coma or subsequent recovery. ATP levels dropped in both CON and HS locusts after 30 minutes of anoxia and remained stable until locusts were removed from the anoxic environment. ATP levels increased to around pre-anoxia values after one hour in normally oxygenated air. Sample sizes (CON, HS): N_{0min}=16,16; N_{15min}=12,11; N_{30min}=11,11; N_{60min}=9,9; N_{120min}=12,11; N_{150min}=11,12; N_{180min}=10,10. Asterisks indicate significant differences from 0 and 15 minutes and daggers indicate significant differences from 180 minutes (or 60 minutes recovery) according to *post hoc* Tukey tests ($P < 0.05$).

Ganglionic ATP levels were depressed at failure induced by anoxia, hyperthermia (CON), and NaN_3 and at subsequent recovery in NaN_3-treated locusts (*post hoc* Dunnett's test, $P < 0.05$). Stress treatment and the state of motor pattern generation, i.e. failure vs. recovery, both affected ATP levels (two-way ANOVAs: $P < 0.001$, $F_{(4,75)} = 17.435$; $P = 0.002$, $F_{(1,75)} = 10.193$). At failure of the motor pattern, NaN_3-treated locusts had lower ganglionic ATP levels than all other groups. Locusts subjected to anoxia and hyperthermia (CON) had lower ATP levels than locusts treated with 10^{-4}M ouabain (*post hoc* Tukey tests, $P < 0.05$). At recovery of the motor pattern NaN_3-treated locusts had lower ganglionic ATP levels than locusts subjected to 10^{-4}M ouabain and hyperthermia (HS) suggesting that recovery was independent of metabolic state (*post hoc* Tukey tests, $P < 0.05$). ATP levels in ganglia at failure and recovery of the motor pattern were not different except in NaN_3-treated locusts (*post hoc* Tukey tests, $P < 0.05$). Notably, HS preconditioning did not increase ATP levels at hyperthermic failure or subsequent recovery of the motor pattern compared to CON-hyperthermia locusts (Figure 4.5A). The lack of effect of HS on MTG ATP levels was also evident during and after two hours of whole animal anoxia (Figure 4.5B). HS pre-treatment did not affect ATP levels prior to anoxia, at 15, 30, 60, and 120 minutes of anoxia exposure, and at 30 and 60 minutes post-anoxia (two-way ANOVA, $P = 0.467$, $F_{(1,147)} = 0.531$). Anoxia exposure affected ganglionic ATP (two-way ANOVA, $P < 0.001$, $F_{(6,147)} = 11.418$). Anoxia (15 minutes) did not affect ATP levels in either CON or HS locusts, even though locusts entered anoxic coma within 1 minute. ATP levels dropped after 30 minutes of anoxia and remained stable for 90 minutes in CON and HS locusts (*post hoc* Tukey tests, $P < 0.05$).

Following 2 hours in an anoxic environment, ATP increased after 60 minutes of normoxia in CON and HS locusts (*post hoc* Tukey tests, $P < 0.05$).

HS pre-treatment changed $[K^+]_o$ homeostasis in the MTG.

We used 10^{-5}M ouabain to test whether increased Na^+/K^+ ATPase activity could underlie the increased thermotolerance conferred by HS pre-treatment (Newman et al. 2003). 10^{-5}M ouabain is not normally sufficient to induce the SD-like events of Figure 4.2A but is sufficient to inhibit the Na^+/K^+ ATPase (see below). HS pre-treatment and 10^{-5}M ouabain bath application affected $[K^+]_o$ before and during a temperature ramp (Figure 4.6). Heat shock pre-treatment increased initial $[K^+]_o$ measured after 10 minutes of bath application with standard locust saline (*t*-test, $t = -3.195$, $P = 0.002$, d.f. = 49; Figure 4.6A). Changes in extracellular potassium ($\Delta[K^+]_o$) were examined after 15 minutes of ouabain treatment at room temperature and in response to the initial 5°C increase of the temperature ramp to determine the effects of HS pre-treatment and 10^{-5}M ouabain treatment on K^+ homeostasis (Figure 4.6B and C). HS pre-treatment had no effect on $\Delta[K^+]_o$ after 15 minutes of bath application, however there was an effect of 10^{-5}M ouabain treatment (two-way ANOVAs: $P = 0.407$, $F_{(1,43)} = 0.703$; $P < 0.001$, $F_{(1,43)} = 42.772$) (Figure 4.6B). CON-OUA and HS-OUA locusts had a greater increase in $[K^+]_o$ than CON and HS locusts after 10^{-5}M ouabain bath application for 15 minutes (*post hoc* Tukey tests, $P < 0.05$). HS pre-treatment affected $\Delta[K^+]_o$ after a 5°C increase in temperature, however there was no effect of 10^{-5}M ouabain treatment (two-way ANOVAs: $P < 0.001$, $F_{(1,43)} = 15.584$; $P = 0.988$, $F_{(1,43)} = 0.000223$) (Figure 4.6C).

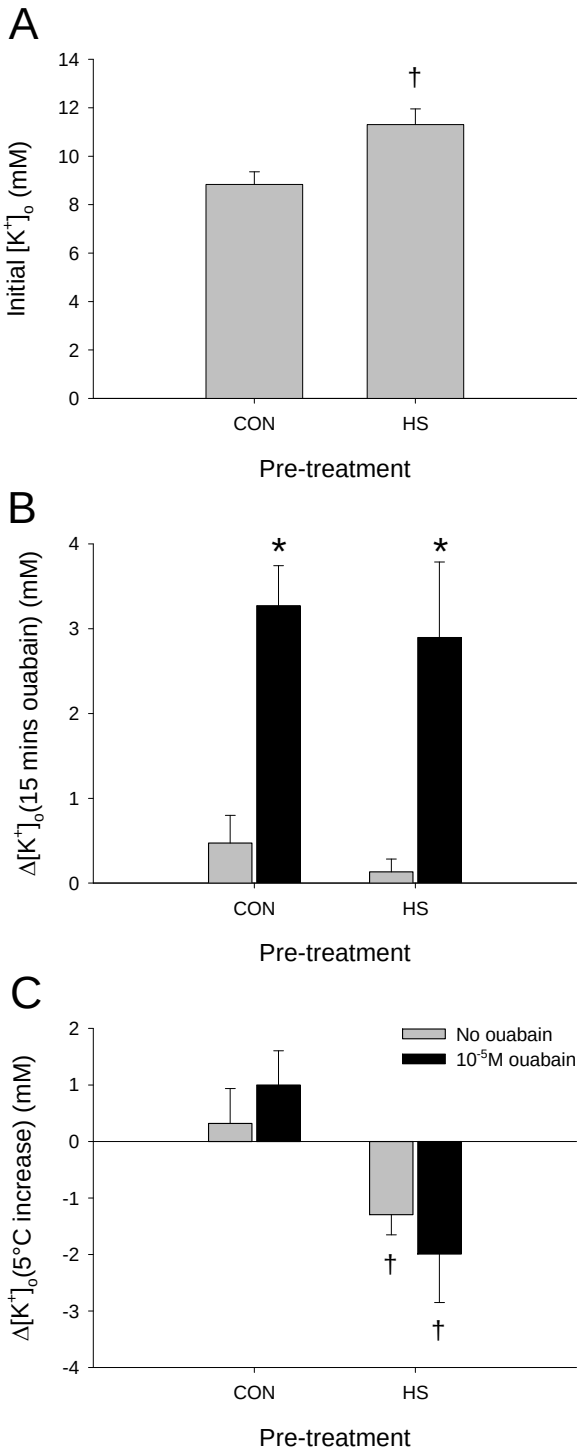
A
Initial [K+]o (mM)
14
12
10
8
6
4
2
0
†
CON
HS
Pre-treatment
B
Δ[K+]o(15 mins ouabain) (mM)
4
3
2
1
0
*
*
CON
HS
Pre-treatment
C
Δ[K+]o(5°C increase) (mM)
2
1
0
-1
-2
-3
-4
No ouabain
10-5M ouabain
†
†
CON
HS
Pre-treatment

Figure 4.6

Figure 4.6. HS and ouabain affect $[K^+]_o$. **A.** Heat shock preconditioning resulted in a significantly higher $[K^+]_o$ in HS locusts compared to CON locusts. All animals pooled: $N_{CON} = 25$; $N_{HS} = 26$. **B.** CON-OUA and HS-OUA locusts had a significantly greater increase in $[K^+]_o$ after 15 minutes of bath application with 10^{-5}M ouabain compared to CON and HS locusts. HS pre-treatment did not have an effect on $\Delta[K^+]_o$ over this 15 minute period ($N_{CON} = 12$; $N_{CON\text{-}OUA} = 10$; $N_{HS} = 17$; $N_{HS\text{-}OUA} = 8$). **C.** CON and HS locusts had a markedly different $\Delta[K^+]_o$ in response to a 5ºC increase in temperature. $\Delta[K^+]_o$ was positive in CON locusts and negative in HS locusts after only one minute of temperature increase. There was no effect of 10^{-5}M ouabain treatment on $\Delta[K^+]_o$ one minute into the temperature ramp ($N_{CON} = 12$; $N_{CON\text{-}OUA} = 10$; $N_{HS} = 17$; $N_{HS\text{-}OUA} = 8$). Asterisks indicate a significant effect of ouabain and daggers indicate a significant effect of pre-treatment according to *t*-test (**A**) and *post hoc* Tukey tests ($P < 0.05$) (**B,C**).

CON and CON-OUA locusts had a greater $\Delta[K^+]_o$ than HS and HS-OUA locusts (*post hoc* Tukey tests, $P < 0.05$).

Time to recovery is correlated with failure temperature in control and HS locusts.
HS preconditioning delayed the onset of the $[K^+]_o$ event and subsequently hastened recovery and re-establishment of normal $[K^+]_o$ (Figure 4.7). However HS had no effect on the amplitude of the $[K^+]_o$ event at failure (Figure 4.S2) and there was no correlation between time to recovery and peak $[K^+]_o$ in C and HS locusts (data not shown) indicating that the effect of HS on rate of recovery was not due to a decrease in the initial ionic disturbance. There was a strong positive correlation between time to recovery and failure temperature in control locusts that was shifted by HS and by 10^{-5}M ouabain (Pearson Product Moment Correlations: CON, $r = 0.91$, $P < 0.0001$; HS, $r = 0.90$, $P < 0.0001$; CON-OUA, $r = 0.88$, $P = 0.00172$; HS-OUA, $r = 0.85$, $P = 0.00785$) (Figure 4.7A and B). Thus high failure temperatures were correlated with slower recovery under all conditions. HS improved performance by increasing failure temperatures and speeding recovery whereas ouabain impaired performance of both CON and HS preparations.

HS pre-treatment increases failure temperature and decreases time to recovery.
HS pre-treatment increased the upper temperature limit and shortened time to recovery when these measures were examined independently (Figure 4.7C and D). HS pre-treatment and 10^{-5}M ouabain treatment affected failure temperature though there was no interaction between treatments suggesting that the effect of ouabain did not depend on the

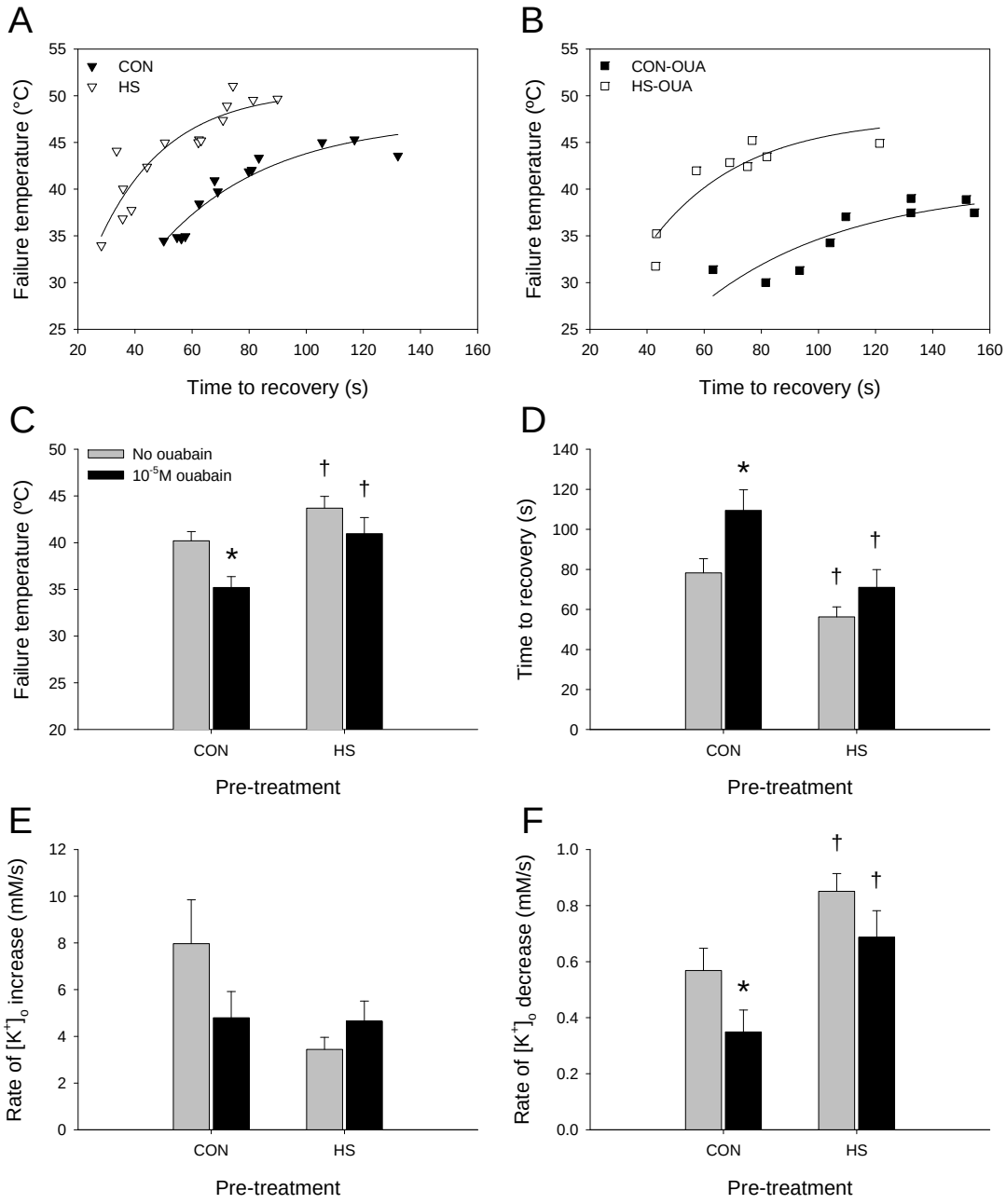
A
CON
HS
Failure temperature (°C)
Time to recovery (s)
B
CON-OUA
HS-OUA
Failure temperature (ºC)
Time to recovery (s)
C
No ouabain
10-5M ouabain
Failure temperature (ºC)
CON
HS
Pre-treatment
D
Time to recovery (s)
CON
HS
Pre-treatment
E
Rate of [K+]o increase (mM/s)
CON
HS
Pre-treatment
F
Rate of [K+]o decrease (mM/s)
CON
HS
Pre-treatment

Figure 4.7

Figure 4.7. HS delays the $[K^+]_o$ event and speeds recovery by increasing the rate of $[K^+]_o$ clearance. **A.** Time to recovery was positively correlated with failure temperature in CON and HS locusts (N_{CON} = 13; N_{HS} = 15). Animals whose ventilatory motor pattern failed at a higher temperature had a longer time to recovery when temperature returned to normal levels. **B.** The correlations seen in CON and HS animals were shifted in animals treated with 10^{-5}M ouabain ($N_{CON\text{-}OUA}$ = 9; $N_{HS\text{-}OUA}$ = 8). The relationship between failure temperature and time to recovery in HS-OUA animals resembled CON animals. Data points for each group were fitted with exponential curves that rise to a plateau (**A, B**). **C.** Ventilatory motor pattern generation in HS locusts failed at a significantly higher temperature than in CON locusts with and without 10^{-5}M ouabain treatment. There was a significant effect of ouabain on the ability to withstand high temperature stress in CON locusts but not in HS locusts (N_{CON} = 15; $N_{CON\text{-}OUA}$ = 9; N_{HS} = 17; $N_{HS\text{-}OUA}$ = 8). **D.** Ventilatory motor pattern generation in HS locusts took significantly less time to recover following heat-induced failure than in CON locusts with and without ouabain treatment. CON-OUA locusts took significantly more time to recover than CON locusts, however there was no significant effect of ouabain treatment on time to recovery in HS locusts (N_{CON} = 13; $N_{CON\text{-}OUA}$ = 10; N_{HS} = 15; $N_{HS\text{-}OUA}$ = 8). **E.** Overall there were no main effects of HS pre-treatment or ouabain treatment on the rate of $[K^+]_o$ increase (mM/s) associated with failure of the motor pattern (N_{CON} = 15; $N_{CON\text{-}OUA}$ = 10; N_{HS} = 18; $N_{HS\text{-}OUA}$ = 7). **F.** The rate of $[K^+]_o$ decrease (mM/s) associated with recovery of the motor pattern was significantly greater in HS locusts than in CON locusts and this effect of pre-treatment was conserved in ouabain-treated locusts. Ouabain treatment significantly

decreased the rate of $[K^+]_o$ clearance in CON locusts but not in HS locusts (N_{CON} = 15; $N_{CON\text{-}OUA}$ = 10; N_{HS} = 18; $N_{HS\text{-}OUA}$ = 8). Asterisks indicate a significant effect of ouabain and daggers indicate a significant effect of pre-treatment according to *post hoc* Tukey tests ($P < 0.05$) (**C-F**).

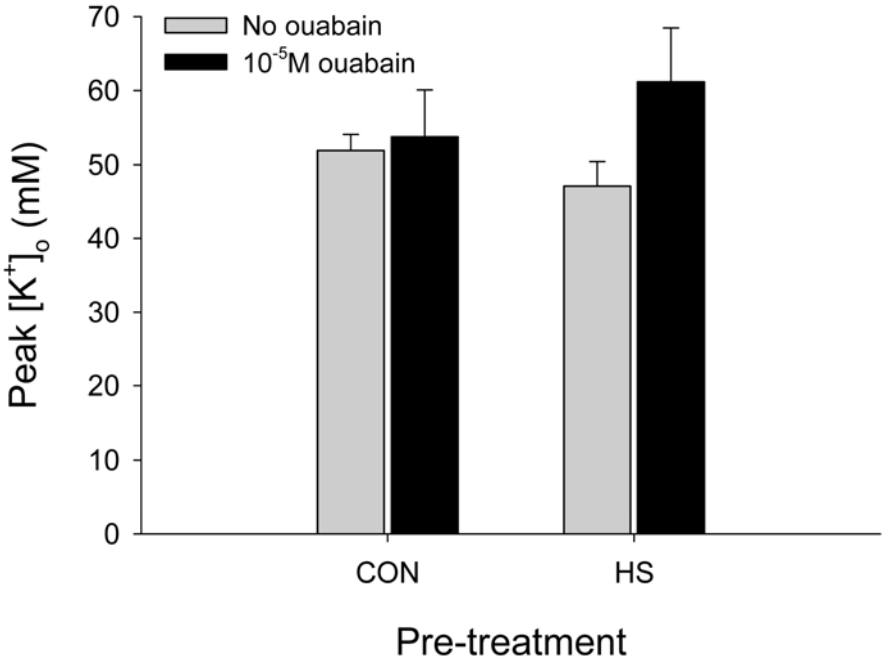

Figure 4.S2. The degree of the $[K^+]_o$ disturbance was the same in CON and HS locusts. There were no main effects of HS pre-treatment or 10^{-5} M ouabain treatment on the peak $[K^+]_o$ associated with failure of the motor pattern ($N_{CON} = 17$; $N_{CON\text{-}OUA} = 10$; $N_{HS} = 18$; $N_{HS\text{-}OUA} = 8$).

pre-treatment (two-way ANOVAs: $P = 0.001$, $F_{(1,45)} = 11.777$; $P = 0.007$, $F_{(1,45)} = 8.140$) (Figure 4.7C). HS increased failure temperatures compared with CON, and ouabain decreased failure temperatures in CON but not HS preparations (*post hoc* Tukey tests, $P < 0.05$). HS pre-treatment and 10^{-5}M ouabain treatment also affected time to recovery of the motor pattern with a similar lack of interaction (two-way ANOVAs: $P < 0.001$, $F_{(1,42)} = 15.302$; $P = 0.005$, $F_{(1,42)} = 8.823$) (Figure 4.7D). HS decreased time to recovery compared with CON, and ouabain increased time to recovery in CON but not HS preparations (*post hoc* Tukey tests, $P < 0.05$).

HS pre-treatment increases the rate of $[K^+]_o$ clearance following hyperthermic failure. Rates of $[K^+]_o$ increase and clearance associated with hyperthermic failure and subsequent recovery of the ventilatory motor pattern were compared among groups to determine if preconditioning improves $[K^+]_o$ stabilization and to test the role of the Na^+/K^+ ATPase in this preconditioning (Figure 4.7E and F). Neither HS pre-treatment nor 10^{-5}M ouabain treatment affected the rate of $[K^+]_o$ increase associated with failure of the motor pattern (two-way ANOVAs: $P = 0.098$, $F_{(1,46)} = 2.846$; $P = 0.482$, $F_{(1,46)} = 0.502$) (Figure 4.7E). However HS pre-treatment and 10^{-5}M ouabain treatment did affect the rate of $[K^+]_o$ decrease associated with recovery of the motor pattern (two-way ANOVAs: $P < 0.001$, $F_{(1,47)} = 14.395$; $P = 0.024$, $F_{(1,47)} = 5.478$) (Figure 4.7F) though there was no interaction between the treatments. HS increased the $[K^+]_o$ clearance rate compared with CON, and ouabain decreased this measure in CON but not in HS preparations (*post hoc* Tukey tests, $P < 0.05$). Thus the proportion of the $[K^+]_o$ clearance

rate sensitive to the 10^{-5}M ouabain treatment was halved by HS from ~40% in control preparations to ~20% after HS.

HS preconditioning does not increase Na^+/K^+ ATPase activity in the MTG.

To complement the results obtained by ouabain treatment on $[K^+]_o$ clearance rates we also measured steady-state Na^+/K^+ ATPase activity within the MTG. Na^+/K^+ ATPase activity (i.e. the ouabain-sensitive fraction of total MTG ATPase activity) was 144 ± 12 nmol ATP/min/mg protein in CON ganglia compared to 133 ± 9 nmol ATP/min/mg protein in HS ganglia (no significant difference; *t*-test, $t = 0.755$, $P = 0.468$, d.f. = 10; $N_{CON}=6$, $N_{HS}=6$). In the presence of phosphatase inhibitors, Na^+/K^+ ATPase activity was 120 ± 7 nmol ATP/min/mg protein in CON ganglia compared to 116 ± 10 nmol ATP/min/mg protein in HS ganglia (no significant difference; *t*-test, $t = 0.430$, $P = 0.672$, d.f. = 18; $N_{CON}=10$, $N_{HS}=10$). This suggests that total Na^+/K^+ ATPase activity is not a target for protection by HS preconditioning.

4.4 Discussion

In a central pattern generator controlling ventilation in the locust, we have shown that hyperthermic failure and recovery of neural function are tightly correlated with an abrupt rise in $[K^+]_o$ and its subsequent restoration when temperature is allowed to return to normal. Anoxia and ATP depletion evoked similar tissue responses, which could also be induced when we disturbed the ionic equilibrium by impairing Na^+/K^+ ATPase activity using ouabain or by local neuropile injections of high $[K^+]$ saline. The fact that a prior anoxia-induced $[K^+]_o$ surge occluded the hyperthermic event suggests that these different stressors converged on the same mechanism. In addition, the nature of these events as large ionic disturbances propagating throughout the MTG neuropile makes it unlikely that different stressors would have additive effects. The amplitude of the hyperthermic $[K^+]_o$ surge was smaller than those induced by either anoxia or ATP depletion and we attribute this partly to the confounding effect of its occurrence at high temperatures (>40°C). This is supported by further analysis that shows a significant negative correlation between the failure temperature during hyperthermia (for CON, HS, CON-OUA, HS-OUA preparations) and $[K^+]_o$ at its peak (Pearson Product Moment Correlation; r = -0.3, P = 0.03; N = 47, one outlier removed), and may be due to the fact that at the point of hyperthermic failure $[K^+]_o$ increased from its room temperature level (t-test, t = -5.085, $P < 0.001$, d.f. = 104) thereby reducing the driving force on K^+ ions. We conclude that the different stressors converged on a single tissue mechanism.

CSD occurs in vertebrate grey matter and is characterized by a rapid and nearly complete depolarization of neurons that propagates at 2-5 mm/min as a wave across the cortex. This propagating wave is due to a disordered regulation of ionic homeostasis evident as a massive redistribution of ions across neuronal membranes, including large increases of $[K^+]_o$ (Somjen, 2001). Each wave results in neuronal hyperexcitation followed by suppression of electrical activity because of spike inactivation. SD events can be evoked by hypoxia (Wu and Fisher, 2000; Somjen, 2001; Kager et al. 2002), ouabain (Balestrino et al. 1999; Wu and Fisher, 2000; Somjen, 2001), simulated ischemia (Anderson et al. 2005), and increased $[K^+]_o$ (Wu and Fisher, 2000; Somjen, 2001; Kager et al. 2002) with normal temperature, as well as hyperthermia (Wu and Fisher, 2000). The locust responses: 1) were all-or-none events of similar magnitude (at least with respect to $[K^+]_o$), 2) were induced by the same stimuli, 3) were not activity-dependent, 4) occurred as repetitive waves with ouabain, 5) propagated at around 2mm/min, 6) did not cross between ganglia through the connectives (equivalent to white matter) and 7) were associated with complete depression of neural activity manifest by failure of ventilatory pattern generation. Thus the locust tissue response, reflected in the all-or-none surge of $[K^+]_o$, shares most, if not all, of the essential characteristics of CSD.

The biophysical mechanism of the extensive redistribution of ions causing CSD is incompletely understood. It nevertheless seems clear that SD-like events in mammals are triggered by positive feedback processes involving an initial ionic disturbance reaching a threshold and caused by neuronal overexcitation or by treatments or conditions that

impair ionic homeostasis (e.g. Grafstein, 1956; van Harrevald, 1978; Balestrino et al. 1999; Somjen, 2001). In a model hippocampal pyramidal neuron, SD-like events can be triggered by manipulating ion clearance mechanisms or levels of excitation, causing the net current in the apical dendrites to turn inward (Kager et al. 2002). The locust responses were triggered by treatments that cause a reduction in energy (i.e. ATP depletion and anoxia). However disruption of energy status was not essential since similar events were triggered by impairment of the Na^+/K^+ ATPase (10^{-4}M ouabain) and by local injection of high $[K^+]$ saline into the neuropile. Moreover there was no correlation between the occurrence of motor pattern failure and recovery with levels of ATP in the MTG. Energy status of a cell (e.g. phosphorylation potential) can change and activate signaling pathways without measureable effects on ATP (Hardie et al. 2006; Evans, 2006), but the size of the sample precluded measurement of any adenylate but ATP. Hyperthermia caused a drop in metathoracic ATP but also increased levels of neuronal excitation in the ganglion. There was an interesting trade-off in our measures of thermotolerance for ventilatory pattern generation such that early failure (i.e. low failure temperature) was associated with shorter times to recovery. This suggests that the triggered event is adaptive and represents a neural off-switch to conserve energy and to prevent hyperexcitation during stressful conditions. In contrast to the insect system, CSD in mammals is associated with local tissue hypoxia and neuronal swelling due to energy consumption that is not met with adequate oxygen supply (Takano et al. 2007). The recovery of motor function was closely associated with the return of $[K^+]_o$ to near normal levels and thus the time taken to recover was related to the rate of clearance of

extracellular K^+ ions. Treatment with 10^{-5}M ouabain rendered preparations more thermosensitive by decreasing failure temperature and increasing recovery time concomitant with a decrease in the rate of extracellular K^+ ion clearance during the recovery period. This indicates an important role for the Na^+/K^+ ATPase pump, as in vertebrate SD-like phenomena. The $[K^+]_o$ disturbance induced by injection of high $[K^+]$ saline propagated within the locust MTG at a similar rate as the depolarizing wave in mammalian brain slices during CSD. Studies suggest opening of intercellular gap junctions as a mechanism of SD propagation in vertebrates (Nedergaard et al. 1995; Largo et al. 1997). Similar mechanisms may exist in the insect CNS in which glia are involved in ion homeostasis, function, and development of the insect brain (Kretzschmar and Pflugfelder, 2002).

Our findings show that the events we recorded in locust ganglia are SD-like ionic disturbances similar to CSD and possibly induced by common mechanisms, which in theory would suggest that these mechanisms have been evolutionarily conserved. Moreover in the locust there is evidence that this is an adaptive event to conserve energy and prevent complete cellular collapse. In the case of hyperthermia this was evident when temperature was increased to the point at which $[K^+]_o$ levels reached a high plateau and motor pattern recovery was precluded.

We found that prior HS preconditioned neural function in the metathoracic ganglion, allowing the ventilatory pattern generator to operate at higher temperatures and to recover

more rapidly from hyperthermic failure on return to normal temperatures. Such preconditioning significantly protects neural function and has been well established in insect preparations (Robertson, 2004a; Robertson, 2004b). HS signals a change to more extreme environmental conditions and it has pleiotropic effects to prepare cells, tissues and organisms for such a change. The shift to higher temperatures of the neural off-switch described here would be appropriate for an organism that has put protective mechanisms in place with a robust HS response (Whyard et al. 1986; Qin et al. 2003). Here we show that at least part of the beneficial effect of HS was on the rate of clearance of extracellular K^+ ions with no change in the initial disturbance. There was no evidence that this was due to improvements of energy status or management; ATP levels in the MTG after HS were not different from control either at rest, during anoxic stress or during hyperthermic stress. Given the thermoprotective effect of a heat shock protein (Hsp70) on mammalian muscle sarco/endoplasmic reticulum Ca^{2+} ATPase (Tupling et al. 2004) we suspected that the SD-like event in the locusts might have been shortened by a protective effect of HS on the activity of the Na^+/K^+ ATPase pump. However measurement of ouabain-sensitive ATPase activity in a biochemical assay of the metathoracic ganglion was not different after HS, with or without the presence of phosphatase inhibitors. Measurements of Na^+/K^+ ATPase activity were made on ganglia of CON and HS locusts at rest, and it is possible that examination of pump activity when stimulated by a rise in $[K^+]_o$ would yield different results suggesting a role for the pump. In addition, this result does not rule out the possibility that HS affected the trafficking of Na^+/K^+ ATPase complexes in neuronal and glial membranes. Nevertheless an effective

concentration of ouabain (10^{-5}M) did not prevent the protective effects of HS on K^+ clearance in the MTG. Indeed the ouabain-sensitive proportion of extracellular K^+ ion clearance was reduced by HS suggesting either that HS somehow rendered membrane-bound Na^+/K^+ ATPase less sensitive to ouabain or that HS was acting via a different mechanism such as glial buffering via inwardly rectifying K^+ channels. This issue is currently unresolved.

In summary we conclude that in locust CNS different stressors converge on an adaptive SD-like event that can be preconditioned by prior HS to delay its occurrence until higher temperatures. We believe that the mechanisms underlying this event are much like those underlying CSD and other SD-like phenomena in mammals and a conserved genetic component to this thermotolerance pathway in insects has recently been demonstrated (Dawson-Scully et al. 2007). It is therefore an intriguing possibility that this phenomenon in the locust and migraine in humans (Lauritzen, 2001; Loder, 2002; van den Maagdenberg et al. 2007 have common evolutionary origins.

4.5 Materials and Methods

Animals: adult male locusts, *Locusta migratoria*, 4-6 weeks past the imaginal ecdysis, were randomly chosen from a crowded colony maintained in the Department of Biology at Queen's University. The animals were housed in cages within the colony under a 12 h:12 h light:dark cycle. Each cage was individually lit with a 40 W fluorescent light bulb. Room temperature was maintained at 25 ± 1ºC, with a constant humidity of 23 ± 1%. Animals were provided with wheat seedlings and carrot slices once daily and an *ad libitum* mixture of 1 part skim milk powder, 1 part torula yeast, and 13 parts bran, by volume. All animals were collected from the colony at the same time each morning and were placed in a two litre ventilated plastic container for 4-8 hours prior to experimentation.

Heat shock pre-treatment: locusts designated for control (CON) and HS pre-treatments were separated into different containers. HS locusts were placed in a humid incubator (45°C) for 3 hours followed by 1-5 hours of recovery at room temperature (21 ± 2°C). CON animals were held at room temperature for 4-8 hours.

Preparation of potassium-sensitive microelectrodes: $[K^+]_o$ was measured with K^+ -sensitive microelectrodes. The K^+-sensitive microelectrodes were made from unfilamented glass pipettes (0.1mm diameter; World Precision Instruments Inc., Sarasota, FL, USA) that were cleaned with methanol (99.9%) and dried on a hot plate, then pulled

to form a low resistance (5-7MΩ) tip. The microelectrodes were silanized by exposure to dichlorodimethylsilane (99%) (Sigma-Aldrich) vapor while baking on a hot plate (100°C) for one hour. After cooling, the microelectrodes were filled at the tip with Potassium Ionophore I - Cocktail B (5% Valinomycin; Sigma-Aldrich) to form an artificial membrane and then back-filled with 500mM KCl. The tips of the K^+ -sensitive microelectrodes were suspended in distilled water until experimentation. Reference electrodes were made by pulling a filamented pipette (0.1mm diameter; World Precision Instruments Inc.) to form a low resistance (5-7MΩ) tip and were filled with 3M KCl.

Semi-intact preparation: following removal of legs, wings and pronotum, the nervous system and ventilatory muscle 161 were exposed by making a dorsal midline incision and pinning the locust open onto a cork board, dorsal side up. The gut, air sacs and fat bodies were removed. A Peri-Star peristaltic pump (World Precision Instruments Inc.) was used for perfusion of standard locust saline into the thoracic and abdominal cavities which contained (in mM) 147 NaCl, 10 KCl, 4 $CaCl_2$, 3 NaOH, and 10 HEPES buffer (pH 7.2) (all chemicals were from Sigma-Aldrich). The saline flow was directed onto the MTG where the ventilatory CPG is located and exited through an incision in the posterior abdominal wall. The tissue covering the MTG was removed as well as the cuticle and attached muscle tissue situated between the connectives. A metal plate was inserted below the MTG to stabilize it. Nerves five and seven of the MTG were cut on both sides to allow saline and pharmacological agents to permeate the ganglion. The preparation was grounded by placing a silver wire in the posterior tip of the abdomen.

Electromyographic recording of the motor pattern: an extracellular recording of the ventilatory motor pattern was obtained by placing a 0.1mm diameter copper wire, insulated except at the tip, onto abdominal muscle 161. The recording was digitized using a DigiData 1200 Series Interface (Axon Instruments Inc., Union City, CA, USA) and displayed using AxoScope 9.0 software (Axon Instruments Inc.). Ventilation can be monitored as a series of rhythmic electrical bursts in the abdominal muscles (e.g. Figure. 4.1d and e). Failure was characterized as the cessation of electrical activity in the extracellular recording and the lack of visible contractions of the ventilatory muscles. Recovery was defined as the first visible sign of rhythmical abdominal contractions coincident with resumption of rhythmic electrical activity.

Extracellular potassium recording: K^+ -sensitive microelectrodes were connected to a pH/Ion amplifier (Model 2000; A-M Systems Inc., Carlsborg, WA, USA) by an electrode holder with a chloride-coated silver wire. Preceding each experiment, a K^+ -sensitive and a reference electrode were calibrated at room temperature (~21°C) using 15mM and 150mM KCl solutions to determine the voltage change, or 'slope', which was needed for determination of $[K^+]_o$ (mM) using the Nernst equation. Electrode sensitivities ranged from 54 to 58mV for a 10-fold change in $[K^+]$. A reference and K^+ -sensitive electrode pair were discarded if the slope did not fall within this range or if the voltage reading exhibited atypical sensitivities. The K^+ -sensitive microelectrode was inserted through

the sheath of the MTG adjacent to the reference electrode in the area of the ventilatory CPG.

The voltage of the K^+ -sensitive electrode is logarithmically related to the potassium concentration which was obtained by transforming the $[K^+]_o$ trace in mV to mM using the Nernst equation:

$$E_K = RT / zF \cdot \ln[K^+]_o / [K^+]_i.$$

In the above equation, E_K is the membrane potential at which K^+ is at equilibrium, R is the gas constant (8.315 $J \cdot K^{-1} \cdot mol^{-1}$), T is the temperature in ° Kelvin ($T_{Kelvin} = 273.16 + T_{Celsius}$), F is Faraday's constant (96,485 $C \cdot mol^{-1}$), z is the valence of the ion, and $[K^+]_o$ and $[K^+]_i$ are the concentrations of K^+ outside and inside the cell, respectively. For a membrane permeable only to K^+ at room temperature (20°C), substituting the appropriate numbers and converting natural log (ln) into log base 10 ($\log_{10}$) results in the equation:

$$E_K = 58.2 \log_{10}[K^+]_o / [K^+]_i.$$

The K^+-sensitive electrode voltage recording was set to zero in a stock solution of 15mM KCl and the following conversion of the above equation was used for determination of extracellular potassium concentrations (corrections for temperature differences were made when appropriate):

$$[K^+]_o = 15 \cdot 10^{\text{voltage / slope}(\sim 58.2)}.$$

Hyperthermia: Preparations were bathed for 25 minutes with saline before starting the temperature ramp to allow the ventilatory rhythm to stabilize and the $[K^+]_o$ to settle at

around 10mM. Saline passed through a glass pipette wrapped in Nichrome^{TM} wire, and the temperature of the saline was controlled by varying the amount of current passed through the wire. Temperature at the ganglion was monitored using a thermocouple connected to a digital thermometer (BAT-12; Physitemp Instruments Inc., Clifton, NJ, USA). Internal temperature was raised in a ramped manner 5ºC per minute from room temperature (~20ºC) until failure of the motor pattern (Figure 4.1A, Figure 4.6C, and Figure 4.7), until the abrupt rise in $[K^+]_o$ was observed (Figure 4.4A), or raised beyond the first $[K^+]_o$ plateau (not necessarily in a ramped manner) until a second plateau was reached (Figure 4.3 and Figure 4.4B). At this time, the heater was switched off allowing the saline temperature to return to ambient levels and the motor pattern to recover.

Anoxia: the locust preparation was enclosed in a sealed chamber. Nitrogen gas (N_2) was first bubbled into the superfusing saline for 5 minutes then blown over the preparation within the chamber. 100% N_2 was maintained until 1 minute post-failure of the motor pattern at which point the preparation was re-oxygenated.

Pharmacological treatments: all drugs were dissolved in standard locust saline and bath-applied in semi-intact preparations as described above (all drugs were obtained from Sigma-Aldrich). Preparations were bathed in standard locust saline for a 10 minute stabilization period prior to pharmacological treatment. Drugs were bath-applied continuously for the full duration of each experiment with the exception of 10^{-3}M sodium azide (NaN_3), an electron transport chain inhibitor that prevents cells from using oxygen,

which was bath-applied until 1 minute post-failure. 10^{-4}M ouabain, a Na^+/K^+ ATPase toxin, was bath-applied continuously for 1 hour. 10^{-6}M tetrodotoxin (TTX), a Na^+ channel blocker, and 10^{-1}M tetraethylammonium chloride (TEA), a voltage-gated K^+ channel blocker, were bath-applied for 15 minutes prior to a ramped increase in temperature (5°C per minute). For TTX experiments, the heater was turned off once the $[K^+]_o$ surge was observed and the temperature at the $[K^+]_o$ surge was taken as the temperature at half the maximum amplitude of the $[K^+]_o$ increase. For TEA experiments, the temperature ramp was continued beyond the first $[K^+]_o$ plateau until a second plateau was reached, at which point the heater was turned off.

CON and HS locusts were treated with 10^{-5}M ouabain to determine the role of ouabain-sensitive Na^+/K^+ ATPase activity in thermotolerance and $[K^+]_o$ homeostasis. Animals were divided into four groups: 1) CON, N = 17; 2) HS, N = 18; 3) CON locusts treated with 10^{-5}M ouabain (CON-OUA), N = 10; 4) HS locusts treated with 10^{-5}M ouabain (HS-OUA), N = 8. Experiments on animals receiving different (pre-) treatments were interspersed over time with each other. All preparations were bathed for 25 minutes with saline before starting the temperature ramp. For 10^{-5}M ouabain treatment, the ganglion was bathed with standard locust saline for 10 minutes, and then with 10^{-5}M ouabain for 15 minutes prior to the temperature ramp. At 25 minutes, internal temperature was raised in a ramped manner 5ºC per minute until failure of the motor pattern. Failure temperature (ºC) and time to recovery (s) were scored as the temperature at which rhythmical ventilator activity ceased and the length of time taken to recover motor pattern

function, respectively. In order to determine the nature of the relationships between time to recovery and failure temperature for each group, values were log-transformed to make the relationships linear, which allowed accurate statistical analyses of the data. The correlations are shown in Figure 4.7 as scatterplots of the untransformed data fit with exponential curves that rise to a plateau. Rates of $[K^+]_o$ increase and decrease associated with hyperthermic failure and recovery of the motor pattern were also determined. Rate of $[K^+]_o$ increase (mM/s) was calculated as the slope between the baseline at the inflection point of the $[K^+]_o$ increase and the maximum peak $[K^+]_o$. Rate of $[K^+]_o$ decrease (mM/s) was calculated as the slope between the maximum peak $[K^+]_o$ and the baseline $[K^+]_o$ inflection point. The sample sizes for each analysis varied depending on the ability to measure parameters in some or all locusts within each group.

To locally increase $[K^+]$ in the MTG neuropile we pressure-injected using a PicoSpritzer III (INTRACEL, Shepreth, UK) a small volume (35nl) of locust saline containing a 15-fold higher $[K^+]$ (147mM NaCl, 150mM KCl, 4mM $CaCl_2$, 3mM NaOH, 10mM HEPES buffer, pH 7.2). Two K^+ -sensitive microelectrodes were inserted into the MTG, one next to the injection point and another in a different region of the ganglion. The distance between the recording electrodes (~0.4 to 0.6mm) was determined as well as the time to onset of the $[K^+]_o$ surge measured by each electrode. Using these values the speed of propagation (mm/s) of the $[K^+]_o$ disturbance between the two recording electrodes was calculated.

ATP extraction and assay for locust ganglia: metathoracic ganglia were removed from locust preparations prior to stress, at stress-induced failure, and at recovery of the motor pattern for ATP measurement. ATP levels in the ventilatory neuropile of HS locusts at hyperthermic failure and subsequent recovery of the motor pattern were also measured in order to determine if preconditioning confers protection by increasing energy availability. In addition, metathoracic ganglia were removed from CON and HS locusts at normal oxygen levels (pre-anoxia) and at 15, 30, 60, and 120 minutes of anoxia exposure. Locusts were then removed from the anoxic environment and ganglia were removed at 30 and 60 minutes post-anoxia for ATP measurement.

Immediately after removal, each ganglion was added to 220µl of ice-cold 3.5% perchloric acid in a 1.5ml centrifuge tube. The ganglion was homogenized thoroughly with a pestle and the solution was centrifuged for 5 minutes at maximum speed. Then, 200µl of the supernatant were transferred to a new centrifuge tube on ice containing 20µl Tris (saturated), 20µl KCl (2M), 10µl phenol red (0.005%), and 120µl KOH (1M) to neutralize the sample. The neutralized sample was stored at -80°C until the ATP assays were performed. At that time, samples were thawed and centrifuged for five minutes at maximum speed. A volume of 2.5µl of supernatant was used for the ATP assay.

ATP was quantified using a luciferin-luciferase reaction in which ATP is consumed and light is emitted when firefly luciferase catalyzes the oxidation of D-luciferin. Since ATP is the limiting reagent, the light emitted is proportional to the ATP present, measured by

an L_{max} luminometer (Molecular Devices, Sunnyvale, CA, USA). A reaction mix was prepared by diluting one volume of luciferin-luciferase ATP Assay Mix (lyophilized powder containing luciferin, luciferase, $MgSO_4$, DTT, EDTA Na_4, BSA, and tricine buffer salts dissolved in 5ml of sterile water) with 100 volumes of ATP Assay Mix Dilution Buffer (250ml: 300mg $MgSO_4$, 4mg DTT, 100mg EDTA Na_4, 250mg BSA, 2.25g tricine buffer salts, pH 7.5). The diluted luciferin-luciferase reaction mix was added by auto injector in 200µl aliquots to 2.5µl of sample, pre-dispensed in a 96-well microplate. Light was collected for 20 seconds. Measures of light intensity were compared to a standard curve generated using known quantities of ATP prepared in water, acidified and neutralized as were samples.

Assay of Na^+/K^+ ATPase activity in locust MTG: the Na^+/K^+ ATPase activity was assessed using a pyruvate kinase/lactate dehydrogenase assay in the presence or absence of ouabain. Single metathoracic ganglia from control and HS locusts were homogenized on ice in 300µL of lysis buffer (150mM sucrose, 10mM EDTA, 50mM imidazole and 0.1% deoxycholate, pH 7.3). In one experiment, inhibitors of phosphorylation and dephosphorylation were also added to the lysis buffer to prevent changes in the phosphorylation status of the ATPase. The additional compounds included (in mM) 10 EGTA, 50 NaF, 10 tetrasodium pyrophosphate, 1 phospho-serine, 1 phospho-threonine, and 1 phospho-tyrosine. After homogenization, 0.01 volumes of 100mM PMSF (dissolved in isopropanol) were added to the homogenate.

The measurement of ATPase activity was measured as the production of NADH spectrophotometrically for 10 minutes at 340 nm. Each sample was assayed in six wells on the 96 well plate, three containing ouabain. Each well contained a 300µL reaction mixture consisting of the following solutions (in order): 228µL of assay buffer (50mM imidazole, 100mM NaCl, 20mM KCl, and 5mM $MgCl_2$), 3µL each of 0.2mM NADH, 0.5mM PEP, 10U/mL LDH, and 10U/mL PK, 15µL of either ouabain (0.5mM) or assay buffer, and 30µL sample homogenate. The reaction was started with the addition of 15 µL ATP (3mM). The slope of absorbance over 10 minutes was compared between samples with and without ouabain to give a value for activity of only Na^+/K^+ ATPase. This value was normalized to total protein within the sample, which was measured from each homogenate using a standard protocol based on the Bradford method (Bradford, 1976).

Statistical analyses: Data were plotted using SigmaPlot 8.0 (SPSS Inc., Chicago, IL, USA) and results are reported as the mean ± standard error (s.e.m.). Data were analyzed using SigmaStat 3.0 statistical analysis software (SPSS Inc.) and statistical differences were determined using appropriate parametric tests as indicated in the text. A 95% confidence interval was used to determine significance among means.

4.6 References

Anderson, T.R. Jarvis, C.R. Biedermann, A.J. and R.D. Andrew. Blocking the anoxic depolarization: neuroprotection without functional compromise following simulated stroke in cortical brain slices. *J. Neurophysiol.* 93: 963-979 (2005).

Armstrong, G.A.B. Shoemaker, K.L. Money, T.G.A. and R.M. Robertson. Octopamine mediates thermal preconditioning of the locust ventilatory central pattern generator via a cAMP/protein kinase A signaling pathway. *J. Neurosci.* 26: 12118-12126 (2006).

Balestrino, M. Young, J. and P.G. Aitken. Block of (Na^+,K^+)ATPase with ouabain induced spreading depression-like depolarization in hippocampal slices. *Brain Res.* 838: 37-44 (1999).

Banks, W.M. Bruce, A.S. and H.T. Peart. The effects of temperature, sex and circadian rhythm on oxygen consumption in two species of cockroaches. *Comp. Biochem. Physiol.* 52A: 223-227 (1975).

Bradford, M.M. A rapid and sensitive method for the quantitation of microgram quantities of protein utilizing the principle of protein-dye binding. *Anal. Biochem.* 72: 248-254 (1976).

Bustami, H.P. and R. Hustert. Typical ventilatory pattern of the intact locust is produced by the isolated CNS. *J. Insect. Physiol.* 46: 1285-1293 (2000).

Davenport, A.P. and P.D. Evans. Stress-induced changes in the octopamine levels of insect haemolymph. *Insect Biochem.* 14: 135-143 (1984).

Dawson-Scully, K. Armstrong, G.A.B. Kent, C. Robertson, R.M. and M.B. Sokolowski Natural variation in the thermotolerance of neural function and behavior due to a cGMP-dependent protein kinase. *PLoS ONE* 2: e773 (2007).

Evans, A.M. AMP-activated protein kinase and the regulation of Ca^{2+} signalling in O_2-sensing cells. *J. Physiol.* 574: 113-123 (2006).

Gidday, J.M. Cerebral preconditioning and ischaemic tolerance. *Nat. Neurosci.* 7: 437-448 (2006).

Grafstein, B. Mechanism of spreading cortical depression. *J. Neurophysiol.* 19: 154-171 (1956).

Gulinson, S.L. and J.F. Harrison. Control of resting ventilation rate in grasshoppers. *J. Exp. Biol.* 199: 379-389 (1996).

Hardie, D.G. Hawley, S.A. and J.W. Scott. AMP-activated protein kinase - development of the energy sensor concept. *J. Physiol.* 574: 7–15 (2006).

Henderson, D.R. Johnson, S.M. and H.D. Prange. CO_2 and heat have different effects on directed ventilation behaviour of grasshoppers *Melanoplus differentialis*. *Respir. Physiol.* 114: 297-307 (1998).

Hustert, R. Neuromuscular coordination and proprioceptive control of rhythmical abdominal ventilation in intact *Locusta migratoria migratorioides*. *J. Comp. Physiol.* A 97: 159-179 (1975).

Kager, H. Wadman, W.J. and G.G. Somjen. Conditions for the triggering of spreading depression studied with computer simulations. *J. Neurophysiol.* 88: 2700-2712 (2002).

Kretzschmar, D. and G.O. Pflugfelder. Glia in development, function, and neurodegeneration of the adult insect brain. *Brain Res. Bull.* 57: 121-131 (2002).

Largo, C. Tombaugh, G.C. Aitken, P.G. Herreras, O. and G.G. Somjen. Heptanol but not fluoroacetate prevents the propagation of spreading depression in rat hippocampal slices. *J. Neurophysiol.* 77: 9-16 (1997).

Lauritzen, M. Cortical spreading depression in migraine. Cephalalgia 21: 757-60 (2001).

Leão, A.A.P. Spreading depression of activity in the cerebral cortex. *J. Neurophysiol.* 7: 359-390 (1944).

Lighton, J.R.B. and B.G. Lovegrove. A temperature-induced switch from diffusive to convective ventilation in the honeybee. *J. Exp. Biol.* 154: 509-516 (1990).

Loder, E. What is the evolutionary advantage of migraine? *Cephalalgia* 22: 624-632 (2002).

Nedergaard, M. Cooper, A.J.L. and S.A. Goldman. Gap junctions are required for the propagation of spreading depression. *J. Neurobiol.* 28: 433-444 (1995).

Newman, A.E.M. Foerster, M. Shoemaker, K.L. and R.M. Robertson. Stress-induced thermotolerance of ventilatory motor pattern generation in the locust, *Locusta migratoria*. *J. Insect. Physiol.* 49: 1039-1047 (2003).

Qin, W. Tyshenko, M.G. Wu, B.S. and Walker, V.K. and R.M. Robertson. Cloning and characterization of a member of the Hsp70 gene family from *Locusta migratoria*, a highly thermotolerant insect. *Cell Stress Chaperones* 8: 144-52 (2003).

Ramirez, J.M. Elsen, F.P. and R.M. Robertson. Long-term effects of prior heat shock on neuronal potassium currents recorded in a novel insect ganglion slice preparation. *J. Neurophysiol.* 81: 795-802 (1999).

Robertson, R.M. Modulation of neural circuit operation by prior environmental stress. *Integr. Comp. Biol.* 44: 21-27 (2004a).

Robertson, R.M. Thermal stress and neural function: adaptive mechanisms in insect model systems. *J. Therm. Biol.* 29: 351-358 (2004b).

Smith, J.M. Bradley, D.P. and M.F. James. Huang CL Physiological studies of cortical spreading depression. *Biol. Rev. Camb. Philos. Soc.* 81: 457-481 (2006).

Snyder, G.K. Ungerman, G. and M. Breed. Effects of hypoxia, hypercapnia, and pH on ventilation rate in *Nauphoeta cinerea*. *J. Insect. Physiol.* 26: 699-702 (1980).

Somjen, G.G. Mechanisms of spreading depression and hypoxic spreading depression-like depolarization. *Physiol. Rev.* 81: 1065-1096 (2001).

Somjen, G.G. Ion regulation in the brain: implications for pathophysiology. *Neuroscientist* 8: 254-267 (2002).

Takano, T. Tian G.-F. Peng, W. Lou, N. Lovatt, D. Hansen, A.J. Kasischke, K.A. and M. Nedergaard. Cortical spreading depression causes and coincides with tissue hypoxia. *Nature Neurosci.* 10: 754-762 (2007).

Tupling, A.R. Gramolini, A.O. Duhamel, T.A. Kondo, H. and M Asahi. HSP70 binds to the fast-twitch skeletal muscle sarco(endo)plasmic reticulum Ca^{2+}-ATPase (SERCA1a) and prevents thermal inactivation. *J. Biol. Chem.* 279: 52382-52389 (2004).

van den Maagdenberg, A.M. Haan, J. Terwindt, G.M. and M.D. Ferrari. Migraine: gene mutations and functional consequences. *Curr. Opin. Neurol.* 20: 299-305 (2007).

van Harrevald A. Two mechanisms for spreading depression in the chicken retina. *J. Neurobiol.* 9: 419-431 (1978).

Walther, C. and K.E Zittlau. Resting membrane properties of locust muscle and their modulation. II. Actions of the biogenic amine octopamine. *J. Neurophysiol.* 80: 785-797 (1998).

Whyard, S. Wyatt, G.R. and V.K. Walker. The heat shock response in *Locusta migratoria*. *J. Comp. Physiol.* B 156: 813-817 (1986).

Wu, J. and R.S. Fisher. Hyperthermic spreading depressions in the immature rat hippocampal slice. *J. Neurophysiol.* 84: 1355-1360 (2000).

Chapter 5

Suppression of spreading depression-like events in locusts by inhibition of the NO/cGMP/PKG pathway.

Gary A.B. Armstrong*, Corinne I. Rodgers, Tomas G.A. Money and R. Meldrum Robertson.

Department of Biology, Queen's University, Kingston ON, Canada, K7L 3N6.

* To whom correspondence should be sent: G.A.B. Armstrong, Department of Biology, Queen's University, Biosciences Complex, Kingston, Ontario, Canada K7L 3N6. Email (9ga1@queensu.ca).

Citation: The Journal of Neuroscience 29:8225-8235 (2009).

5.1 Abstract

In spite of the considerable research attention focused on the mechanisms underlying neural spreading depression (SD) due to its association with several important human CNS pathologies such as stroke and migraine, little attention has been given to explaining its occurrence and regulation in invertebrates. In the locust metathoracic ganglion (MTG) an SD-like event occurs during heat and anoxia stress which results in cessation of neuronal output for the duration of the applied stress. SD-like events were characterized by an abrupt rise in extracellular potassium ion concentration ($[K^+]_o$) from a baseline concentration of around 8 mM to greater than 30 mM which returned to near baseline concentrations upon removal of the applied stress. Following return to baseline $[K^+]_o$ neuronal output from the MTG recovered. Neuronal output was measured by monitoring ventilatory motor pattern activity electromyographically. We show here that unlike mammalian neurons which depolarize almost completely during SD, locust neurons only partially depolarize. We further show that SD-like events in the locust CNS are suppressed by pharmacological inhibition of the nitric oxide / cyclic guanosine monophosphate / protein kinase G (NO/cGMP/PKG) pathway and are exacerbated by its activation. Moreover we show that environmental stressors such as heat and anoxia increase production of NO in the locust CNS. Finally we show, for the intact animal, that manipulation of the pathway affects the speed of recovery from suffocation by immersion under water. We propose that SD-like events in locusts provide an adaptive mechanism for surviving extreme environmental conditions (e.g. promoting hyperthermia or anoxia).

The highly conserved nature of the NO/cGMP/PKG signaling pathway suggests that it may be involved in modulating SD in other organisms including mammals.

5.2 Introduction

Neuronal hyperexcitability associated with elevated concentrations of extracellular potassium ions ($[K^+]_o$) is a hallmark of cortical spreading depression (CSD) in mammals (Somjen, 2001). This phenomenon is critically involved in stroke, head trauma and migraine and the discovery of cellular mechanisms capable of preventing or attenuating CSD has great potential health benefits. We have used a locust model of CNS function to investigate methods of manipulating SD-like events by monitoring the activity of the ventilatory central pattern generator (vCPG), which is vital for organismal health.

Under anoxic conditions many insects enter a reversible state of coma (e.g. supplemental video 1) during which electrical activity in the nervous and muscular systems is shut down. This is considered to be an adaptive strategy to conserve energy and prevent neuronal hyperexcitation (Walter and Nelson, 1975; Rodgers et al., 2007), and recovery is complete upon return to normoxia, often after many hours (up to at least 6 hours in locusts (Wu et al., 2002)). Anoxic conditions arise in the environment during flash floods and monsoons and recovery occurs quickly (e.g. supplemental video 2). Recently we have shown that the arrest of CNS function during anoxia in locusts is accompanied by an abrupt increase in $[K^+]_o$ in the neuropile (Rodgers et al., 2007). Similar increases in $[K^+]_o$ are induced by hyperthermia and by disrupting mitochondrial function. Moreover manipulation of ionic gradients, either by direct injection of high K^+ saline into the extracellular space or by reducing Na^+/K^+ATPase activity with ouabain, generates

waves of increased $[K^+]_o$ that propagate throughout the neuropile and are associated with transient depression of motor pattern activity (Rodgers et al., 2007). These phenomena share all the major characteristics of CSD, though the extent of neuronal depolarization during the locust SD-like event is unknown.

A genetic component to hyperthermic neural depression has been demonstrated for the *foraging* gene in *Drosophila* (Dawson-Scully et al., 2007). The gene encodes for a protein kinase G (PKG) and the naturally occurring populations with different alleles of this gene (*rover* and *sitter*) differ in the levels of gene transcript and PKG (Osborne et al., 1997). Pharmacologically or genetically reducing levels of PKG, or its downstream targets, increases thermotolerance of the larval *Drosophila* neuromuscular junction. Similar treatments also increase the locust vCPG's tolerance to heat-stress (Dawson-Scully et al., 2007) suggesting evolutionary conservation of the mechanism. Hyperthermic arrest of vCPG operation in the locust CNS is associated with SD-like increases of $[K^+]_o$ that occur prior to irreversible cellular collapse (Rodgers et al., 2007). Hence we reasoned that manipulation of the PKG pathway would modulate the occurrence and severity of locust SD-like events induced by direct manipulation of ion gradients, in the absence of heat. We tested this idea by measuring SD-like events induced by ouabain or by neuropile injections of K^+ and by pharmacologically manipulating the NO/cGMP/PKG pathway. We monitored ventilatory motor activity in a semi-intact preparation because of the excellent accessibility of this system during its

normal operation and because the points of failure and recovery of neural function are unequivocal.

5.3 Results

SD-like events coincides with neuronal depolarization and reduced input resistance.

To determine the extent of neuronal depolarization during SD-like events we used sharp intracellular microelectrodes to record neuronal activity in the metathoracic ganglion (MTG) concurrently with recordings of the ventilatory motor pattern and $[K^+]_o$ (Figure 5.1a,b). To induce SD-like events we either superfused the MTG with ouabain (0.1 mM) (Figure 5.1c) or briefly (~30 s) applied sodium azide (1 mM) (Figure 5.1d). By inhibiting mitochondrial function sodium azide mimics anoxic coma whereas treatment with ouabain provides a more gradual and less extreme impairment of ionic homeostasis in the CNS. We recorded from a total of 19 neurons of which 10 were active in phase with ventilation and 9 were tonically active. Both ouabain and sodium azide treatments reliably generated SD-like events characterized by surges of $[K^+]_o$ (30 – 50 mM) associated with arrest of vCPG activity and depolarization of neurons. During SD-like events, neurons depolarized from a mean interburst membrane potential of -49.0 mV to a maximal depolarization to -36.6 mV and then repolarized to -50.9 mV when $[K^+]_o$ recovers to baseline values (Figure 5.2a). To account for neuronal variability and for statistical comparisons we normalized changes in membrane potential to the pre-SD-like event values (Figure 5.2b). There was a statistically significant 30% decrease in membrane potential of MTG neurons during SD-like events evoked by sodium azide. Recovery of vCPG activity occurred when $[K^+]_o$ returned towards normal values and neurons repolarized.

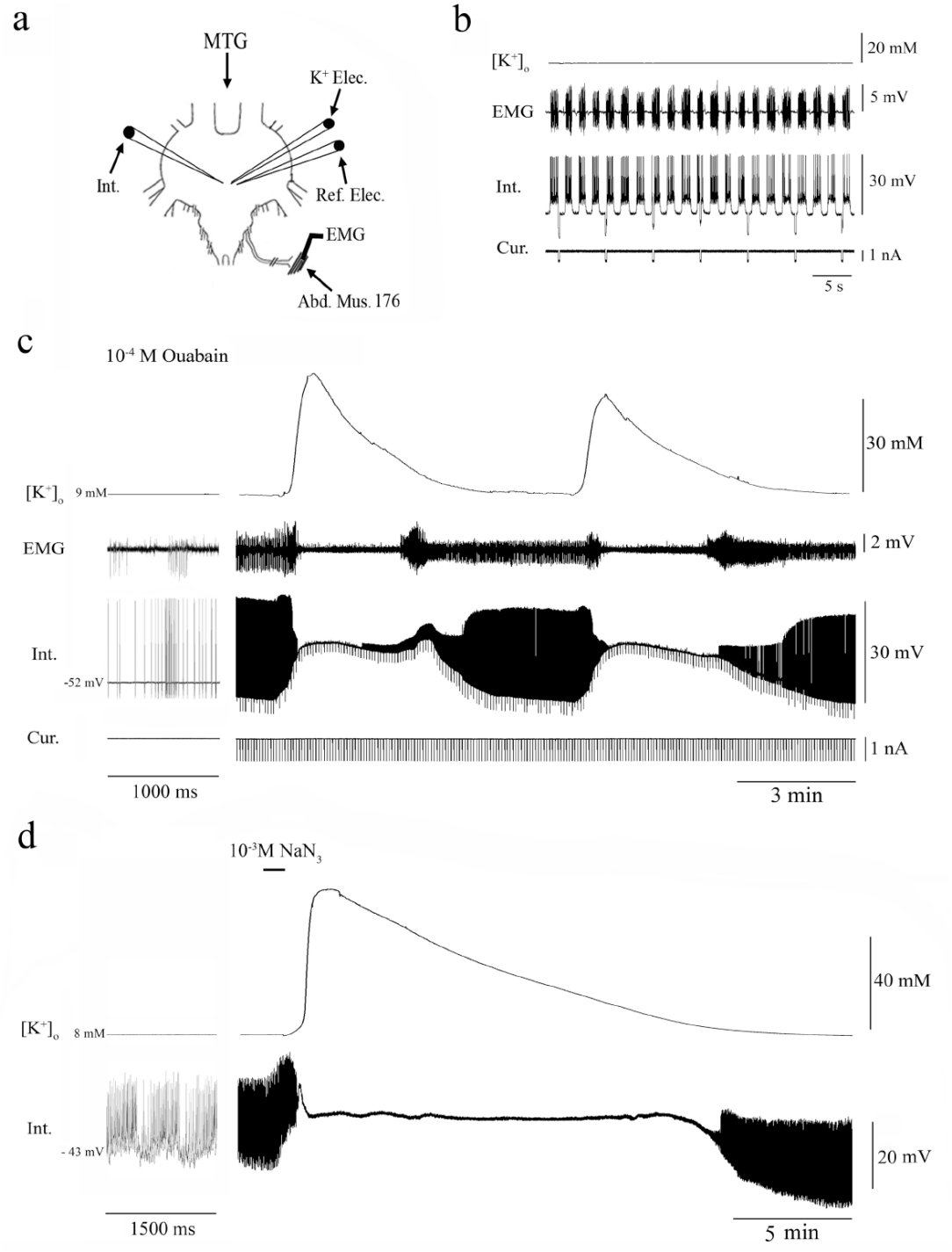
a
MTG
K+ Elec.
Int.
Ref. Elec.
EMG
Abd. Mus. 176
b
[K+]o
20 mM
EMG
5 mV
Int.
30 mV
Cur.
1 nA
5 s
c
10-4 M Ouabain
30 mM
[K+]o 9 mM
EMG
2 mV
Int.
-52 mV
30 mV
Cur.
1 nA
1000 ms
3 min
d
10-3M NaN3
40 mM
[K+]o 8 mM
Int.
- 43 mV
20 mV
1500 ms
5 min

Figure 5.1

Figure 5.1. SD-like events in the metathoracic ganglion (MTG) of the migratory locust (*Locusta migratoria*). **a**, Schematic diagram of the MTG and recording electrodes used (Int., intracellular electrode; K^+ Elec., potassium ion electrode; Ref. Elec., reference electrode for measuring $[K^+]_o$; EMG, electromyographic electrode; Abd. Mus. 176, abdominal muscle 176, one of the ventilatory muscles). **b**, Sample recording from a ventilatory interneuron (Int.) and associated motor activity (EMG). Baseline level of $[K^+]_o$ is 8 mM. Lower trace (Cur.) shows -1 nA hyperpolarizing current pulses (6 Hz). **c**, Sample trace showing a preparation bath applied with the Na^+/K^+ATPase inhibitor, ouabain; note the two ouabain-induced SD-like events. During the surge the neuron depolarized and then repolarized when $[K^+]_o$ returned to near baseline levels. Current pulses (-1 nA) were delivered at 4.5 Hz. **d**, Sample trace following a brief exposure to sodium azide (30 sec.) which quickly induced a surge in $[K^+]_o$, coinciding with membrane depolarization and cessation of neuronal activity. Following superfusion with saline, neuronal activity recovered, and membrane potential was restored.

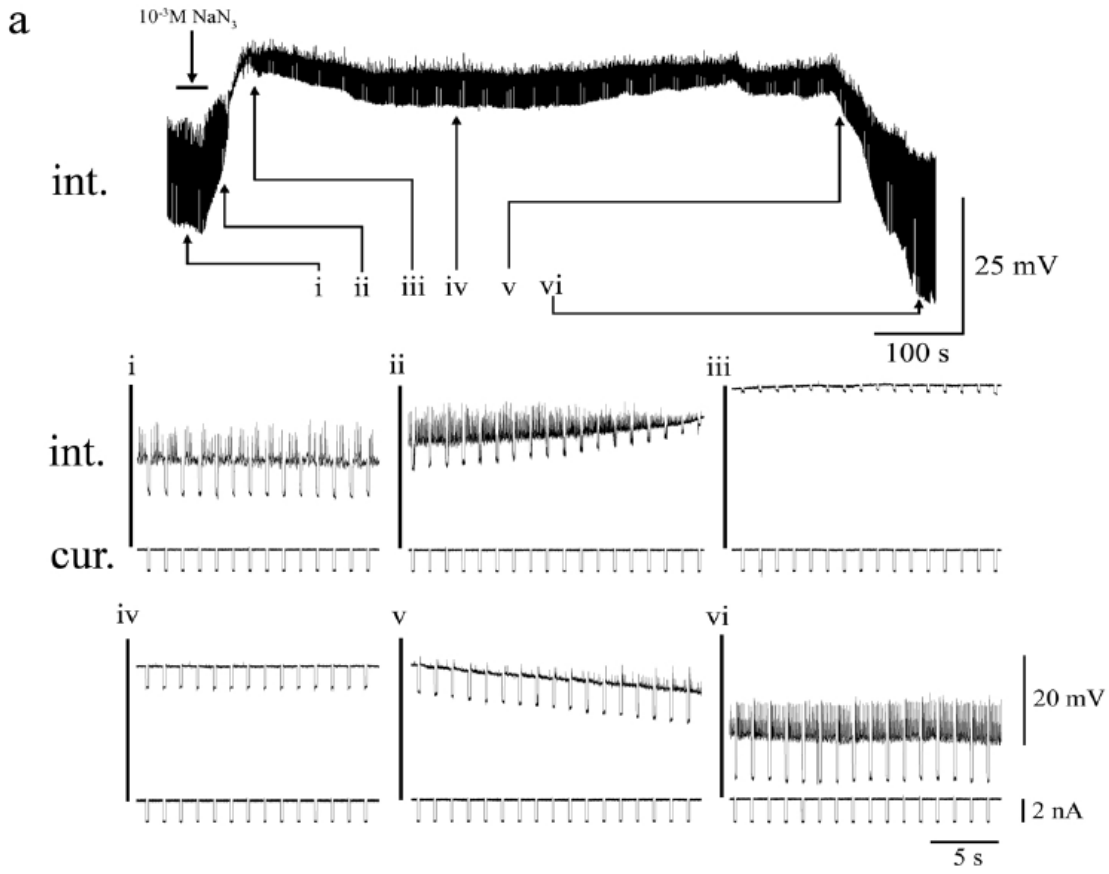
a
10-3M NaN3
int.
i
ii
iii
iv
v
vi
25 mV
100 s
i
ii
iii
int.
cur.
iv
v
vi
20 mV
2 nA
5 s

Figure 5.2

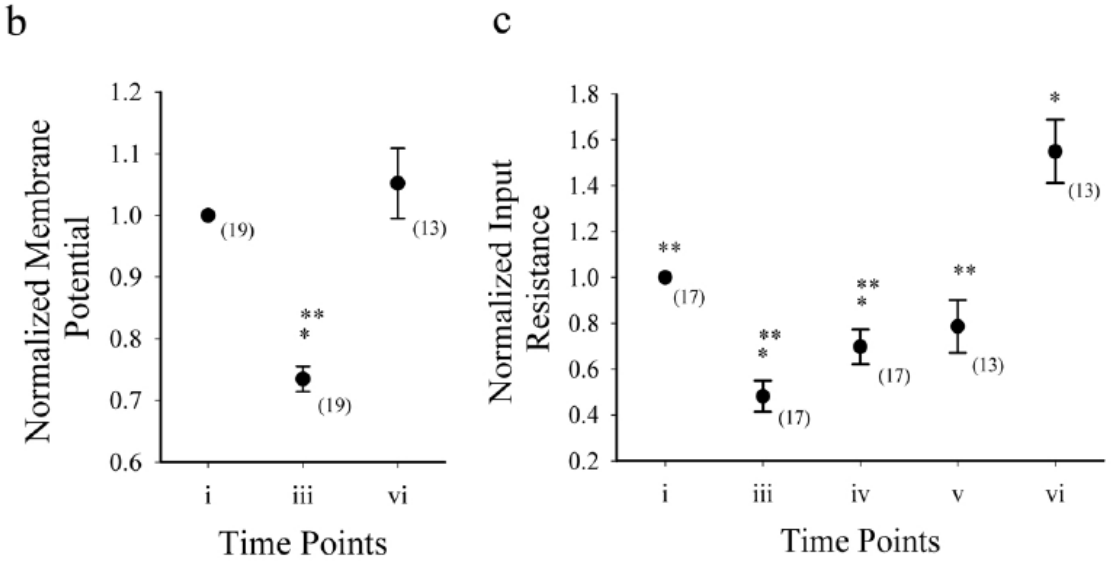
b
Normalized Membrane Potential
1.2
1.1
1.0
0.9
0.8
0.7
0.6
(19)
**
*
(19)
(13)
i
iii
vi
Time Points
c
Normalized Input Resistance
1.8
1.6
1.4
1.2
1.0
0.8
0.6
0.4
0.2
**
(17)
**
*
(17)
**
*
(17)
**
(13)
*
(13)
i
iii
iv
v
vi
Time Points

Figure 5.2. Effect of SD-like events on membrane potential and input resistance of neurons in the MTG. **a**, Above, sample intracellular recording in the neuropil from a spontaneously active neuron during an SD-like event. Following a 30 second sodium azide perfusion over the MTG (NaN_3) the neuron depolarized, timing coincides with the onset of SD-like event (see figure 5.1). Below, various time points (i-vi) were used to quantify membrane characteristics. i, before NaN_3 treatment; ii, during depolarization; iii, maximal depolarization; iv, 5 minutes following azide wash off; v, prior to repolarization; vi, restoration of membrane potential. Note that the lower trace in each time point is showing the current pulses (cur., 1 Hz) and the upper trace is the intracellular recording (int.). **b**, Changes in membrane potential normalized to initial values before sodium azide treatment show depolarization during the SD-like event with subsequent recovery. **c**, During SD-like events there was a significant decrease in input resistance. Upon restoration of activity and resting membrane potential, input resistance was higher than pre-SD-like event values. Numbers in brackets represent sample size. Single asterisks indicate significant differences from i. Double asterisks indicate significant differences from vi (one-way ANOVA, Post-hoc Tukey test, $p < 0.05$).

To monitor changes in input resistance we delivered hyperpolarizing -1 nA current pulses through the recording electrode and measured changes in membrane potential (Figure 5.2a). Before the SD-like event, the mean input resistance from neuropil recordings was 9.3 ± 1.5 MΩ which decreased to 4.4 ± 0.9 MΩ at the maximal depolarization of each neuron and then recovered to a value of 13.4 ± 2.1 MΩ following restoration of the K^+ gradient. For statistical comparisons we normalized changes in input resistance to pre-SD-like event values and found a significant decrease in input resistance in neurons during the SD-like event (Figure 5.2c). Just prior to repolarization, input resistance increased, to the point where it was not significantly different from pre-SD-like event values. However input resistance following restoration of K^+ gradient was significantly higher than pre-SD-like event values (Figure 5.2c).

These data confirm that SD-like events in the locust MTG are associated with neuronal hyperexcitation and a decrease in input resistance likely caused by opening of voltage-dependent channels.

PKG inhibition suppresses ouabain-induced SD-like events.

Using a model whereby repetitive SD-like events were induced by inhibiting the Na^+/K^+-ATPase during a 30 minute exposure to 0.1 mM ouabain, we examined if altered PKG activity would affect the occurrence of repetitive SD-like events. Coinciding with ouabain-induced cessation of vCPG activity there was a rapid rise in $[K^+]_o$ followed by restoration of $[K^+]_o$ to near baseline levels corresponding with vCPG recovery (Figure 5.3a).

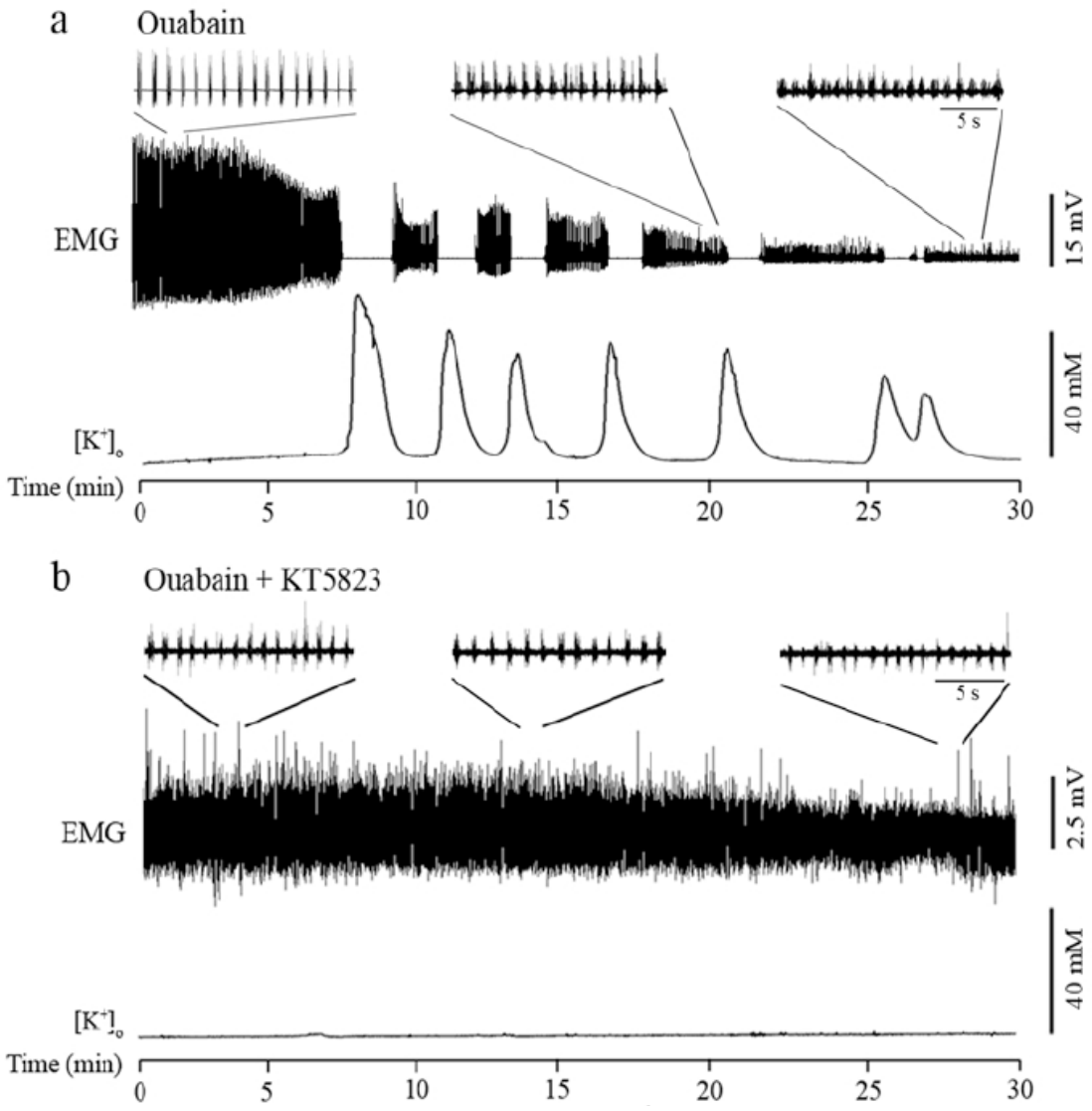
a
Ouabain
5 s
EMG
15 mV
40 mM
[K+]o
Time (min)
0
5
10
15
20
25
30
b
Ouabain + KT5823
5 s
EMG
2.5 mV
40 mM
[K+]o
Time (min)
0
5
10
15
20
25
30

Figure 5.3

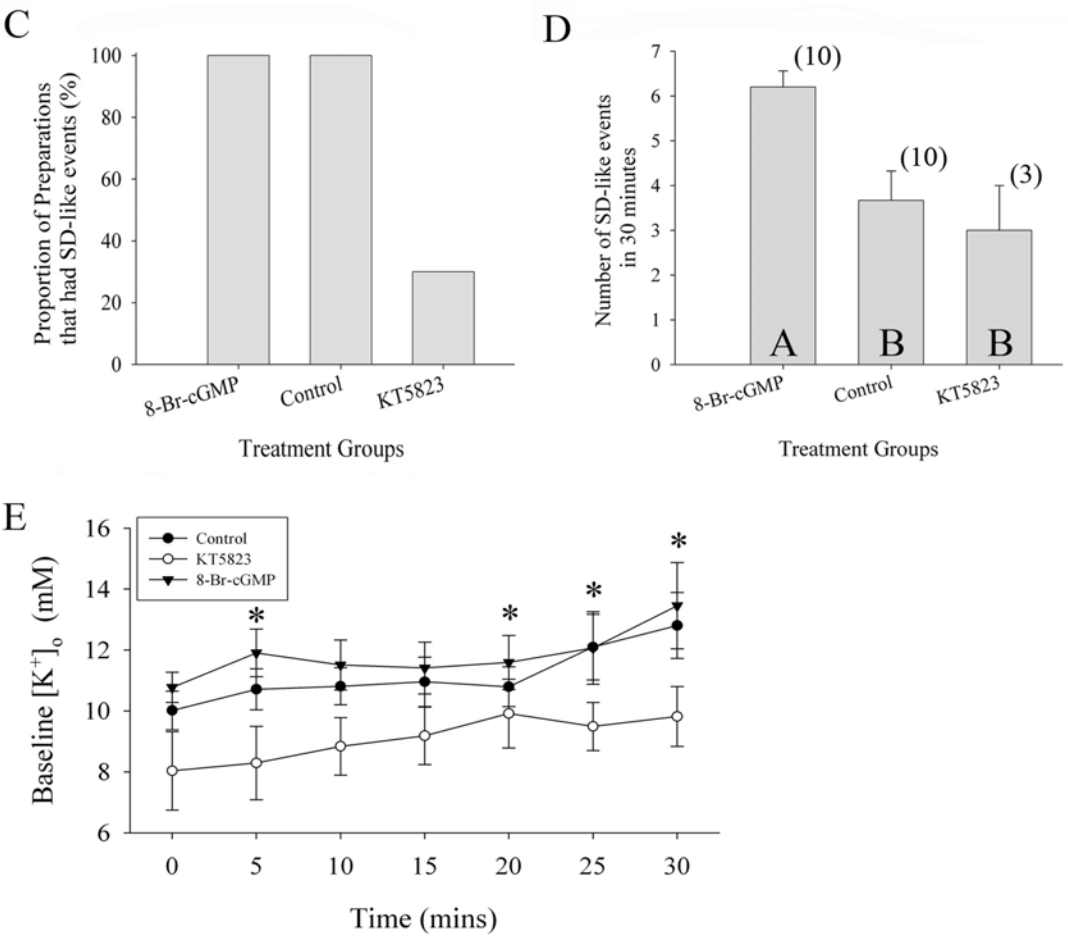
C
Proportion of Preparations that had SD-like events (%)
100
80
60
40
20
0
8-Br-cGMP
Control
KT5823
Treatment Groups
D
Number of SD-like events in 30 minutes
7
6
5
4
3
2
1
0
(10)
(10)
(3)
A
B
B
8-Br-cGMP
Control
KT5823
Treatment Groups
E
Baseline [K+]o (mM)
16
14
12
10
8
6
Control
KT5823
8-Br-cGMP
*
*
*
*
0
5
10
15
20
25
30
Time (mins)

Figure 5.3. Effects of PKG manipulation on ouabain-induced SD-like events in the MTG. (**A**) SD-like events were identified as abrupt increases in $[K^+]_o$ coinciding with cessation of motor output from the MTG monitored by electromyographic recordings of ventilatory motor patterns (EMG) during a 30 minute exposure to 100 μM ouabain. Insets show expansions of the EMG trace, revealing the ventilatory rhythm. (**B**) Sample recordings from a preparation pre-treated with the PKG inhibitor KT5823 showing protection from ouabain-induced SD-like events. Semi-intact preparations were dissected in saline, then switched to saline containing either 10 μM KT5823, 10 μM 8-Br-cGMP (PKG agonist), or saline as a control for 10 minutes. Following drug treatment, saline containing ouabain was superfused over the MTG. (**C**) All control and 8-Br-cGMP-treated preparations co-treated with ouabain generated SD-like events, whereas only 30% of KT5823-treated preparations generated these events. (**D**) Treatment with 8-Br-cGMP significantly increased the number of individual events occurring in a 30 minute period, whereas the few animals treated with KT5823 that exhibited this phenomena (n=3) did not differ in the number of events when compared to control preparations. (**E**) Preparations treated with KT5823 had lower baseline $[K^+]_o$ during the course of ouabain exposure than 8-Br-cGMP-treated and control preparations (n = 10 for each group). Asterisks indicate significant differences between KT5823-treated animals and control animals (Two-way repeated measures ANOVA with a post-hoc Tukey multiple comparisons test $p \leq 0.05$). Numbers in brackets represents sample size. Letters in histogram bars represent statistical groupings using a post-hoc test, whereby bars with

different letters are significantly different (one-way ANOVA, Post-hoc Tukey test, $p < 0.05$).

All preparations treated with 0.1 mM ouabain generated SD-like events in the MTG, however preparations pretreated with the PKG inhibitor KT5823 showed a 70% reduction in the number of preparations generating SD-like events (Fig. 2b,c). All locusts pretreated with the PKG activator 8-Br-cGMP showed ouabain-induced SD-like events. Furthermore these animals had significantly more SD-like events in the same period than locusts treated with ouabain (Fig. 3d). Moreover, treatment with the PKG activator made this model more sensitive to ouabain-induced SD-like events, observed as a reduction in the time to the first SD-like event (control, 542 ± 142 s; 8-Br-cGMP, 252 ± 26 s mean ± s.e.m; Mann-Whitney Rank Sum Test, $P = 0.076$). We found no difference in mean amplitude or duration measured at half the maximum amplitude of each ouabain-induced SD-like event, but there was a general trend of decreased amplitude following each successive SD-like event. Preparations treated with the PKG inhibitor maintained a lower baseline level of $[K^+]_o$ during the 30 minute exposure to ouabain (Fig. 3e).

These data demonstrate that pharmacological manipulation of PKG has profound effects on the occurrence and severity of repetitive SD-like events induced by disturbing ion homeostasis in the locust.

PKG inhibition attenuates SD-like event evoked by extracellular K^+ injection.

To investigate the effect of PKG pathway manipulation on SD-like events without the confounding effects of ouabain we tested a variety of pharmacological agents on single SD-like cycles evoked by local injections of high KCl saline directly into the MTG

(150mM vs. 10mM; 50 nl). All preparations, regardless of drug treatment, reliably generated SD-like events following each injection. We used a within animal experimental paradigm to compare various drug treatments on SD-like event duration (measured at half the maximum amplitude) and the length of time to recover vCPG function after motor pattern arrest. KCl-evoked SD-like events were compared before and after 10 minutes of recovery followed by 10 mins of bath-applied drug treatment. Within 10-15 seconds of the first injection (depending on how close the ion-sensitive electrodes were to the injection site) there was a surge in $[K^+]_o$ with concurrent cessation of vCPG activity (Figure 5.4a). Mean SD-like event duration and vCPG recovery time of the first evoked SD-like event was 102.3 ± 9.2 s and 156.6 ± 11.1 s (n = 14; mean ± s.e.m) respectively. Following the second injection, SD-like event duration and vCPG recovery time were longer (130.5 ± 16.0 s and 174.6 ± 10.3 s respectively; n = 11) (Figure 5.4a,b). The increases in mean SD-like event duration and vCPG recovery time were significant (SD-like event duration: Wilcoxon signed rank test, w = 83.00, P = 0.007; vCPG recovery time: Paired t-test, t = - 3.308, P = 0.006).

Consistent with the ouabain experiments, single KCl-evoked SD-like events were significantly altered by PKG inhibition. To quantify the change in SD-like event duration and vCPG recovery time following drug treatments we normalized these measures to the

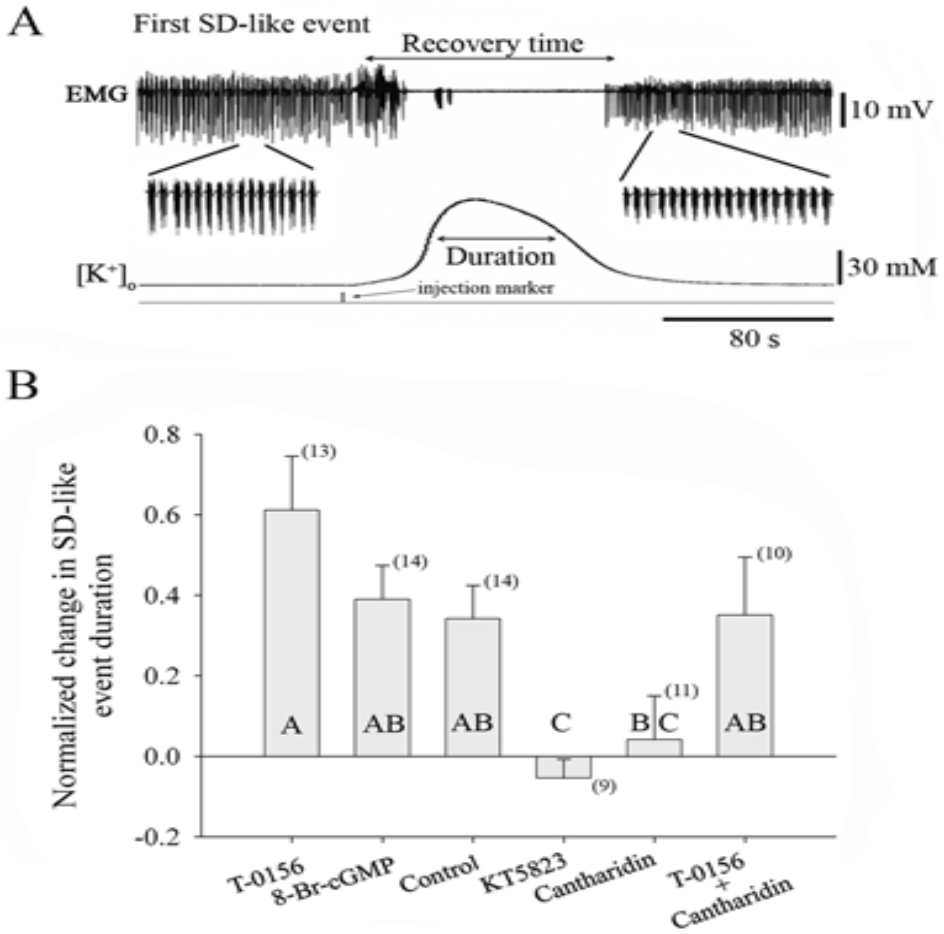
A
First SD-like event
Recovery time
EMG
10 mV
Duration
[K+]o
30 mM
injection marker
80 s
B
Normalized change in SD-like event duration
0.8
0.6
0.4
0.2
0.0
-0.2
(13)
(14)
(14)
(9)
(11)
(10)
A
AB
AB
C
B C
AB
T-0156
8-Br-cGMP
Control
KT5823
Cantharidin
T-0156 + Cantharidin

Figure 5.4

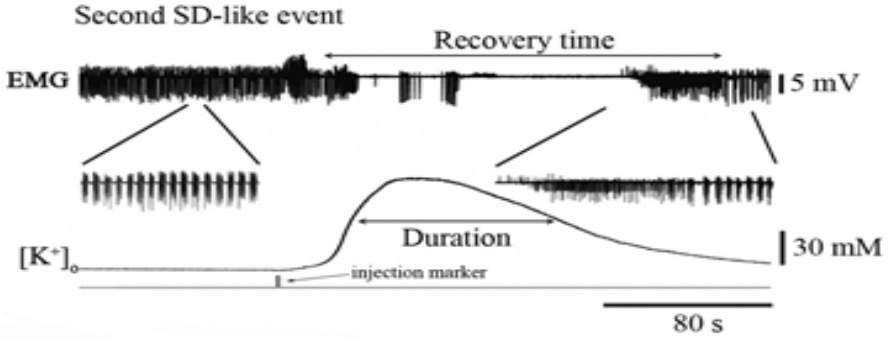
Second SD-like event
Recovery time
EMG
5 mV
Duration
30 mM
injection marker
80 s

C

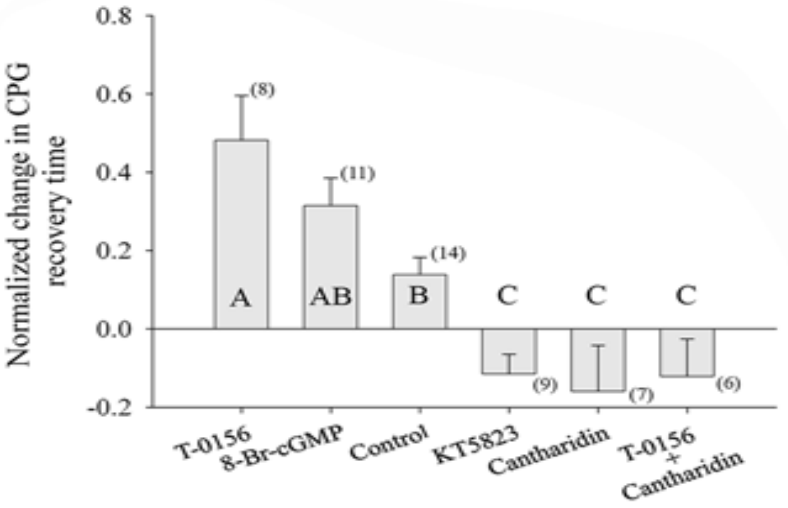
Normalized change in CPG recovery time
0.8
0.6
0.4
0.2
0.0
-0.2
(8)
(11)
(14)
(9)
(7)
(6)
A
AB
B
C
C
C
T-0156
8-Br-cGMP
Control
KT5823
Cantharidin
T-0156 + Cantharidin

Figure 5.4. Effects of activation and inhibition of the cGMP/PKG pathway on KCl-induced SD-like events. **a**, Single SD-like events were evoked by injecting saline (50 nl) containing elevated potassium chloride (150mM vs. 10mM) directly into the MTG. SD-like events was characterized by a transient increase of extracellular potassium ion concentration ($[K^+]_o$). During SD-like events ventilatory motor activity monitored electromyographically (EMG) ceased and recovered upon restoration of the potassium ion gradient. We measured the duration of the $[K^+]_o$ event at half its maximal amplitude and the time from failure of the ventilatory motor pattern to the recovery of the rhythm. **b**, 20 minutes following recovery of ventilatory motor pattern activity a second injection was delivered into the MTG, evoking a second SD-like event, permitting within animal comparisons. 10 minutes before the second injection was made, various pharmacological antagonists or agonists were bath applied to manipulate PKG activity or protein phosphatase 2A activity. **c**, In control preparations the second event was about 30% longer than the first. Event duration was increased by T-0156 (phosphodiesterase inhibitor) though not by 8-Br-cGMP, and reduced by KT5823 and cantharidin (PP2A antagonist). The effect of T-0156 was offset by cantharidin but not significantly reduced. **d**, In control preparations motor pattern recovery time was about 10% longer for the second event compared with the first. The recovery time was increased by 8-Br-cGMP and T-0156 and reduced by KT5823 and cantharidin. The effect of T-0156 was significantly offset by co-treatment with cantharidin. These data indicate that PKG inhibition (KT5823) reduces the duration of SD-like events and hastened the time to recover neural function following SD; whereas activation of the pathway (8-Br-cGMP, T-

0156) had the opposite effect. Numbers in brackets represent sample size. Letters in histogram bars represent statistical groupings using a post-hoc test, whereby bars with different letters are significantly different (Tukey, $p < 0.05$). Error bars represent s.e.m.

values obtained as a result of the first injection (e.g. normalized SD-like event duration equals (1^{st} injection SD-like event duration minus 2^{nd} injection SD-like event duration) divided by 1^{st} SD-like event duration time). For instance, a normalized change in SD-like event duration of zero would indicate that there was no change between the first and second SD-like event duration. Treatment with the PKG inhibitor KT5823 shortened SD-like event durations more than all other treatments (Figure 5.4c). Using cantharidin to inhibit protein phosphatase 2A (PP2A), a downstream target of PKG that acts on K^+ channels (Zhou et al. 1996), we found a similar decrease in SD-like event duration (Figure 5.4c). Neither PKG activation (via 8-Br-cGMP) or phosphodiesterase (PDE) inhibition (via T-0156; Mochida et al. 2002) significantly affected SD-like event duration beyond that of control experiments, although there was a general trend of increased SD-like event duration.

Perhaps a more relevant measure of neuronal activity recovery following KCl-evoked SD-like events is the time taken for motor pattern activity to recover operation (see methods for assessment of vCPG recovery time). Preparations treated with either KT5823 or cantharidin after their first KCl-evoked SD-like event, generated shorter recovery times. This was in contrast to either control preparations or those treated with 8-Br-cGMP or T-0156 which were statistically longer (Figure 5.4d). In addition, preparations co-treated with cantharidin and T-0156, had shorter vCPG recovery times, confirming that inhibition of downstream steps can prevent the exacerbating effects of upstream activation of the PKG pathway by T-0156 (Figure 5.4d).

Thus the severity of the depression of neural activity during individual cycles of SD-like events can be modulated by altering levels of PKG and one of its downstream targets.

Inhibition of NOS attenuates SD-like events evoked by extracellular K^+ injection.

In the CNS of invertebrates and vertebrates, nitric oxide (NO)-activated soluble guanylate cyclase (sGC) is one of the enzymes responsible for the production of cGMP and subsequent activation of PKG (Elphick et al. 1993; Moncada et al. 1991), though other activators of PKG do exist (Morton and Giunta, 1992; Ewer et al. 1994; Müller, 1997). Histochemical techniques and immunocytochemistry have been used to identify cells in the locust thoracic nerve cord that contain NO synthase (NOS), the key enzyme that produces NO as it converts L-arginine to L-citrulline (Moncada et al. 1991; Müller, 1997; Bullerjahn and Pflüger, 2003). To examine the role of NO in modulation of KCl-evoked SD-like events we used the same double injection experimental paradigm used previously. We either treated preparations with L-NAME (NOS inhibitor) or we augmented endogenous NO using the NO donors SNAP or SNOG (Figure 5.5a). Although treatment with L-NAME or the NO donors did not significantly alter SD-like event duration compared with control preparations, preparations treated with L-NAME generated significantly shorter SD-like event durations than preparations treated with SNOG. There was a general trend of increased duration following bath application of both NO donors (Figure 5.5a). There was a strong effect of L-NAME on the time to recover circuit function which was significantly different from all other treatments (Figure 5.5b). The presence of NO donors did not significantly increase the length of time needed for vCPG activity to recover but did offset the effect of L-NAME.

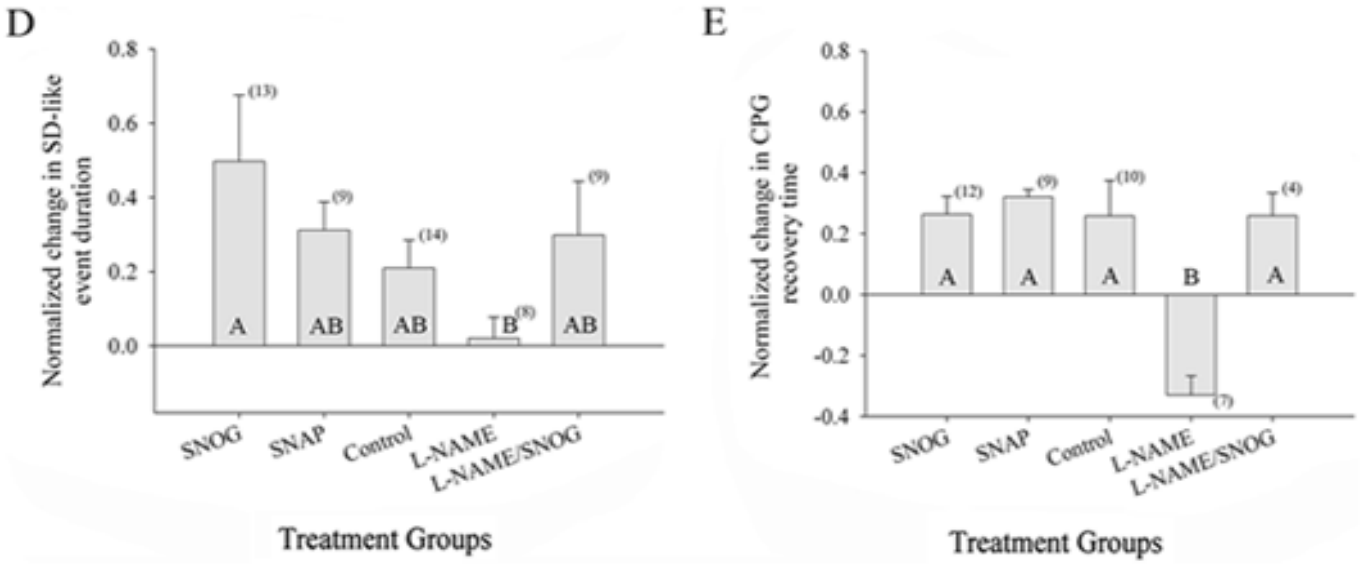
D
Normalized change in SD-like event duration
0.8
0.6
0.4
0.2
0.0
(13)
(9)
(14)
(8)
(9)
A
AB
AB
B
AB
SNOG
SNAP
Control
L-NAME
L-NAME/SNOG
Treatment Groups
E
Normalized change in CPG recovery time
0.8
0.6
0.4
0.2
0.0
-0.2
-0.4
(12)
(9)
(10)
(7)
(4)
A
A
A
B
A
SNOG
SNAP
Control
L-NAME
L-NAME/SNOG
Treatment Groups

Figure 5.5

Figure 5.5. Effect of NO on KCl-induced SD-like events. **a**, Animals were treated with either the NOS inhibitor L-NAME (100 μM), the NO donors SNAP (1μM) or SNOG (1μM), or a combination of L-NAME and SNOG. Control animals were superfused with locust saline. Animals treated with L-NAME had significantly shorter SD-like event durations than animals treated with SNOG. **b**, Following L-NAME treatment the length of time taken to recover CPG function following SD-like events was shorter than for all other drug treatments. This effect was abolished by concurrent exposure to the NO donor SNOG (L-NAME + SNOG). Letters in histogram bars represent statistical groupings using a post-hoc test, whereby bars with different letters are significantly different (One-way ANOVA, Tukey, $p < 0.10$). Error bars represent s.e.m.

These data demonstrate that inhibition of NOS mimics the effect of reduced PKG activity on reducing SD-like event duration in the MTG.

Abiotic stress increases NO production in the MTG.

A plausible interpretation of anoxic and hyperthermic comas is that they are adaptive, conserving energy during periods of abiotic stress (Walter and Nelson 1975; Rodgers et al. 2007). Thus we looked for evidence that abiotic stressors would activate the NO/PKG pathway by measuring the production of NO in the MTG. We dissected out the MTG and mesothoracic ganglion (MSG) and incubated both for 1 hour in 30 μM 4,5-diaminofluorescein-2 diacetate (DAF-2 DA), a selective membrane permeable marker, which is converted by cellular esterases to DAF-2 that fluoresces in the presence of NO (Kojima et al. 1998; Brown et al. 2000). NO levels were estimated as the difference in fluorescence between the DAF-2 loaded neurons and tissue background arising during a 500 ms exposure. Fluorescence readings were collected every 5 min. Labeled cell patterns were similar to previously reported cells that contain NOS in the desert locust, *Schistocerca gregaria* (Müller and Bicker, 1994; Ott and Burrows, 1998). Cell sizes ranged from 9.4μM to 39.0μM with an average size of 18.9 ± 2.9μM (mean ± s.e.m.; n = 11).

In untreated ganglia, DAF-2 fluorescence (corrected for background) remained nearly constant for 65 min. The modest (not significant) decrease with time in these ganglia is likely due to a combination of low NO production with photobleaching and leakage.

When ganglia were treated with sodium azide, there was no significant change in DAF-2 fluorescence during the 15 min treatment, but after azide removal, DAF-2 fluorescence increased linearly for the next 25 min. After this point, DAF-2 fluorescence remained greater than untreated cells, but did not further increase, suggesting either a reduction in NO production or saturation of the available DAF-2. (Figure 5.6a.b). When azide-treated cells were compared to untreated cells, DAF-2 fluorescence was significantly increased (two-way rm ANOVA, $p < 0.001$; $n = 6$; Figure 5.6c). To assess the role of NOS in this phenomenon, we pretreated cells with the NOS inhibitor L-NAME by including it as a pretreatment during DAF-2 loading (n=3). Under these conditions, L-NAME completely abolished the azide-induced increase in DAF-2 fluorescence (two-way rm ANOVA, $p = 0.449$).

We also investigated if temperature stress would alter NO production in these cells. We briefly raised the temperature of saline flowing over these ganglia to 35 °C and then

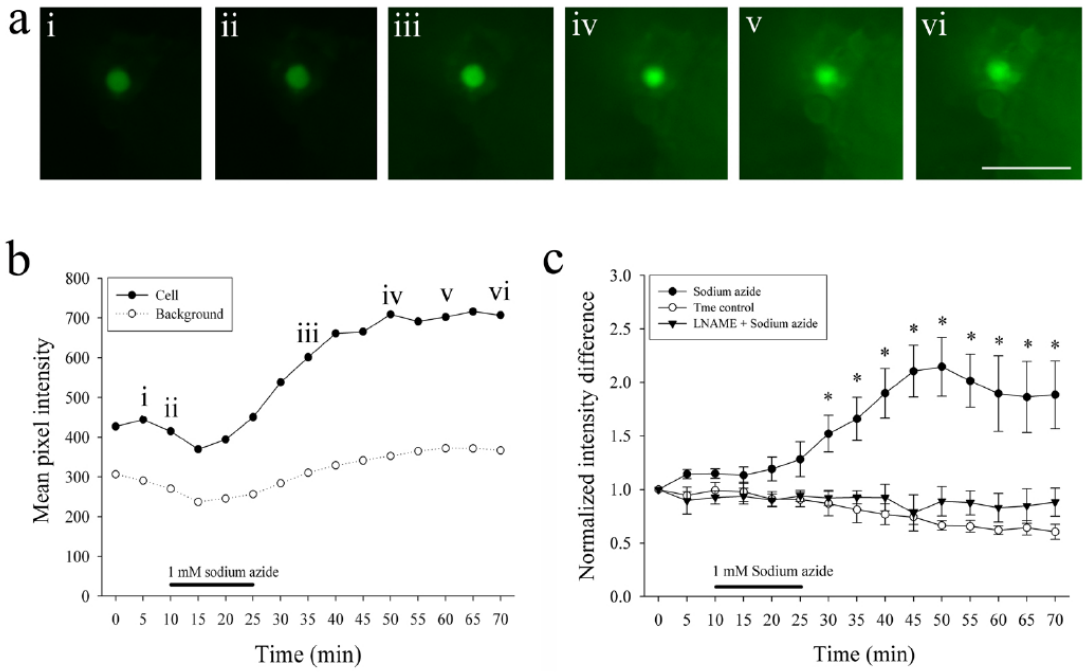
a
i
ii
iii
iv
v
vi
b
Cell
Background
Mean pixel intensity
1 mM sodium azide
Time (min)
c
Sodium azide
Tme control
LNAME + Sodium azide
Normalized intensity difference
1 mM Sodium azide
Time (min)

Figure 5.6

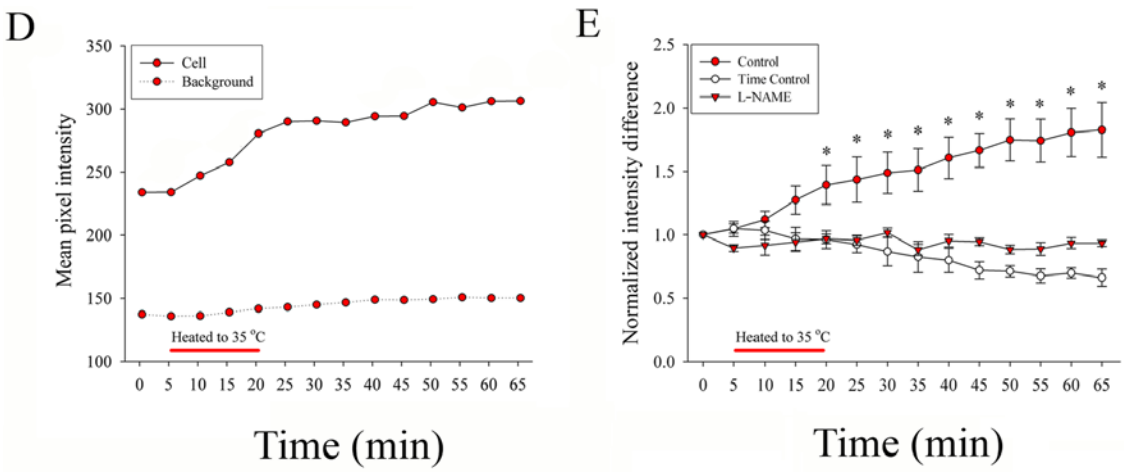
D
Cell
Background
Mean pixel intensity
Heated to 35 °C
Time (min)
E
Control
Time Control
L-NAME
Normalized intensity difference
Heated to 35 °C
Time (min)

Figure 5.6. Chemical anoxia and heat stress increase NO production in thoracic ganglia. (**A**) Example images of a DAF-2 DA loaded cell body at various time points during exposure to 1 mM sodium azide. Scale bar is 50 μm. (**B**) Cell body and background fluorescence changes following chemical anoxia. (**C**) Normalized change in intensity difference (cell body to background) fluorescence over a 65 minute time period in tissue treated with sodium azide (n = 6), tissue treated with sodium azide and the NOS inhibitor L-NAME (n = 3) , and non-treated tissues (time control, n = 3). Exposure to sodium azide significantly increased fluorescence but this rise in fluorescence was not observed in tissue first treated with L-NAME. (**D**) Cell body and background fluorescence changes following exposure to 35 °C. (**E**) Control cells in ganglia exposed to heat (Control, n = 4) showed a significantly larger increase in intensity difference than those in non-heated time controls (n = 3). L-NAME treated tissues (n = 4) did not significantly produce NO when exposed to heat. Asterisk indicates significant differences from time controls (two-way ANOVA with a Tukey test, $p < 0.05$).

allowed the saline to return to room levels. We found a significant increase in intensity difference between control preparations that were heated and unheated preparations (two-way rm ANOVA, $p < 0.001$; Fig. 5.6d,e). In alignment with what we found following exposure to sodium azide, in L-NAME and DAF-2 DA co-treated tissues, exposure to heat did not significantly increase the fluorescence intensity difference (two-way rm ANOVA, $p = 0.156$; Fig. 5.6e).

These experiments demonstrate that the stressors that induce coma associated with SD-like events in the MTG also increase the production of NO in this ganglion. This suggests that NO may be the upstream effector of the PKG pathway that modulates SD-like event duration.

Recovery from coma induced by suffocation under water is faster following inhibition of the NO/cGMP/PKG pathway

In a final data set we examined if the length of time required to recover from anoxic coma in intact behaving animals could be altered by modulating the NO/cGMP/PKG signalling pathway. To test this we treated animals with pharmacological manipulators and submerged intact animals in water for 30 minutes. All animals were incapacitated (no movement) within 10 minutes following immersion in water, recovered ventilatory motor pattern activity and stood upright following removal from the water, and survived to reproduce normally. In alignment with our previous data, locusts injected with L-

NAME, KT5823, and Cantharidin recovered ventilatory activity significantly faster and took less time to stand upright (Fig. 5.7a,b). Animals treated with 8-Br-cGMP took significantly longer to start ventilating again than control animals but no differences were found in the length of time required to stand upright (Fig. 5.7b). Locusts treated with the phosphodiesterase inhibitor T-0156 were not different from control animals.

This data set confirms that activity of the NO/cGMP/PKG signalling pathway in intact animals can alter the time required to recover from incapacitating environmental conditions. Inhibition of this signalling pathway reduced the time to recover ventilatory activity and reduced the time before the animal is able to stand upright.

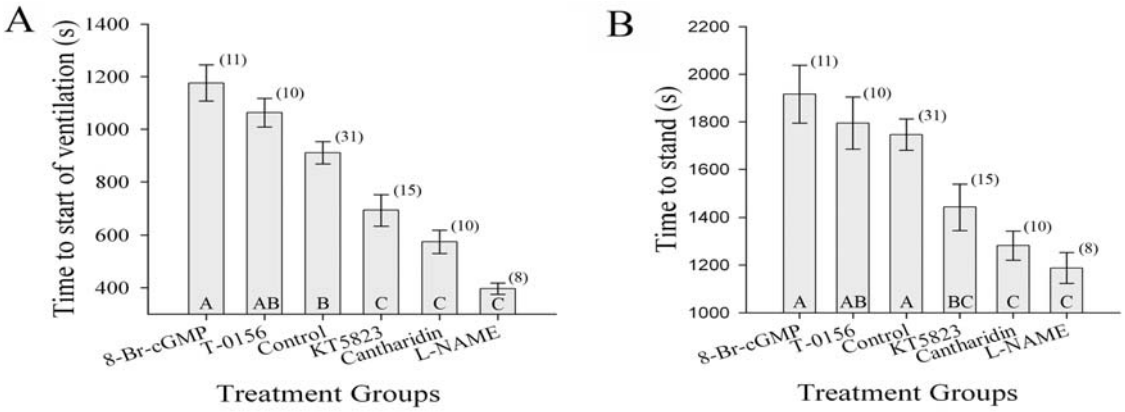
A
Time to start of ventilation (s)
1400
1200
1000
800
600
400
(11)
(10)
(31)
(15)
(10)
(8)
A
AB
B
C
C
C
8-Br-cGMP
T-0156
Control
KT5823
Cantharidin
L-NAME
Treatment Groups
B
Time to stand (s)
2200
2000
1800
1600
1400
1200
1000
(11)
(10)
(31)
(15)
(10)
(8)
A
AB
A
BC
C
C
8-Br-cGMP
T-0156
Control
KT5823
Cantharidin
L-NAME
Treatment Groups

Figure 5.7

Figure 5.7. Inhibition of NO production and PKG activity reduced the time to recover from coma as a result of suffocation by immersion in water. Locusts treated with the NOS inhibitor (L-NAME) or the PP2A inhibitor (Cantharidin) or the PKG inhibitor (KT5823) recovered ventilatory motor pattern activity significantly faster and took less time to stand upright than control animals. Conversely, locusts treated with the PKG activator (8-Br-cGMP) took a significantly longer time to recover ventilatory motor pattern activity than control animals. The phosphodiesterase inhibitor, T-0156, did not significantly alter the time required to start ventilation again nor the length of time needed to stand upright. Letters represent statistical groupings whereby bars with different letters are significantly different (One-way ANOVA, Tukey, $p < 0.05$).

5.4 Discussion

Genetic and pharmacological down-regulation of the cGMP/PKG pathway in *Drosophila* attenuates hyperthermic neural failure and similar pharmacological treatments modulate the temperature sensitivity of the vCPG in *L. migratoria* (Dawson-Scully et al., 2007). Given that hyperthermic ventilatory arrest in the locust is an SD-like event (Rodgers et al., 2007); our primary goal in this investigation was to test the hypothesis that inhibition of PKG would reduce the severity of SD-like events monitored in the locust MTG. We found a striking effect of PKG manipulation on ouabain-induced SD-like events such that PKG inhibition completely suppressed SD-like events evoked by 10^{-4}M ouabain in 70% of preparations. Conversely, PKG activation reduced the time to SD-like event onset and exacerbated it by increasing the frequency of individual SD-like events. These results were confirmed in a model of SD-like events induced by KCl injection and were extended to show that inhibition of a downstream target of PKG (PP2A) reduced the duration of SD-like events. This effect could offset the exacerbating effect of phosphodiesterase inhibition to increase PKG levels. We have also shown that manipulation of NO levels also affects SD-like events induced by KCl injection. Finally we demonstrated that two cellular stressors known to generate SD (chemical anoxia and hyperthermia) increase the production of NO in the thoracic ganglia of this system and that this can be prevented by incubation with an inhibitor of NO synthase. Thus we conclude that the NO/cGMP/PKG pathway acting through PP2A has an important role in modulating the incidence and severity of SD-like events in this system. Finally we show

that differing activity levels of this pathway can alter the time taken to recover from incapacitating environmental conditions such as water immersion.

In order to consider the potential mechanisms underlying the attenuation of SD-like events by inhibition of the NO/cGMP/PKG pathway we propose the following model for SD-like events in the locust MTG (Fig. 5.8). This model is based on models proposed for CSD (Kager et al., 2002; Somjen, 2002; Cestèle et al., 2008) and the described characteristics of locust SD-like events whereby $[K^+]_o$ shows accelerating transitions between two stable states (Rodgers et al., 2007). The core feature is the balance between K^+ accumulation and K^+ clearance in a relatively restricted extracellular volume. Normally, extracellular volume buffering and mechanisms of K^+ clearance are more than sufficient to accommodate the increased flux of K^+ associated with increased neural activity. However when processes leading to K^+ accumulation predominate over processes of clearance sufficiently to increase $[K^+]_o$ and reduce the K^+ equilibrium potential, the system becomes unstable and enters a positive feedback cycle (Fig. 5.8a). This requires either movement of large quantities of ions or a small extracellular volume. Reduction of the K^+ equilibrium potential depolarizes neurons, which in turn leads to more K^+ accumulation and further depolarization until neuronal activity ceases when voltage-dependent Na^+ channels remain inactivated: SD-like event. The positive feedback accounts for the acceleration and rapidity of the increase of $[K^+]_o$ to a new equilibrium. Different manipulations that predispose towards the generation of an SD-like event act at different points in the model. Thus hyperthermia and other forms of

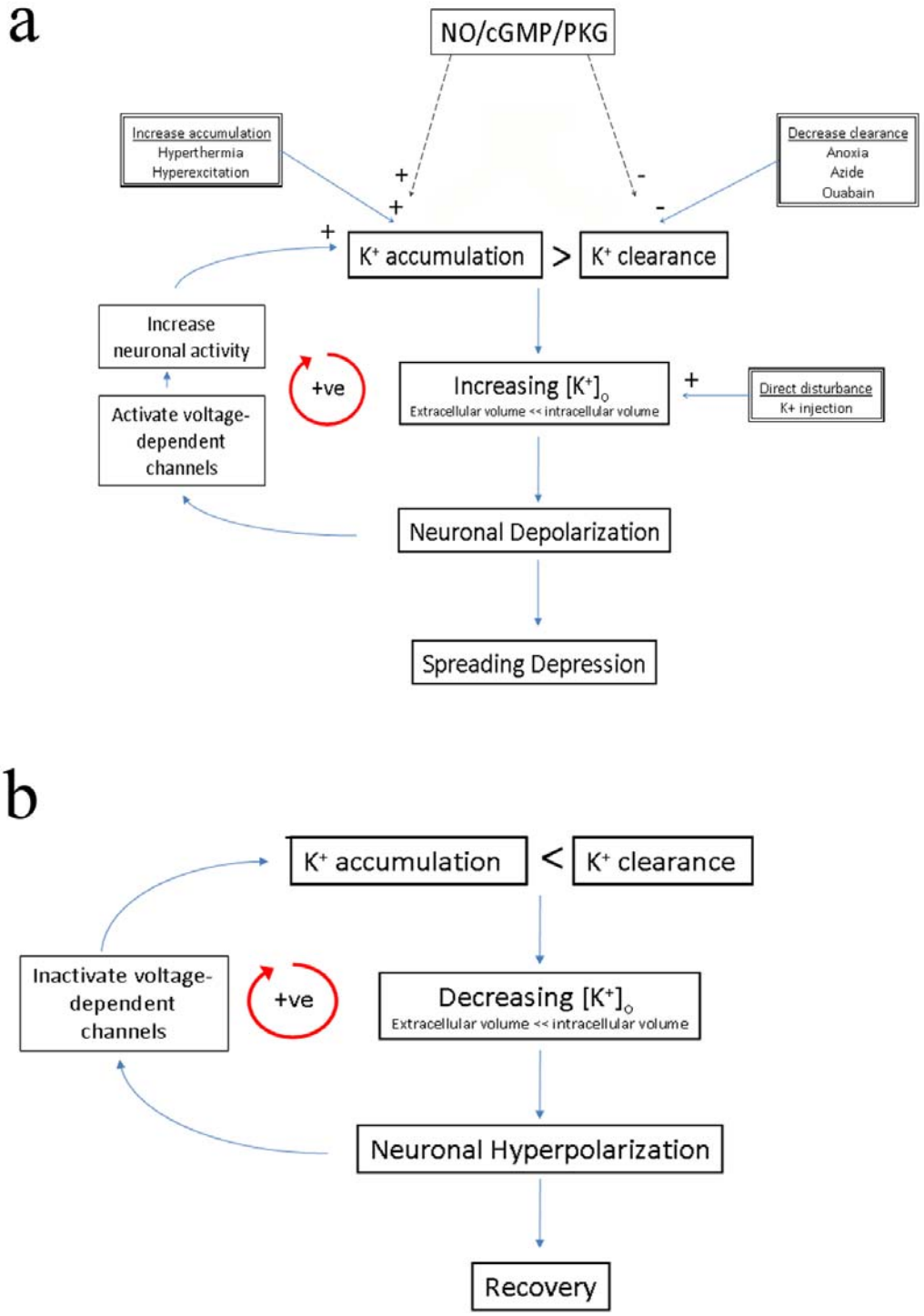
a
NO/cGMP/PKG
Increase accumulation
Hyperthermia
Hyperexcitation
Decrease clearance
Anoxia
Azide
Ouabain
+
+
-
-
+
K+ accumulation
>
K+ clearance
Increase neuronal activity
+ve
Increasing [K+]o
Extracellular volume << intracellular volume
+
Direct disturbance
K+ injection
Activate voltage-dependent channels
Neuronal Depolarization
Spreading Depression
b
K+ accumulation
<
K+ clearance
Inactivate voltage-dependent channels
+ve
Decreasing [K+]o
Extracellular volume << intracellular volume
Neuronal Hyperpolarization
Recovery

Figure 5.8

Figure 5.8. Model of spreading depression-like events in the locust metathoracic ganglion. **a,** Onset. SD-like event is evoked when extracellular K^+ accumulation exceeds clearance under conditions when $[K^+]_o$ can appreciably affect the K^+ equilibrium potential and cause neuronal depolarization thus entering a positive feedback cycle (+ve). This can be induced by increasing accumulation, decreasing clearance or directly manipulating $[K^+]_o$ (double bordered boxes). **b,** Recovery. If cessation of neural activity is sufficient to enable K^+ clearance to predominate then the system enters a positive feedback cycle that restores $[K^+]_o$ and membrane potentials to pre-SD-like event levels. Further details in text.

hyperexcitation increase K^+ accumulation whereas metabolic inhibition and inhibition of the Na^+/K^+ ATPase decrease K^+ clearance and K^+ injection is a direct disturbance of K^+ homeostasis, but all eventually result in the same end state of an SD-like event.

Some treatments are extreme enough that the SD-like event is maintained until normal conditions are restored (e.g. anoxic coma). Nevertheless the repetitive nature of ouabain-induced SD-like events, seen here, and occasionally in hippocampal slices (Balestrino et al., 1999), is striking and can be accommodated in the model (Fig. 5.8b). When the reduction of K^+ clearance is modest (e.g. using 10^{-4}M ouabain) then the onset of an SD-like event reduces K^+ accumulation by arresting neuronal activity and allows processes of clearance to predominate again. At this point the system enters the restorative positive feedback cycle whereby decreasing $[K^+]_o$ increases the K^+ equilibrium potential, hyperpolarizes neurons and inactivates voltage-dependent K^+ channels, which decreases $[K^+]_o$. At some threshold, neuronal activity can be restored but this causes processes of accumulation to predominate and the cycle repeats (e.g. Fig 5.3a).

Our findings with respect to the model described above suggest that activation of the NO/cGMP/PKG pathway predisposes towards K^+ accumulation (by increasing accumulation and/or by decreasing clearance), whereas inhibition of this pathway predisposes towards K^+ clearance (Fig. 5.8a). Although the details of the mechanisms in this system remain to be determined it is probable that numerous and diverse targets contributing to a coordinated tissue response to stress are involved. Nevertheless there is

evidence from other systems to suggest direct effects on K^+ conductances and the Na^+/K^+ ATPase. Notably, reduced PKG activity in the *sitter* variants of the *Drosophila foraging* gene is associated with reduced peak and steady-state voltage-activated K^+ currents and this can be mimicked by pharmacological inhibition of PKG (Renger et al., 1999). Moreover, activation of K^+ conductances by the NO/cGMP/PKG pathway has been demonstrated in mammalian systems (Kubokawa et al., 1998; Van Cuong et al., 2006). Elevated NO both activates leak K^+ current through a PKG-dependent mechanism in forebrain neurons (Kang et al., 2007) and can indirectly decrease Na^+/K^+ ATPase activity when ATP production is impaired in cortical neurons (Travalin et al., 1997; Zhang et al., 1994). NO responses that are normally stabilizing and protective (Andoh et al., 2002), such as stress-induced activation of K^+ conductances to hyperpolarize neurons and prevent excitotoxicity, could promote SD-like events under conditions when there are insufficient resources to maintain K^+ homeostasis, particularly with a restricted extracellular volume.

NO modulation of neural function (Calabrese et al., 2007) has been implicated in several important processes including synaptic plasticity (e.g. Antonov et al., 2007), tuning of locomotor circuits in the spinal cord (McLean and Sillar, 2002), in response to increased CNS activity in insects (Zayas et al., 2002) and as a response to environmental stressors including hypoxia (Wingrove and O'Farrell, 1999). Indeed NO has been shown to modulate the threshold for spreading depolarization in human and rodent cortex (Petzold et al., 2008) though in this study the threshold was reduced by decreasing levels of NO

and was primarily dependent on endothelial NOS. In insects the neuroanatomical substrate has been well described (e.g. Bicker, 1998), especially in locusts (Ott and Burrows, 1998; Bullerjahn and Pflüger, 2003), and several studies have investigated its effect on motor patterning, sensory processing and neuronal excitability (Newland and Yates, 2007; Müller and Hildebrandt, 2002). In contrast the conditions under which NO production increases are less well known and thus the behavioural relevance of the motor pattern modulation is not always clear. We found that treatments that mimic environmental stress (chemical anoxia and hyperthermia) increased DAF-2 fluorescence of particular neurons in the thoracic ganglia. Some caution in interpretation is warranted because ascorbic acid and dehydroascorbic acid react with DAF-2 to produce fluorescent compounds (Zhang et al. 2002). However treatment with L-NAME did produce less fluorescence suggesting that a significant portion of measured fluorescence was derived from NO. Nevertheless, taking all the observations together, we believe that in this system stress activates the NO pathway and the subsequent adaptive responses make the system more likely to generate SD-like events. Several possibilities exist such as increasing K^+ conductance to prevent neuronal hyperexcitation (as mentioned above) or reducing energy consumption by the ion pumps. Downregulation of this pathway would have immediate consequences of reducing the likelihood of generating SD-like events but could have unforeseen, longer term consequences.

We have argued previously that the phenomena we describe here as SD-like in the MTG of the locust and CSD in vertebrates are substantially the same. We provide further

support for this by demonstrating that metathoracic neurons depolarize during SD-like events and this is associated with a large decrease in input resistance suggesting the opening of voltage-dependent membrane channels. The levels of depolarization we recorded (around 13mV) are consistent with previous reports in insects (10-25 mV during hypoxia in cockroaches (Le Corronc et al., 1999); 10-18mV during hyperthermic failure in flight motoneurons (Wu et al., 2001)) but are markedly smaller than the depolarizations to zero evident in mammalian neurons (Collewijn and Van Harreveld, 1966). It is unclear why insect neurons do not depolarize completely during SD-like events but it may account for the ability of insects to survive long periods of anoxic coma without neuronal damage and thus it would be of considerable interest to find out.

In mammals, CSD and anoxic depolarization are considered to be related phenomena which differ primarily in severity and mechanism of induction (Somjen, 2001; Anderson and Andrew, 2002; Joshi and Andrew, 2001). Although CSD is closely associated with migraine pathology it is generally thought to be benign whereas anoxic depolarization lasting longer than a few minutes is damaging largely due to cell swelling (Jarvis et al., 2001). In our preparation SD-like events are similarly related to the depolarization and neural failure associated with anoxic coma. A major difference from mammals is that insects recover from several hours of anoxic coma apparently none the worse for the experience (see supplemental videos). It is hard to avoid the interpretation that anoxic coma in insects (and thus the SD-like event that generates it) is adaptive in nature, allowing insects to cope temporarily with extreme environmental conditions by entering a

state of neural arrest that conserves energy and prevents complete neuronal depolarization and associated cell swelling and damage. The idea stills requires conclusive substantiation but the discovery of a genetically-encoded pathway that can modulate SD-like events, particularly its initiation and duration, lends support to this interpretation. Conversely, in humans it is hard to accept the interpretation that SD and migraine might have adaptive roles, though arguments along these lines have been made (Loder, 2002). In spite of these fundamentally different perspectives, and given the strong functional similarity at the cellular level that allows invertebrates to be used as genetic models for human diseases, we propose that much can be learned about general mechanisms of CSD by investigations of SD-like events in the locust MTG. Moreover, it is a reasonable assumption that anoxic coma in *Drosophila*, which can be manipulated genetically (Haddad et al., 1997), is generated by the same mechanisms as SD-like events in the locust. This would permit powerful, high throughput, molecular genetic tools to be brought to bear on the problem (Farahani and Haddad, 2003).

In conclusion, we have shown in the locust the generation of SD-like events can be manipulated in the long term by pretreatments requiring protein synthesis like HS (Rodgers et al. 2007), and in the short term by targeting well-defined cellular signaling pathways like the NO/cGMP/PKG pathway. The fact that these pathways are evolutionarily conserved suggests that insect models of SD-like events will be fruitful avenues for future investigation.

5.5 Materials and Methods

Locusts

All experiments were performed on 3- 4 week postimaginal moult male locusts (*Locusta migratoria*). Animals were collected from a crowded colony maintained in the Department of Biology at Queen's University. Locusts were reared under a 12 h light/dark cycle. Prior to experimentation locusts were held in a ventilated 2 litre plastic container. All electrophysiological experiments were performed 4-8 hours after locusts were collected from the colony.

Semi-intact preparation

Locusts were secured to a corkboard ventral-side down and dissected to expose the ventral nerve cord. The MTG was stabilized on a stainless steel plate and nerves 5 on both sides of the ganglion were cut to improve access for saline and drugs. Standard locust saline (in mM: 147 NaCl, 10 KCl, 4 $CaCl_2$, 3 NaOH, 10 HEPES buffer, pH 7.2) was used to superfuse the thoracic and abdominal cavities at 5 ml/min. Saline temperature was held at 22 °C.

Water immersion

Locusts were placed within a mesh-lidded clear plastic container which was then submerged in a larger bucket filled with water (water temperature ~19-21 °C) for 30 minutes. Animals were completely submerged in water and all were incapacitated by this treatment. Following removal from the water, locusts were placed on their side on piece

of paper towel. The time to recover ventilation was calculated as the length of time between removal from the water to the start of ventilatory movements monitored by visual inspection. Motor pattern activity was assumed to have recovered at the time when repetitive movements could be observed). Time to stand was scored by measuring the time required to stand upright following removal from the water.

Motor patterns

Ventilatory motor patterns were recorded using a 0.1 mm diameter copper electromyographic (EMG) electrode placed on muscle 161. Signals were amplified using a model P15 preamplifier (Grass Instruments, West Warwick, RI) and digitized using a Digidata 1322A (Molecular Devices, Union City, CA). Data were analyzed using Clampfit 9.0 (Molecular Devices). Motor patterns were allowed to stabilize for 10 minutes before beginning an experiment. Following dissection, motor pattern frequency is around 1 Hz with an expiratory muscle burst duration of 250-300 ms (Armstrong et al. 2006). vCPG recovery time was calculated by examining the time difference between the last rhythmic muscle burst resulting from the KCl-evoked SD event to the first rhythmic muscle burst following recovery of the $[K^+]_o$ to baseline levels. A rhythmic burst is a muscle burst having a minimum duration of 100 ms and a period of at least 300 ms for at least 3 consecutive cycles.

Intracellular recordings

Intracellular recordings of neurons were made using sharp microelectrodes (1 M KAc, 30-40 MΩ) and amplified using a Model 1600 Neuroprobe Amplifier (A-M Systems Inc., Carlsborg, WA). Hyperpolarizing -1 or -2 nA current pulses were used to measure input resistance.

Extracellular potassium-sensitive microelectrodes

Low resistance (4-8 MΩ) microelectrodes were made from unfilamented glass pipettes with a diameter of 1 mm (World Precision Instruments Inc., Sarasota, FL) that had been washed with methanol (99.9%, Sigma-Aldrich) and dried on a hot plate prior to being pulled. The inner glass wall was then made hydrophobic by silanization with hot dichlorodimethylsilane (100°C. 99%, Sigma-Aldrich) vapor. Following silanization electrodes had their tips filled with Potassium Ionophore I-Cocktail B (5% Valinomycin, Sigma-Aldrich) forming an artificial membrane and then back-filled with 500 mM KCl. Reference electrodes were made from low resistance (4-8 MΩ) filamented pipettes filled with 3 M KCl.

Extracellular potassium recordings

Potassium-sensitive microelectrodes were connected to a DUO 773 2-channel intracellular/extracellular amplifier (World Precision Instruments Inc., Sarasota, FL) and calibrated at room temperature (22°C). 15 mM and 150 mM KCl solutions were used to

determine the voltage change needed to establish $[K^+]_o$ (mM) using the Nernst equation (see Rodgers et al 2007 for details).

Pharmacology

All chemicals were obtained from Sigma-Aldrich and dissolved in standard locust saline using a minimum amount of DMSO (0.5 ml/100 ml of saline) and bath applied to the semi-intact preparations. Concentrations used to modulate activity of the NO/cGMP/PKG pathways are as follows: to augment endogenous NO levels we bath applied 10 μM SNAP or 10 μM SNOG, a donor and a source of NO; to inhibit the endogenous production of NO we bath applied L-NAME (100 μM), a NOS inhibitor; to increase cGMP and PKG levels we either bath applied 10 μM 8-Br-cGMP, a phosphodiesterase resistant analog of cGMP or 10 μM T-0156, a phosphodiesterase inhibitor; to inhibit PKG activity we bath applied 10 μM KT5823, to inhibit protein phosphatase 2A activity (next step in the NO/cGMP/PKG pathway) we bath applied 1 μM cantharidin. To evoke repetitive SD-like events we bath applied 100 μM ouabain, a Na^+/K^+ATPase inhibitor. To induced chemical anoxia we bath applied 1 mM sodium azide, an electron transport chain inhibitor.

Pharmacology treatment for animals submerged in water was as follows: animals were injected with 10 μL of various drugs into the haemocoel (for methods see Armstrong et al., 2006). Drug concentrations used were: 8-Br-cGMP, 100 μM; T-0156, 100 μM; KT5823, 100 μM; Cantharidin 100 μM; L-NAME, 10 μM. Control locusts were injected

with standard locust saline containing 0.5% DMSO. Locusts were immersed in water 1 h after injection.

Potassium injections

To generated K^+-evoked SD-like events we delivered 50 nl volumes of saline containing higher than normal KCl (150 mM vs. 10 mM) directly into the anterior region of the MTG. We have previously reported that this concentration and volume is the minimum needed to generate SD-like events in the MTG (Armstrong et al., 2006; Armstrong and Robertson, 2006; Rodgers et al., 2007). Occasionally the mechanical disturbance of the injection was sufficient to cause a disturbance in vCPG activity; however this did not last longer than one rhythm cycle and normal rhythm continued thereafter. Long-tipped pipettes were pulled and filled with the modified saline and attached to a picoSpritzer III (INTRACELL, Shepreth, UK). Pressure was set to 10 psi, and pulse duration was varied to produce a bolus of 50 nl.

DAF-2 DA Imaging

Thoracic ganglia were dissected out and incubated for 1 hour in 30 μM 4,5-diaminofluorescein-2 diacetate (DAF-2 DA), a selective membrane permeable marker that fluoresces in the presence of NO (Kojima et al. 1998). The ganglia were then rinsed several times over a 20 minute period before being pinned to sylgard-coated chamber for examination under a fluorescence microscope (Olympus BX50WI). Fluorescence excitation wave length was 460-490 nm and emission wavelength was 510 nm using an

Olympus FITC filter (product # U-N31001). Images were analyzed using SlideBook 4 (Intelligent Image Innovations). A perfusion system with external heater allowed saline composition and temperature to be changed while imaging. Temperature was monitored with a BAT12 thermometer and copper/constantan thermocouple placed adjacent to the ganglia.

Statistics

SigmaStat 3.1 and JMP 7.0 were used to assess data groupings for significance. Statistical analyses used one-way and two-way ANOVA, followed by a post-hoc Tukey multiple comparison test. Figures show significant differences using letter designations, treatments containing same letters are not significantly different from one another. Significance was assessed at $P < 0.10$ however the majority of P values are less than 0.05. Asterisks indicate significant differences from control.

5.6 References

Anderson TR, Andrew RD (2002) Spreading depression: imaging and blockade in the rat neocortical brain slice. *J Neurophysiol* 88:2713-2725.

Andoh T, Chock PB, and Chiueh CC (2002) Preconditioning-mediated neuroprotection: role of nitric oxide, cGMP, and new protein expression. *Ann NY Acad Sci* 962:1-7.

Antonov I, Ha T, Antonova I, Moroz LL, Hawkins RD (2007) Role of nitric oxide in classical conditioning of siphon withdrawal in *Aplysia*. *J Neurosci* 10: 10993-11002.

Armstrong GAB, Robertson RM (2006) A role for octopamine in coordinating thermoprotection of an insect nervous system. *J Thermal Biol* 31:149-158.

Armstrong GAB, Shoemaker KL, Money TGA, Robertson RM (2006) Octopamine mediates thermal preconditioning of the locust ventilatory central pattern generator via a cAMP/Protein Kinase A signaling pathway. *J Neurosci* 26:12118-12126.

Balestrino M, Young J, Aitken P (1999) Block of (Na^+,K^+)ATPase with ouabain induces spreading depression-like depolarization in hippocampal slices. *Brain Res* 838:37-44.

Bicker G (1998) NO news from insect brains. *Trends Neurosci* 21:349-355.

Brown LA, Key BJ, Lovick TA (2000) Fluorescent imaging of nitric oxide production in neuronal varicosities associated with intraparenchymal arterioles in rat hippocampal slices. *Neurosci Lett* 294:9-12.

Bullerjahn A, Pflüger H-J (2003) The distribution of putative nitric oxide releasing neurons in the locust abdominal nervous system: a comparison of NADPHd histochemistry and NOS-immunocytochemistry. *Zoology* 106:3-17.

Calabrese V, Mancuso C, Calvani M, Rizzarelli E, Butterfield DA Anna Maria Giuffrida S (2007) Nitric oxide in the central nervous system: neuroprotection versus neurotoxicity. *Nat Rev Neurosci* 8:766-775.

Cestèle S, Scalmani P, Rusconi R, Terragni B, Franceschetti S, Mantegazza M (2008) Self-limited hyperexcitability: functional effect of a familial hemiplegic migraine mutation of the $Na_v1.1$ (SCN1A) Na^+ channel. *J Neurosci* 28:7273-7283.

Collewijn H, van Harreveld A (1966) Membrane potential of cerebral cortical cells during spreading depression and asphyxia. *Exp Neurol* 15:425-436.

Dawson-Scully K, Armstrong GAB, Kent C, Robertson RM, Sokolowski MB (2007) Natural variation in the thermotolerance of neural function and behavior due to a cGMP-dependent protein kinase. *PLoS ONE* 8:e773.

Elphick MR, Green IC, O'Shea M (1993) Nitric oxide synthesis and action in an invertebrate brain. *Brain Res* 619:344-346.

Ewer J, Gammie SC, Truman JW (1994) Control of insect ecdysis by a positive-feedback endocrine system: roles of eclosion hormone and ecdysis triggering hormone. *J Neurosci* 14:7704-7712.

Farahani R, Haddad GG (2003) Understanding the molecular responses to hypoxia using *Drosophila* as a genetic model. *Respir Physiol Neurobiol* 135:221-229.

Haddad GG, Sun Y-A, Wyman RJ, Xu T (1997) Genetic basis of tolerance to O_2 deprivation in *Drosophila melanogaster*. *Proc Natl Aca Sci* 94:10809-10812.

Jarvis CR, Anderson TR, Andrew RD (2001) Anoxic depolarization mediates acute damage independent of glutamate in neocortical brain slices. *Cereb Cortex* 11:249-259.

Joshi I, Andrew RD (2001) Imaging anoxic depolarization during ischemia-like conditions in the mouse hemi-brain slice. *J Neurophysiol* 85:414-424.

Kager H, Wadman WJ, Somjen GG (2002) Conditions for the triggering of spreading depression studies with computer simulations. *J Neurophysiol* 88:2700-2712.

Kang Y, Dempo Y, Ohashi A, Saito M, Toyoda H, Sato H, Koshino H, Maeda Y, Hirai T (2007) Nitric oxide activates leak K^+ currents in the presumed cholinergic neuron of basal forebrain. *J Neurophysiol* 98:3397-3410.

Kojima H, Nakatsubo N, Kawahara S, Kirino Y, Nagoshi H, Hirata Y, Nagano T (1998) Detection and imaging of nitric oxide with novel fluorescent indicators: diaminofluoresceins. *Anal Chem* 70:2446-2453.

Kubokawa M, Nakaya S, Yoshioka Y, Nakamura K, Sato F, Mori Y, Kubota T (1998) Activation of inwardly rectifying K^+ channel in OK proximal tubule cells involves cGMP-dependent phosphorylation process. *Jpn J Physiol* 48:467-476.

Le Corronc H, Hue B, Pitman RM (1999) Ionic mechanisms underlying depolarizing responses of an identified insect motor neuron to short periods of hypoxia. *J Neurophysiol* 81:307-318.

Loder E (2002) What is the evolutionary advantage of migraine? *Cephalalgia* 22:624-634.

McLean DL, Sillar KT (2002) Nitric oxide selectively tunes inhibitory synapses to modulate vertebrate locomotion. *J Neurosci* 22:4175-4184.

Mochida H, Takagi M, Inoue H, Noto T, Yano K, Fujishige K, Sasaki T, Yuasa K, Kotera J, Omori K, Kikkawa K (2002) Enzymological and pharmacological profile of T-0156, a potent and selective phosphodiesterase type 5 inhibitor. *Eur J Pharm* 456:91-98.

Moncada S, Palmer RM, and Higgs EA (1991) Nitric oxide: physiology, pathophysiology, and pharmacology. *Pharmacol Rev* 43:109-142.

Morton DB, Giunta MR (1992) Eclosion hormone stimulates cyclic GMP levels in *Manduca sexta* nervous tissue via arachidonic acid metabolism with little or no contribution from the production of nitric oxide. *J Neurochem* 59:1522-1530.

Müller U (1997) The nitric oxide system in insects. *Prog Neurobiol* 51:363-381.

Newland PL, Yates P (2007) Nitrergic modulation of an oviposition digging rhythm in locusts. *J Exp Biol* 210:4448-4456.

Müller U, Bicker G (1994) Calcium-activated release of nitric oxide and cellular distribution of nitric oxide-synthesizing neurons in the nervous system of the locust. *J Neurosci* 14:7521-7528.

Müller U, Hildebrandt H (2002) The nitric oxide/cGMP-mediated protein kinase A activation in the antennal loves plays an important role in appetitive reflex habituation in the honeybee. *J Neurosci* 22:8739-8747.

Osborne KA, Robichon A, Burgess E, Butland S, Shaw RA, Coulthard A, Pereira HS, Greenspan RJ, Sokolowski MB (1997) Natural behavior polymorphism due to a cGMP-dependent protein kinase of *Drosophila*. *Science* 277:834-836.

Ott SR, Burrows M (1998) Nitric oxide synthase in the thoracic ganglia of the locust: distribution in the neuropiles and morphology of neurons. *J Comp Neurol* 395:217-230.

Petzold GC, Haack S, von Bohlem und Halback O, Priller J, Lehmann T-N, Heinemann U, Dirnagl U, Dreier JP (2008) Nitric oxide modulates spreading depolarization threshold in the human and rodent cortex. *Stroke* 39:1292-1299.

Ramirez JM, Elsen FP, Robertson RM (1999) Long-term effects of prior heat shock on neuronal potassium currents recorded in a novel insect ganglion slice preparation. *J Neurophysiol* 81:795-802.

Renger JJ, Yoa WD, Sokolowski MB, Wu CF (1999) Neuronal polymorphism among natural alleles of a cGMP-dependent kinase gene, *Foraging*, in *Drosophila*. *J Neurosci* 19,:RC28.

Rodgers CI, Armstrong GB, Shoemaker KL, LaBrie JD, Moyes CD, Robertson RM (2007) Stress preconditioning of spreading depression in the locust CNS. *PLoS ONE* 12:e1366.

Somjen GG (2002) Ion regulation in the brain: implications for pathophysiology. *Neuroscientist* 8, 254-267.

Somjen GG (2001) Mechanisms of spreading depression and hypoxic spreading depression-like depolarization. *Physiol Rev* 81:1065-1096.

Travalin SJ, Ellis EF, Satin LS (1997) Inhibition of the electrogenic Na pump underlies delayed depolarization of cortical neurons after mechanical injury or glutamate. *J Neurophysiol* 77:632-638.

Van Cuong D, Kim N, Youm JB, Joo H, Warda M, Lee J-W, Park WS, Kim T, Kang S, Kim H, Han J (2006) Nitric oxide-cGMP-protein kinaseG signalling pathway induces anoxic preconditioning through activation of ATP-sensitive K^+ channels in rat hearts. *Am J Physiol Heart Circ Physiol* 290:H1808-H1817.

Walter DC, Nelson SR (1975) Energy metabolism and nerve function in cockroaches (*Periplaneta americana*). *Brain Res* 94:485-490.

Wingrove JA, O'Farrell PH (1999) Nitric oxide contributes to behavioral, cellular, and developmental responses to low oxygen in *Drosophila*. *Cell* 98:105-114.

Wu BS, Lee JK, Thompson KM, Walker VK, Moyes CD, Robertson RM (2002) Anoxia induces thermotolerance in the locust flight system. *J Exp Biol* 205:815-827.

Wu BS, Walker VK, Robertson RM (2001) Heat shock-induced thermoprotection of action potentials in the locust flight system. *J Neurobiol* 49:188-199.

Zayas RM, Qazi S, Morton DB, Trimmer BA (2002) Nicotinic-acetylcholine receptors are functionally coupled to the nitric oxide/cGMP-pathway in insect neurons. *J Neurochem* 83:421-431.

Zhang J, Dawson VL, Dawson TM, Snyder SH (1994) Nitric oxide activation of poly(ADP-ribose) synthetase in neurotoxicity. *Science* 263:687-689.

Zhang X, Kim W-S, Hatcher N, Potgieter K, Moroz LL, Gillette R, Sweedler JV (2002) Interfering with nitric oxide measurements. *J Biol Chem* 277:48472-48478.

Zhou XB, Schlossmann J Hofmann F, Ruth P, Korth M (1996) Protein phosphatase 2A is essential for the activation of Ca^{2+}-activated K^{+} currents by cGMP-dependent protein kinase in tracheal smooth muscle and Chinese hamster ovary cells. *J Biol Chem* 271:19760-19767.

Chapter 6

6.1 General Discussion

Environmental temperature fluctuation can strongly influence neuronal circuit function and the behaviour of animals. While temperature is a major stress for insects inhabiting highly variable thermal environments; other biotic and abiotic stresses, and the complex interactions between them, should not be discounted. Resource availability, predatory stress, osmotic stress, and toxins can limit the ability of locust populations to reproduce and survive. Even within individuals localized tissue hypoxia could conceivably occur when increased oxygen consumption rates, due to stress or physical activity outstrip the capacity of the tracheal system to deliver oxygen. Whereas non-thermal stressors undoubtedly affect the locust nervous system, work conducted during the course of my Ph.D. essentially focused on thermal stress. Nevertheless, in my last chapter I investigate the effects of water submersion (anoxia by suffocation) and chemical anoxia on neuronal function.

For insects inhabiting hot arid environments temperature variability can be large and at extremes neuronal function can be impaired. Adaptations exist that allow for small extensions in the upper thermal operating range of neuronal function during acute heat stress. In the laboratory these adaptations can be switched on by preconditioning locusts with a high sub-lethal exposure to temperature for three hours (HS treatment). Extensions in operating range are usually manifested in the hours that follow HS

treatment (Whyard et al.1986) and can last for several weeks (Robertson et al. 1996). The neuronal mechanisms that allow for this extension in thermal operating range are beginning to be understood. The overall objective of my thesis was to investigate the involvement of various neuromodulators (and their cellular signalling pathways) in conferring vCPG thermotolerance.

The vCPG is a reliable neuronal circuit which coordinates a persistent motor pattern that regulates the movement of gas through the tracheal system. It is an ideal circuit to study adaptations that exist in the nervous system, because any impairment in its function would have severe repercussions for the entire animal. Thus, it is not surprising that the vCPG displays a robust response to HS treatment. Two measurements of thermotolerance were used to assess the extent of neuroprotection conferred via HS treatment. The first was a measurement of CNS temperature when the vCPG failed during a rising temperature ramp, and the second was a measure of how long it took the vCPG to recover function following heat-induced failure and a return to room temperature. vCPG activity in HS-treated locusts was able to remain in operation 4-9 °C higher than control animals during thermotolerance tests (Armstrong et al. 2006; Dawson-Scully et al. 2007). The length of time taken to recover vCPG activity following cooling was also found to be quicker in HS-treated animals (60 s vs. 180 s) (Dawson-Scully et al. 2007). These basic measurements of thermotolerance formed a cornerstone for my investigation of the physiological mechanisms these animals employ which provide thermotolerance.

In the second chapter of my thesis, I investigated whether the thermoprotective effects of HS treatment could be mimicked by increased OA neuromodulation. The rationale for testing OA's involvement came from two notable observations. First OA concentrations in the haemolymph increases from ~ 7.5 to 15.5 pg/μL following heat stress, and second, the vCPG is excited by OA neuromodulation (Davenport and Evans, 1985; Sombati and Hoyle, 1984; Armstrong et al. 2006). This led to an early hypothesis that HS treatment might increase OA release during stress and aid in maintaining vCPG activity by stimulating the rhythm. No evidence for this was found. Short OA applications (20 minutes) which did excite the rhythm did not confer vCPG thermotolerance. However, longer application (1 hour) of OA did confer vCPG thermotolerance. Two other neuromodulators (dopamine and tyramine) were also investigated but neither appeared to affect thermotolerance within our experimental paradigm.

Using a variety of pharmacological tools we were able to confirm that activation of the neuronal β-adrenergic-like OA receptor and increased activity of various steps along the neuronal octopaminergic signalling pathway (cAMP/PKA) could also induce vCPG thermotolerance. In one compelling experiment vCPG thermotolerance was generated by blocking β-adrenergic-like OA receptors with an antagonist and then pharmacologically increasing PKA activity (Armstrong et al. 2006). This chapter further showed that OA-induced changes in thermotolerance appear to be dependent upon transcription and translation. An intriguing possibility is that the octopaminergic signalling pathway leads

to the transcription of heat shock proteins (HSPs). There have been reports that both antagonists of PKA and PKC activity attenuate the transcription and translation of HSP72 in human glioblastoma cell lines, whereas agonists of these pathways promote production of this protien (Ohnishi, 1998). Further, *hsp70* gene expression in cardiac tissue following hemodynamic stress is regulated by PKA- and PKC-dependent activity (Osaki et al. 1998). Although HSP levels were not examined, it is conceivable that OA application may have lead to an increase in their production.

The third chapter investigated the role of PKG signalling in generating vCPG thermotolerance. The rationale for studying this pathway came from observations made of flies with differing cellular levels of PKG. In *Drosophila* populations, two naturally occurring variants of the *foraging* (*For*) gene exists (Osborne et al. 1997). Rovers (For^R) have reduced PKG levels and sitters (For^S) have high levels of PKG. This naturally occurring polymorphism gives rise to differing feeding strategies where For^R move more in the presence of food and For^S move less (Osborne et al. 1997). These altered foraging strategies may be a result of differing neuronal voltage-gated K^+ currents. Both peak and sustained currents were attenuated in For^S variants (Renger et al. 1999). Interestingly, this altered K^+ conductance is very similar to what is found in neuronal cell bodies of preconditioned locusts (Ramirez et al. 1999; Wu et al. 2002).

It was hypothesized that synaptic transmission across the neuromuscular junction in the For^S variant would be maintained at a higher temperature. Synaptic transmission in For^R

and *For*^{S} failed at 35.5 °C and 37.5 °C respectively. This thermoprotective effect can be removed by pharmacologically increasing PKG activity. Moreover, maintained synaptic transmission at high temperatures in the *For*^{R} variant could be pharmacologically induced by treating the flies with an antagonist of PKG activity (Dawson-Scully et al. 2007). Similar to the fly, pharmacologically reducing PKG activity in the locust was found to increase vCPG thermotolerance, manifested as a 9°C increase in the failure temperature. Further, the length of time required to recover vCPG activity following heat-induced failure was much quicker in locusts treated with the PKG inhibitor (60 s vs. 175 s) (Dawson-Scully et al. 2007). The results from this chapter suggest a more ubiquitous role for this pathway in the regulation of acute stress tolerance across species.

The fourth chapter of my thesis examined the physiological events that occur during heat-induced neuronal failure. In an initial set of experiments, measurements of $[K^+]_o$ rose from a baseline level of 10 mM to > 50 mM at the moment of heat-induced vCPG failure (Rodgers et al. 2007). $[K^+]_o$ recovered to baseline levels when temperature was allowed to return to room levels and vCPG activity resumed. This observation is very similar to what Wu and Fisher (2000) report in the rat hippocampus during hyperthermia-induced SD. At heat-induced neuronal failure, V_m depolarized by 38 mV and $[K^+]_o$ rose from 6 mM to 44 mM. When thermal stress was removed, $[K^+]_o$ returned to baseline levels, and V_m and neuronal activity recovered (Wu and Fisher, 2000). HS treatment did not abolish the occurrence of SD-like events occurring in the locust but delayed the onset of the heat-induced SD-like event (Rodgers et al. 2007). We believe that a delay of the onset of the

SD-like event allows for continued vCPG operation at elevated temperature in HS-treated animals. Additionally, HS-treated locusts showed an increase in $[K^+]_o$ clearance rates, which was correlated with a quicker vCPG recovery time (Rodgers et al. 2007).

In the mammalian nervous system SD can also be evoked by mitochondrial blockers, inhibition of Na^+/K^+ATPase activity, and KCl application (Müller and Ballanyi, 2003; Balestrino, 1999; Leão, 1944; Leão and Morrison, 1945). In this chapter we showed that these same stimuli can also reliably induce SD-like events in the locust. Experiments performed in a nitrogen gas filled chamber (anoxia) or preparations treated with sodium azide (mitochondrial blocker) produced SD-like events in the MTG (Rodgers et al. 2007). Recovery from SD-like events occurred when air was allowed to renter the chamber or when sodium azide was flushed out of the preparation. It is likely that the triggering of the SD-like events was caused by the inability to provide enough energy required to maintain ionic gradients.

The Na^+/K^+ATPase plays a major role in maintaining ionic gradients needed for proper neuronal activity. Experiments performed by my colleagues using ouabain (an inhibitor Na^+/K^+ATPase activity) in chapter 4 and myself in chapter 5 demonstrated repetitive SD-like events (Rodgers et al. 2007; Armstrong et al. unpublished 5 chapter). In hippocampal slices ouabain can occasionally induce repetitive SD-like events (Balestrino et al. 1999). This finding is also supported by computer simulations of SD (Kager et al. 2002). The repetitive nature of ouabain-induced SD-like events can be explained as

follows (see also Figure 5.8). As ouabain begins to impair Na^+/K^+ATPase function neuronal activity outpaces the ability of neurons and glia to sequester accumulating $[K^+]_o$, resulting in increased $[K^+]_o$. This rise in $[K^+]_o$ decreases the potassium equilibrium potential (E_k) and in doing so slowly depolarizes the V_m (V_m is largely dependent upon E_k). When the depolarization reaches the voltage-gated Na^+ channels threshold, these channels open and further depolarize the neuron. During ionic homeostasis E_k is sufficiently large and K^+ driving forces are able to repolarize the neuron. However in situations when E_k is reduced such as during ouabain exposure, K^+ driving forces may be insufficient to restore V_m. Recovery from ouabain-induced SD might be afforded through cessation of neuronal activity allowing non-inhibited Na^+/K^+ATPases to clear excess K^+ from the extracellular space thereby restoring E_k.

Another reliable way of inducing SD in the locust is to artificially reduce E_k. This was achieved by delivering nanoinjections of saline containing high KCl content directly into the ventilatory neuropil (Rodgers et al. 2007; Armstrong et al. unpublished 5 chapter). Application of KCl is regularly used to initiate SD in mammals (Leão, 1944; Leão and Morrison, 1945; Jing et al. 1993; Czéh et al. 1993; Urenjak and Obrenovitch, 2000; Gorji et al. 2001; Anderson and Andrew, 2002). Raising the $[K^+]_o$ in this manor would decrease E_k and depolarize the V_m. Recovery of neuronal activity following KCl-induced SD might be dependent on clearance of excess K^+ from the extracellular space and restoration of E_k.

One of the more interesting observations described in this chapter is that SD-like events in the locust MTG propagate. In mammals, propagation speeds range from 2 mm/min to as high as 9 mm/min with most reports describing a mean speed around 3 mm/min (Van Harreveld et al. 1956; Grafstein, 1956; Hull and Van Harreveld, 1964; Nicholoson et al. 1978). In this chapter we report a mean KCl-evoked SD-like propagation speed of 2.4 mm/min (Rodgers et al. 2007). Additionally, these events only propagated locally within the MTG and were unable to propagate through white matter (connectives), an observation that is constant with SD phenomena occurring in mammals (Van Harreveld, 1956).

In the final chapter of this thesis, I investigated the extent of neuronal depolarization that occurs during SD-like events. Using intracellular microelectrodes I monitored activity in both rhythmic ventilatory interneurons and non-rhythmic neurons in the MTG. As previously reported a modest depolarization of neuronal V_m (between 11-17 mV) occurs in the MTG at the moment of heat-induced failure (Wu et al. 2001). In the cockroach (*Periplaneta americana*) a similar depolarization occurs during exposure to hypoxia (Le Corronc et al. 1999). In this chapter we used sodium azide to evoke SD-like events while concomitantly monitoring neuronal activity. We observed a modest depolarization by 13 mV coinciding with a surge in $[K^+]_o$ (Armstrong et al. unpublished chapter 5). This modest depolarization is in contrast to that of neurons in the mammalian CNS which depolarize briefly to zero during SD (Collewijn and Van Harreveld, 1966). However, the modest depolarizations we recorded are similar to anoxic tolerant species of vertebrates

(Pamenter and Buck, 2008). It remains to be determined why a limited and not a complete neuronal depolarization of V_m occurs during anoxia and heat stress in this terrestrial insect.

A major aim of the last chapter was to investigate the correlation, if any, of the thermoprotective role inhibition of PKG activity (chapter three) on the propensity to generate and severity of SD-like events occurring in the locust CNS (chapter four). In experiments in which SD-like events were evoked by nanoinjections of KCl we found that pretreatment with an antagonist of PKG activity decreased the length of the SD-like event, whereas treatment that increases activity of PKG made the duration of the SD-like event longer. In addition to a reduced SD-event duration the length of time required to recover vCPG activity was also found to be shorter in locusts pharmacologically treated with an antagonist of PKG activity, whereas locusts treated with an agonist of PKG activity required more time to recover vCPG activity following a KCl-induced SD-like event. These data show that the duration of the SD-like event can be altered by differing levels of PKG activity. As previously mentioned there is a tight correlation between heat-induced failure and recovery of vCPG activity and the start and finish of an SD-like event in the locust CNS. This observation may account for our earlier observations (chapter three) which showed a faster recovery time, following heat-induced failure, in locusts pharmacologically treated to have reduced PKG activity.

A bigger question addressed in this final chapter was whether biologically relevant factors (environmental stress) can alter PKG activity in the locust CNS. To determine this we examined the production of NO which stimulates a rise in $[cGMP]_i$ in the locust CNS by augmenting soluble guanylyl cyclase (sGC) activity (Elphick et al. 1993). Using a selective membrane-permeable fluorescent marker for the presence of NO (Zhang et al. 2002) we examined if NO production was increased during stress. Following both chemical anoxia and hyperthermia we found a significant increase in NO production in the cell bodies of discrete neurons. Interestingly, tissue from HS-treated animals or ganglia treated with a NOS inhibitor produced less NO during chemical anoxia and hyperthermia. This work represents the first description of biologically relevant stimuli affecting NO production in locusts.

The data presented in this thesis have significantly improved our understanding of how thermotolerance in central neuronal circuits can be modulated by cellular signalling pathways. A few notable differences between these two pathways and their ability to confer thermotolerance in the locust vCPG need recapping. OA-induced thermotolerance is a relatively slow process requiring 1 hour of OA application. It is dependent upon increased cAMP levels and the ability of the nervous system to transcribe and translate new proteins. Conversely, we found that reduced PKG activity also confers vCPG thermotolerance. But, in contrast to OA-induced thermotolerance, inhibition of PKG activity achieved a HS-like thermotolerance in about 3 minutes. The rapidity with which this occurs suggests a transcriptional- and translational-independent mechanism for

conferring tolerance to acute heat stress. The mechanisms that underlie the ability of PKG inhibition to confer thermotolerance include the modulation of SD-like events in the locust. However we do not know which downstream target proteins this pathway acts upon to alter SD-like phenomena. Perhaps more critical to the future advancement in our understanding of how these neuromodulators regulate stress tolerance would be to investigate interactions between them. For example, does NO modulate the activity of DUM neurons? It is conceivable that nitrergic neuromodulation of DUM neurons during stress increases their release of OA into the haemolymph. Conversely, it is possible that octopaminergic neuromodulation alters the production of NO in the thoracic ganglia.

Despite the advances described in this thesis which showed that at the moment of heat-induced CNS failure an SD-like event occurs, important questions remain. First, why is it that neurons in the CNS only partially depolarize during the SD-like event and does this account for the ability of the locust to survive long periods of anoxic coma? Second, are SD-like events adaptive? It is tempting to suggest that SD-like events are adaptive; however the experiments described in this thesis have not addressed this question. It will also be important to determine the extent to which the pathways and mechanisms for heat tolerance in the locust are shared by other organisms and thus the extent to which the findings of this thesis represent a description of general cellular strategies for neural stress tolerance.

6.2 Summary

1) Protection of neural operation (e.g. ventilation) at high temperature is crucial.

2) At high temperature an SD-like event occurs in the thoracic ganglia that shuts down CNS activity.

3) Heat-induced SD-like events in the locust are characterized by membrane potential depolarization, a rapid rise in $[K^+]_o$ and cessation of neuronal activity.

4) Recovery from Heat-induced SD-like events occurs when thermal stress is removed.

5) SD-like events can also be generated following exposure to ouabain, KCl, N_2 gas, and sodium azide application.

6) We conclude that SD-like events in the locust are very similar to SD in vertebrates.

7) Animals have evolved mechanisms to protect themselves from extreme temperatures.

8) These mechanisms can be switched on by treating animals with a prolonged sublethal exposure to heat. Following these exposures to heat, CNS thermotolerance was generated.

9) Thermotolerance was manifested as an increase in the temperature at which the vCPG failed at and a quicker recovery time following removal of heat stress.

10) Octopamine is a major insect neuroactive compound. It functions as a neurotransmitter, neuromodulator and neurohormone and its actions are analogous to norepinephrine.

11) OA modulates central pattern generators including the locust vCPG.

12) We tested if OA treatment generates vCPG thermotolerance. Short applications (20 mins) of OA did not confer thermotolerance but longer (1hr) applications did.

13) Animals preconditioned with HS and concomitantly treated with a β-androgenic-like OA receptor antagonist did not generate thermotolerance.

14) OA-induced vCPG thermotolerance is dependent upon transcription and translation.

15) We also tested if NO/cGMP/PKG signalling pathway is involved in thermotolerance.

16) Pharmacological inhibition (not activation) of PKG activity conferred thermotolerance.

17) Thermotolerance can be generated in less then 3 minutes following PKG inhibition.

18) PKG inhibition also decreased the duration of KCl-evoked SD-like events in the MTG.

19) PKG inhibition also decreased the occurrence of ouabain-induced SD-like events in the MTG during a 30 minute ouabain exposure.

20) Application of a phosphodiesterase increased the duration of KCl-evoked SD-like events in the MTG

21) Application of a phosphodiesterase resistant analog of cGMP increased the number of ouabain-induced SD-like events in the MTG during a 30 minute ouabain exposure.

22) NO production increases following heat stress and chemical anoxia.

23) Inhibition of NO production decreased the duration of KCl-evoked SD-like events in the MTG.

24) NO donors did not increase the duration of KCl-induced SD-like event.

25) Inhibition of NO reduces the time to recover from water immersion.

26) We conclude that both octopaminergic and nitrergic neuromodulation play a role in conferring tolerance to heat stress. However octopaminergic-induced CNS thermotolerance requires 1 hr and nitrergic neuromodulation requires 3 minutes.

27) We do not know what these signalling pathways regulate which provides CNS thermotolerance.

6.3 Literature cited

Anderson T.R. and R.D. Andrew. Spreading depression: imaging and blockade in the rat neocortical brain slice. *J. Neurophysiol.* 88, 2713-2725 (2002).

Andoh T, Chock PB, and Chiueh CC (2002) Preconditioning-mediated neuroprotection: role of nitric oxide, cGMP, and new protein expression. *Ann. NY Acad. Sci.* 962:1-7.

Antonov I, Ha T, Antonova I, Moroz LL, Hawkins RD (2007) Role of nitric oxide in classical conditioning of siphon withdrawal in *Aplysia*. *J. Neurosci.* 10: 10993-11002.

Armstrong GAB, Robertson RM (2006) A role for octopamine in coordinating thermoprotection of an insect nervous system. J. *Thermal. Biol*. 31:149-158.

Armstrong, G.A.B. Shoemaker, K.L. Money, T.G.A. and R.M. Robertson. Octopamine mediates thermal preconditioning of the locust ventilatory central pattern generator via a cAMP/protein kinase A signaling pathway. *J. Neurosci.* 26, 12118-12126 (2006).

Balestrino, M. Young, J. and P. Aitken. Block of (Na^+,K^+)ATPase with ouabain induces spreading depression-like depolarization in hippocampal slices. *Brain Res.* 838: 37-44 (1999).

Collewijn, H. and A. Van Harreveld. Membrane potential of cerebral cortical cells during spreading depression and asphyxia. *Exp. Neurol.* 15: 425-436 (1966).

Czéh, G. Aitken, P.G. and G.G. Somjen. Membrane currents in CA1 pyramidal cells during spreading depression(SD) and SD-like hypoxic depolarization. *Brain Res.* 632: 195-208 (1993).

Dawson-Scully, K. Armstrong, G.A.B. Kent, C. Robertson, R.M. and M.B. Sokolowski. Natural variation in the thermotolerance of neural function and behavior due to a cGMP-dependent protein kinase. *PLoS ONE* 8, e773 (2007).

Davenport, A.P. and P.D. Evans. Stress-induced changes in the octopamine levels of insect haemolymph. *Insect. Biochem.* 14: 135-143 (1984).

Elphick, M.R. Green, I.C. and M. O'Shea. Nitric oxide synthesis and action in an invertebrate brain. *Brain Res.* 619: 344-346 (1993).

Gorji, A. Scheller, D. Straub, H. Tegtmeier, F. Köhling, R. Höhling, J.-M. Tuxhorn, I. Ebner, A. Wolf, P. Panneck, H.W. Oppel, F. Speckmann, E.-J. Spreading depression in human neocortical slices. *Brain Res.* 906: 74-83 (2001).

Grafstein, B. Mechanism of spreading cortical depression. *J. Neurophysiol.* 19: 154-171 (1956).

Hull, C.D. and A. Van Harreveld. Absence of conduction of spreading depression through cortical region damaged by asphyxiation. *Am. J. Physiol.* 207: 921-924 (1964).

Jing, J. Aitken, P.G. and G.G Somjen. Role of calcium channels in spreading depression in rat hippocampal slices. *Brain Res.* 604: 251-259 (1993).

Kager, H. Wadman, W.J. and G.G. Somjen. Conditions for the triggering of spreading depression studied with computer simulations. *J. Neurophysiol.* 88: 2700-2712 (2002).

Leão, AAP. Spreading depression of activity in the cerebral cortex. *J. Neurophysiol*. 7: 359-390 (1944).

Leão, AAP and R.S. Morrison. Propagation of spreading cortical depression. *J. Neurophysiol* 8: 33-45 (1945).

Le Corronc, H. Hue, B. and R.M. Pitman. Ionic mechanisms underlying depolarizing responses of an identified insect motor neuron to short periods of hypoxia. *J. Neurophysiol*. 81: 307-318 (1999).

Müller, M. and K. Ballanyi. Dynamic recording of cell death in the in vitro dorsal vagal nucleus of rats in response to metabolic arrest. *J. Neurophysiol.* 89: 551-561 (2003).

Nicholson, C. Ten Bruggencate, G. Stöckle, H. and R. Steinberg. Calcium and potassium changes in extracellular microenvironement of cat cerebellar cortex. *J. Neurophysiol.* 41: 1026-1039 (1978).

Ohnishi, K. Wang, X, Takahashi, A. Matsumoto, H. Aoki, H. and T. Ohnishi. Effects of protein kinase inhibitors on heat-induced *hsp*72 gene expression in a human glioblastoma cell line. *Cell. Signal.* 24: 259-264 (1998).

Osaki, J. Haneda, T. Kashiwagi, Y. Oi, S. Fukuzawa, J. Sakai, H. Kikuchi, K. Pressure-induced expression of heat shock protein 70 mRNA in adult rat heart is coupled both to protein kinase A-dependent and protein kinase C-dependent systems. *J. Hypertens.* 16: 1193-1200 (1998).

Osborne, K.A. Robichon, A. Burgess, E. Butland, S. Shaw, R.A. Coulthard, A. Pereira, H.S. Greenspan, R.J. and M.B. Sokolowski. Natural behavior polymorphism due to a cGMP-dependent protein kinase of *Drosophila*. *Science* 277: 834- 836 (1997).

Pamenter, M.E. and L.T. Buck. Neuronal membrane potential is mildly depolarized in the anoxic turtle cotrex. *Comp. Biochem. Physiol.* 150: 410-414 (2008).

Ramirez, J.M. Elsen, F.P. and R.M. Robertson. Long-term effects of prior heat shock on neuronal potassium currents recorded in a novel insect ganglion slice preparation. *J. Neurophysiol.* 81: 795-802 (1999).

Renger, J.J. Yoa, W.D. Sokolowski, M.B. and C.F. Wu. Neuronal polymorphism among natural alleles of a cGMP-dependent kinase gene, *foraging*, in *Drosophila*. *J. Neurosci.* 19: RC28 (1999).

Robertsons, R.M. Xu, H. Shoemaker, K.L. and K. Dawson-Scully. Exposure to heat shock affects thermosensitivity of the locust flight system. *J. Neurobiol.* 29: 367-383 (1996)

Rodgers, C.I. Armstrong, G.A.B. Shoemaker, K.L. LaBrie, J.D. Moyes, C.D. and R.M. Robertson. Stress preconditioning of spreading depression in the locust CNS. *PLoS ONE* 2:e1366 (2007).

Sombati, S. and G. Hoyle. Generation of specific behaviors in a locust by local release into neuropil of the natural neuromodulator octopamine. *J. Neurobiol.* 15: 481-506 (1984).

Urenjak, J. and T.P. Obrenovitch. Pharmacological investigation into the involvement of nitric oxide in K^+-induced cortical spreading depression. *Naunyn Schmiedebergs Arch. Pharmacol.* 362: 137-144 (2000).

Van Harreveld, A. Stamm, J.S. and E.I.Christensen. Spreading depression in rabbit, cat and monkey. *Am. J. Physiol.* 184: 312-320 (1956).

Whyard, S., Wyatt, G.R., Walker, V.K. The heat shock response in *Locusta migratoria*. *J. Comp. Physiol. B*. 156: 813-817 (1986).

Wu, J. and R.S. Fisher. Hyperthermic spreading depression in the immature rat hippocampal slice. *J. Neurophysiol*. 84: 1355-1360 (2000).

Wu, B.S. Walker, V.K. and R.M. Robertson. Heat shock-induced thermoprotection of action potentials in the locust flight system. *J. Neurobiol.* 49: 188-199 (2001).

Wu, B.S. Lee, J.K. Thompson, K.M. Walker, V.K. Moyes, C.D. and R.M. Robertson. Anoxia induces thermotolerance in the locust flight system. *J. Exp. Biol.* 205: 815-827 (2002).

Zhang, X. Kim, W.-S. Hatcher, N. Potgieter, K. Moroz, L.L. Gillette, R. and J.V Sweedler. Interfering with nitric oxide measurements. *J. Biol. Chem.* 277, 48472-48478 (2002).